The Pairing of Two-Dimensional Liquid Chromatography and Electrochemical Surface-Enhanced Raman Spectroscopy to Provide Enhanced Separation and Detection of Complex Mixtures

By

Maddison Margaret Eisnor

A Thesis Submitted to
Saint Mary's University, Halifax, Nova Scotia
in Partial Fulfillment of the Requirements for
the Degree of Master of Science in Applied Science.

April 2022, Halifax, Nova Scotia

Approved: Dr. Christa L. Brosseau
Professor
Supervisor

Approved: Prof. Mary Sheppard
Lecturer
Committee Member

Approved: Dr. Laura Weir
Assistant Professor
Committee Member

Approved: Dr. Anthony Tong
Professor
External Examiner

Date: April 25th, 2022

ABSTRACT

The Pairing of Two-Dimensional

Liquid Chromatography and Electrochemical Surface-Enhanced Raman Spectroscopy to Provide

Thorough Separation and Detection of Complex Samples

By

Maddison Margaret Eisnor

Dissolved organic matter (DOM) and green tea are known complex substances requiring advanced separation techniques and ultrasensitive detection methods for characterization and identification. DOM is ubiquitous in water bodies and participates in the global carbon cycle, undergoing complex transformation through photochemical and microbial processes. Green tea is one of the most consumed beverages in the world and is rich in polyphenolic compounds. Separation and identification of components in green tea is useful for gauging tea quality. In this work, 2D-LC and EC-SERS were explored for the first time to analyze compounds in DOM and green tea. 2D-LC offers enhanced separation compared to conventional HPLC systems since there are two dimensions present. EC-SERS was used as an offline detection modality to help identify the compounds in DOM and green tea. 2D-LC-EC-SERS was successfully performed for green tea and preliminary work was conducted for DOM taken from the Sackville River.

April 25th, 2022

Acknowledgements

First and most importantly, I want to thank my research supervisor, Dr. Christa Brosseau for allowing me to have an amazing opportunity to complete my master's degree in your research group. Words cannot explain how much your guidance and endless support have changed my life in the last five years. During analytical, you opened my eyes to how applicable and relevant analytical chemistry is in solving the world's most challenging problems and made me want to pursue chemistry as a result. I am not quite sure what I would have done with my undergrad degree if I did not have you as a professor for that class. Then, when I started working in your lab in my honours year, you made me realize how much I love doing research even though it can be hard and not go as planned sometimes but you learn that is okay or made me see it from a different perspective. I really want you to know that you are the reason why I want to become a chemistry professor and want to inspire students to pursue chemistry like you did for me. Also, I want you to know that your EDI sessions have made me a better person and more empathic for others which I am grateful for. I will forever cherish my time working in your group and always look up to you as a role model.

I would like to thank my committee members: Dr. Laura Weir, and Professor Mary Sheppard for taking the time to meet with me through the past two years. You both have provided me guidance and support, and shared lots of comments and suggestions that guided me through my research. I would like to thank Dr. Anthony Tong for agreeing to be the external examiner and taking the time to read my thesis. I would also like to thank Dr. Heather Reader for introducing me to DOM and always being available for answering my questions.

I would like to thank Melanie Davidson for being my mentor when I first started in the Dr. Brosseau group and for training me on how to operate the 2D-LC. Patricia Granados, thank you so much for all your help and patience with operating and mastering the 2D-LC and countless other instruments at SMU. I have learned so much from you, Patricia and I will always be grateful. Thank you, Dr. Xiang Yang, for helping me obtain SEM images and always providing me a laugh when seeing you. As well as Alyssa Doue, Dr. Najwan Albarghouthi and Dr. Bitu Hurriso for being so helpful and providing me supplies when needed. I want to acknowledge the chemistry faculty for providing me with my incomparable education in chemistry and continuously being inspired. I would like to thank NSERC, FGSR, and the Canada Research Chairs program for providing the financial support required to complete this research.

I want to extend my appreciation to Carolyn Farling and Kaleigh McLeod. You both were always there for me and kept me sane during this time in my life, especially lifting me up when I was down and answering any of my questions. I want to say thank you to past group member especially, Dr. Najwan Albarghouthi, Shruti Bindesri, Gaius St. Marie, Tanner George, and Megan Himmelman. I would like to acknowledge present group members: Sam Julien, Sumayyah Ayesha Bibi Chotoye, Mary Stackaruk, and Jaskaran Singh Anand for your support and help whenever it was given. Thank you to Maka Biton for all of your assistance with this project, it is much appreciated.

I would like to say a huge thank you to my boyfriend, Jordan for always listening to me when I wanted to talk about my research even though he may not have understood, always putting a smile on my face, and being patient and supportive. Finally, I want to say an enormous thank you to my Mom and especially my Dad, since he was able to help me with my water sample collection.

Additionally, for providing me their continuous support and the opportunity to attend university through their hard work and sacrifices they both have made which has allowed me to follow my dreams.

Table of Contents

List of Abbreviations

1D	One-dimensional
^{1}D	First-dimension (column or separation)
2D	Two-dimensional
^{2}D	Second-dimension (column or separation)
2D-LC	Two-dimensional liquid chromatography or multidimensional liquid chromatography
2D-LC-EC-SERS	Two-dimensional liquid chromatography with electrochemical Surface-enhanced Raman spectroscopy
AC	Argentation chromatography
APCI	Atmospheric pressure chemical ionization
AgNPs	Silver nanoparticles
Ag / AgCl	Silver-silver chloride electrode
AuNPs	Gold nanoparticles
CDOM	Chromophoric DOM
CE	Counter electrode
DAD	Diode array detection
DOC	Dissolved organic carbon
DOM	Dissolved organic matter
EC-SERS	Electrochemical surface-enhanced Raman spectroscopy
EDX	Energy-dispersive X-ray spectroscopy
EEM	Excitation emission matrix
EC	(-)-Epicatechin
ECG	(-)-Epicatechin-3-gallate
EGC	(-)-Epigallocatechin
EGCG	(-)-Epigallocatechin-3-gallate
ENV	ENVironmental
ESI	Electrospray ionization
FDOM	Fluorescent DOM
FT-ICR-MS	Fourier transform ion cyclotron resonance mass spectrometry
GC	Gas chromatography
Q-TOF	Quadrupole-time of flight
HILIC	Hydrophilic interaction liquid chromatography
HPLC	High-performance liquid chromatography
HPLC-MS	High performance liquid chromatography with MS detection
HPLC-SERS	High performance liquid chromatography with SERS detection
HWE	Hot water extracts
IEC	Ion-exchange chromatography
IHP	Inner Helmholtz plane
IR	Infrared spectroscopy
LC	Liquid chromatography
LCCC	Liquid chromatography under critical conditions
LC×LC	Comprehensive multidimensional liquid chromatography
LC-LC	Heart-cutting multidimensional liquid chromatography
LSPR	Localised surface plasmon resonance

mLC-LC	Multiple heart-cutting multidimensional liquid chromatography
MS	Mass spectrometry
NP-LC	Normal phase liquid chromatography
NMR	Nuclear magnetic resonance
OCP	Open circuit potential
OHP	Outer Helmholtz plane
PPL®	Priority Pollutant
QTOF	Quadrupole time-of-flight
RE	Reference electrode
RP	Reverse phase
RP-LC	Reverse-phase liquid chromatography
RP-LC-MS	Reverse-phase liquid chromatography-mass spectrometry
SCE	Saturated calomel electrode
SEC	Size exclusion chromatography
SEM	Scanning electron microscopy
SEM-EDX	Scanning electron microscopy-Energy-dispersive X-ray spectroscopy
SERS	Surface-enhanced Raman spectroscopy
sLCxLC	Selective two-dimensional chromatography
SOM	Soil organic matter
SPE	Solid phase extraction
SPE	Screen-printed electrode
SUVA	Specific UV absorption
TLC	Thin layer chromatography
TOC	Total organic carbon
UHPLC	Ultra-high-performance liquid chromatography
UV	Ultra-violet detection
UV-Vis	Ultra-violet visible spectroscopy
WE	Working electrode

List of Figures

List of Tables

Chapter 1: Introduction

1.1 Preamble

This thesis explores the combination of two-dimensional liquid chromatography (2D-LC) with electrochemical surface-enhanced Raman spectroscopy (EC-SERS), because the addition of EC-SERS provides an extra level of sensitivity and selectivity after a LC separation. In this work, EC-SERS is investigated as an offline detection modality for studying green tea and DOM extracts from the Sackville River. These combined techniques allow for a coupling of the great separation power of multidimensional chromatography with the robust molecular fingerprinting capability of EC-SERS. 2D-LC has been shown to be a promising tool for the separation of very complex samples.[1,2,3] However, after a sample is within a 2D-LC system it is reduced in concentration due to longitudinal diffusion or partial peak captured from heart-cutting; subsequently, an ultrasensitive technique is needed for additional investigation after the second separation. EC-SERS has been shown to improve the sensitivity of Raman spectroscopy by up to 10^6-10^8 orders of magnitude versus conventional Raman spectroscopy and this advantage could be very valuable in green tea and DOM analysis after 2D-LC separation. In this thesis work, 2D-LC-EC-SERS was explored for the first time for separation and identification of the various green tea components, and was conducted for two DOM extracts.

1.2 Objective of Thesis

Dissolved organic matter (DOM) is considered one of the most fundamentally complex molecular mixtures known, and it is ubiquitous in various water bodies within the global carbon cycle.[4,5,6] There is still a great deal to be discovered regarding the exact composition of DOM since

it remains quite indiscernible, despite the abundance of literature on the nature and classes of compounds found within DOM.[7]

To improve our understanding of DOM, researchers have started to explore the physical and chemical properties of DOM using a wide array of analytical techniques, such as mass spectrometry (MS), absorbance spectroscopy (UV-Vis), fluorescence spectroscopy, and nuclear magnetic resonance (NMR) spectroscopy in conjunction with various types of separation techniques including chromatography.[4,8] However, each of these techniques have their limitations in DOM research and are not capable of providing detailed and complete information on DOM. Currently, the most widely used technique for the separation and detection of DOM is high performance liquid chromatography (HPLC). Although liquid chromatography is powerful and highly sensitive, it has a limited separation capacity for highly complex samples such as natural extracts, metabolites, and proteins. Multidimensional liquid chromatography, also known as two-dimensional liquid chromatography (2D-LC), is an emerging technique that addresses this issue due to a significantly enhanced peak capacity, allowing adequate separation of highly complex samples, which would be very advantageous in the analysis of DOM.

Green tea was originally chosen as a model of DOM for chromatographic and spectroscopic method development. Green tea is one the most consumed beverages in the world especially in China and Japan.[9] Green tea is made from the harvested leaves of the *Camellia sinensis* plant that have undergone minimal oxidation.[9] Varieties of green tea can differ substantially due to variable growing conditions, horticulture, production processing and harvesting time.[9] Green tea contains phenolics, terpenoids, xanthines, alkaloids, flavones, flavonoids, fatty acids, amino acids, and sugars.[10] Catechins are the highest concentration component of green tea, dominated by (-)-epigallocatechin-3-gallate (EGCG) followed by (-)-epigallocatechin (EGC).[10] Polyphenols are a

group of phytochemicals present in green tea that are responsible for anti-oxidative and anti-carcinogenic health benefits.[9]

Many different analytical techniques paired with various higher level statistical analyses such as principal component analysis (PCA) have been used to identify and quantify components of green tea varieties.[9] These techniques have included gas chromatography-mass spectrometry (GC-MS), inductively coupled plasma mass spectrometry (ICP-MS), high performance liquid chromatography (HPLC), and capillary electrophoresis.[9] However, these methods are commonly time consuming and expensive.[9] Consequently, accurate, cost-effective, and rapid analytical methods for identifying and quantifying the various compounds in complex samples such as green tea are required.

Surface-enhanced Raman spectroscopy (SERS) can be used to overcome the inherent weakness of Raman spectroscopy and to quench competing fluorescence. SERS involves measuring Raman scattering from an analyte adsorbed onto a roughened surface of a nanostructured noble metal such as gold or silver. The free surface electrons in the metal nanoparticles undergo a collective oscillation in response to the oscillating electric field of an incident light beam, resulting in a greatly enhanced Raman signal which is capable of single molecule detection limits. Electrochemical surface-enhanced Raman spectroscopy (EC-SERS) combines electrochemistry and SERS where an electric potential is applied to the modified metallic surface of the working electrode in the presence of an electrolyte. It should be noted that EC-SERS has not yet been used to analyze green tea or DOM taken from water samples in the literature, and hence this thesis work provides additional novel research in this area.

This thesis hypothesizes that with sufficient optimization, EC-SERS will be useful as an alternative offline detection modality for 2D-LC after the separation of various compounds found

in green tea and DOM extracted from natural waters. In this work, 2D-LC-EC-SERS is first used on green tea, as a model of a complex substance and as a model of DOM for method development. The thesis research then moves onto DOM collected from the Sackville River, which includes further method optimization for DOM as well as identification challenges that remain with regards to DOM analysis using 2D-LC-EC-SERS.

1.3 Scope of Thesis

This thesis consists of eight chapters. Chapter 1 gives a brief introduction to the research conducted in this thesis and emphasizes the main goal of this work. Chapter 2 provides a detailed literature review of the important aspects of this project. Chapter 3 provides a detailed description of the theory which underlies the major experimental techniques used in this work including one- and two- dimensional liquid chromatography, Raman spectroscopy, SERS, electrochemistry, and EC-SERS. Chapter 4 summarizes the experimental procedures including the preparation of green tea, collection of Sackville River water, solid phase extraction of DOM, 2D-LC parameters, and EC-SERS methodology. The major 2D-LC and EC-SERS experimental results are presented in Chapter 5 for green tea and extracted DOM. Chapter 5 also focuses on the challenges experienced with DOM but also highlights the successful identification of caffeine in green tea and how 2D-LC-EC-SERS has been used for DOM. Chapter 6 summarizes the most important results obtained from this work and Chapter 7 discusses future work for this project. Finally, Chapter 8 includes the references used in this thesis. An appendix is included at the end of the thesis that contains additional spectra.

Chapter 2: Literature Review

2.1 Dissolved Organic Matter (DOM)

Organic matter found within the global water system can be categorized as either dissolved or particulate matter.[8] Dissolved organic matter (DOM) is considered one of the most complex molecular mixtures known and is ubiquitous in water systems as a heterogeneous combination of dissolved carbon-containing molecules of both aquatic and terrestrial origin.[4,5,6] Figure 2.1 demonstrates how DOM is created through terrestrial and aquatic sources, and highlights how it is altered through different transformations such as photochemical and microbial processes.[4] DOM is a crucial component in aquatic systems as it serves as a major reservoir of carbon in the global carbon cycle, providing an important energy source for the microbial community. In addition, DOM affects the transparency and pH of water and binds and interacts with metals and pollutants.[4,11]

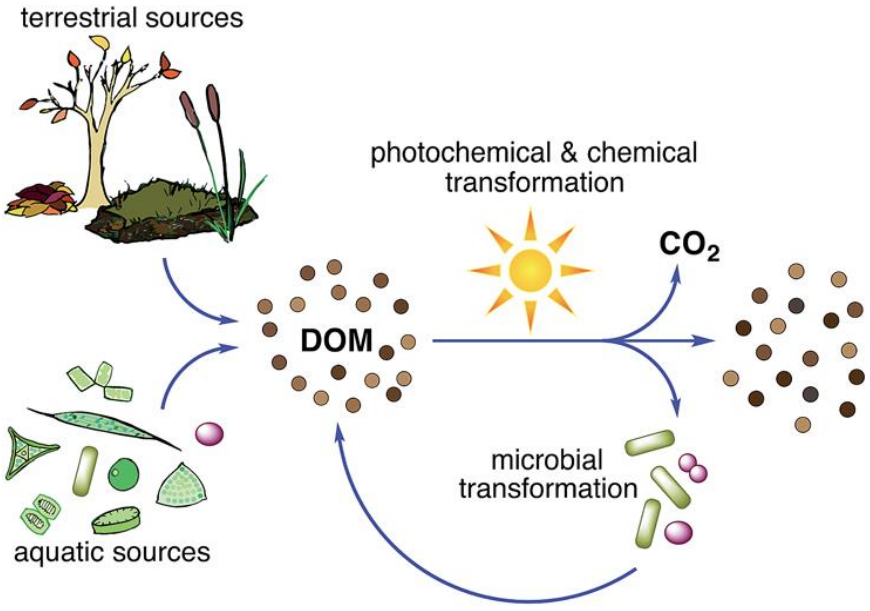

Figure 2.1: Transformation of dissolved organic matter in the environment by selected pathways. Image reproduced with permission from Lin *et al*. 2015.[4]

Some of the carbon-containing molecules found in abundance in DOM include alkyl compounds, unsaturated compounds, amides, carboxylic acids, aldehydes, ketones, amino acids

and phosphate esters.[6,7] The major components found in DOM are humic and fulvic compounds.[12] Humic substances are produced from the decomposition of plant and animal tissues and are found in soils, water systems and sediments.[12,13] Two well-known humic substances in aquatic systems are humic acid and fulvic acid.[13,14] The exact composition of these molecules varies by source. Humic acid is water soluble at a pH above 2 and fulvic acid is water soluble at all pH values. Humic acid and fulvic acid can bind to metals found in water via functional groups found in these acids, such as phenolic, carboxylate, and hydroxyl groups which helps regulate the bioavailability of these metals in aquatic ecosystems.[14] However, humic acid can react with chloride present in water to produce harmful by-products such as trihalomethane, a known carcinogenic substance.[14] The exact nature of DOM constituents remains poorly defined because of the vast number of compounds found in DOM, despite ongoing characterization efforts.[4]

DOM within all seawater and freshwater sources is recognized as one of Earth's largest carbon reservoirs, holding approximately as much carbon as is available in the atmosphere.[8,15,16] Oceanic DOM is the second largest reservoir of organic carbon in the biosphere; about 72% of the global DOC inventory is stored in deep oceanic layers for years to centuries.[17] Oceanic DOM is also the largest reactive component of the global carbon cycle and is understood to be a significant short-term sink for atmospheric carbon.[17] DOM can be viewed as a major transport mechanism for carbon from various terrestrial environments into aquatic systems.[18] DOM is clearly a very important part of the global carbon cycle, and that is one of the reasons why investigations of DOM and its various components is imperative.

DOM undergoes a multitude of biotic and abiotic transformations such as photochemical and microbial degradation, as well as autoxidation in the environment where it occurs, which contributes to the diversity of its components.[4] It is proposed that the combination of both

photochemical and microbial degradation represents the major transformation mechanism for DOM.[16] The impact of photochemical processes on the DOM pool depends on the initial chemical composition of DOM. A study suggests that recently produced autochthonous DOM (DOM produced within the water body) becomes less bioavailable, while allochthonous DOM (DOM produced outside of the water body) becomes more bioavailable to prokaryotes after sunlight exposure (however refer to reference 13).[16] Compared with photochemical reactions that occur only in the photic zone (the uppermost layer of a body of water), microbial degradation proceeds throughout the water body. Microbial degradation can contribute up to 60% of DOM consumption depending on the sources of DOM and its specific size fractions and chemical components.[6] Abiotic processes including self-assembly although autoxidative degradation may also be important.[6] The self-assembly of DOM has received continuous attention due to its critical role in carbon cycling and nutrient dynamics. Studies on the coupling effect of both types of processes on the transformation of DOM between different molecular sizes and components should provide new insights, which could lead to better understanding of the heterogeneous nature of DOM with respect to fate, transport, ecological role, and environmental impacts of DOM in aquatic systems.[11]

2.1.1 DOM Extraction Methods

The isolation of DOM from water samples represents the first step in the majority of DOM studies, and this step could possibly provide the biggest challenge in understanding the exact composition of DOM.[8] This is because it can be difficult to achieve an efficient, reproducible extraction of representative, uncontaminated samples with acceptable recoveries.[8] One of the reasons it is difficult to achieve decent DOM extractions from water samples is because of the very low concentration of organic molecules dissolved in water, compared with the huge amounts of inorganic salts, which remains a major challenge in analytical chemistry.[19] Through isolation of

DOM, highly concentrated organic samples with low salt content can be obtained, and different analytical techniques can then be performed on these samples.[19]

It is important to differentiate between the terms isolation, concentration, and extraction given that there are distinct differences between these terms that are sometimes not noted.[18] Concentration indicates the removal of solvent to increase the dissolved organic carbon (DOC) concentration. Isolation refers to the separation of DOC from other sample components, including inorganic compounds.[18] Ultimately, extraction is the general term that refers to the combination of isolation and concentration.[18] The extraction of DOM is generally done in one of these four ways: reverse osmosis coupled with electrodialysis (RO/ED), ultrafiltration, solid phase extraction (SPE), and direct drying or freeze drying.[18] RO/ED, ultrafiltration and SPE are techniques that both concentrate and isolate dissolved organic matter. For the purposes of this thesis work, SPE will be explained in greater detail as it was the extraction method chosen for this research.

SPE has become a widespread separation method that is very easy to use and can be fairly selective. Further, SPE provides high extraction efficiency, compared to reverse osmosis or ultrafiltration methods.[20,21] The work of Dittmar *et al*., as highlighted in Figure 2.2 demonstrates how to extract DOM from seawater, but this process is applicable for any type of water sample.[22] Firstly, in this process, SPE cartridges are soaked with methanol to ensure the cartridge is clean. Subsequently, the previously acidified and filtered sample is passed through a cartridge with the help of a pump, and molecules in the water sample are adsorbed onto the nonpolar stationary phase, also known as the sorbent, contained in the cartridge. The salt present in the sample is removed by rinsing the cartridges with 0.01 M hydrochloric acid and then the cartridge is dried using air or nitrogen gas. Lastly, the molecules contained in the stationary phase are eluted in a small volume, typically one cartridge volume (~5 mL), of a solvent of suitable polarity such as methanol.

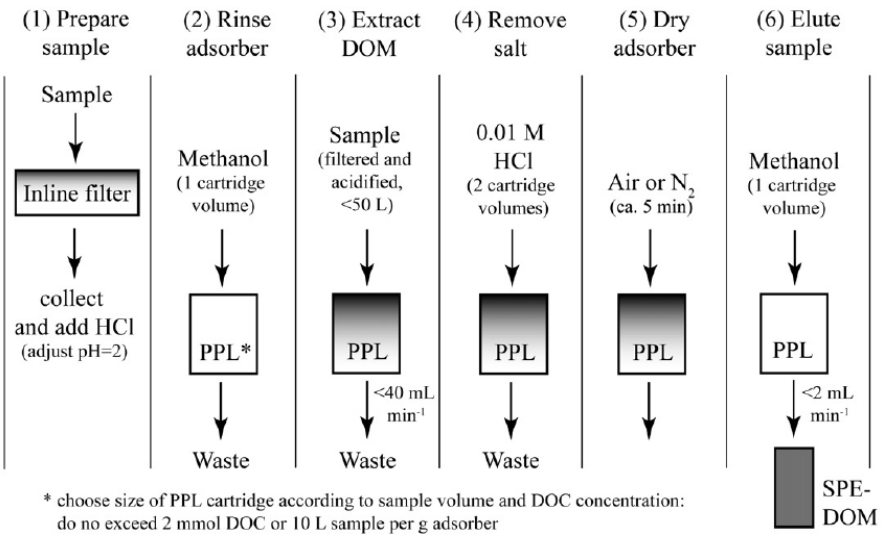

Figure 2.2: Solid phase extraction method for the isolation of DOM. Image reproduced with permission from Dittmar *et al.* 2008.[19]

Originally, Amberlite XAD resins, composed of methyl methacrylate or styrene divinyl benzene polymers, were the most commonly used stationary phases for DOM extraction, however, some of these resins are no longer manufactured.[22] Also, a drawback of silica-based hydrophobic sorbents, another well-known sorbent, is that they can undergo phase collapse in aqueous matrices with concomitant loss of retention. As well, the silica structure can decompose through acidic or basic hydrolysis, which can be problematic for the acidified water samples.[19] However, there are other non-polar stationary phases based on styrene divinylbenzene such as PPL® (Priority Pollutant®), or hydrocarbons bonded to a silica matrix that are typically used. PPL® cartridges rely on interactions between organic molecules of considerable structural variance and a modified styrene divinylbenzene stationary phase. Dittmar *et al*. found through their work that the highest extraction efficiencies of DOC were achieved with PPL® cartridges (62 ± 6% extraction efficiency), as highlighted in Figure 2.3.[19] These sorbents are made for the extraction of a wide range of highly polar to nonpolar substances from large volumes of water, and as such, can capture a much larger fraction of the organic matter pool.[19,22] PPL® has a smaller pore size (150 Å) than the overall similar environment (ENV) sorbent (450 Å), which is likely the reason for the higher

extraction efficiency of DOC by PPL®.[19] In addition, Li *et al*. emphasize how strong the recovery of DOM is by using a PPL® cartridge compared to twenty three other commercially available SPE sorbents under identical conditions while extracting DOM from Suwannee River and North Sea water samples.[20] SPE can also be automated, which greatly reduces operator involvement and increases the reproducibility of extractions through tight control of variables such as flow rates, solvent volumes, and equilibration and drying times.[23]

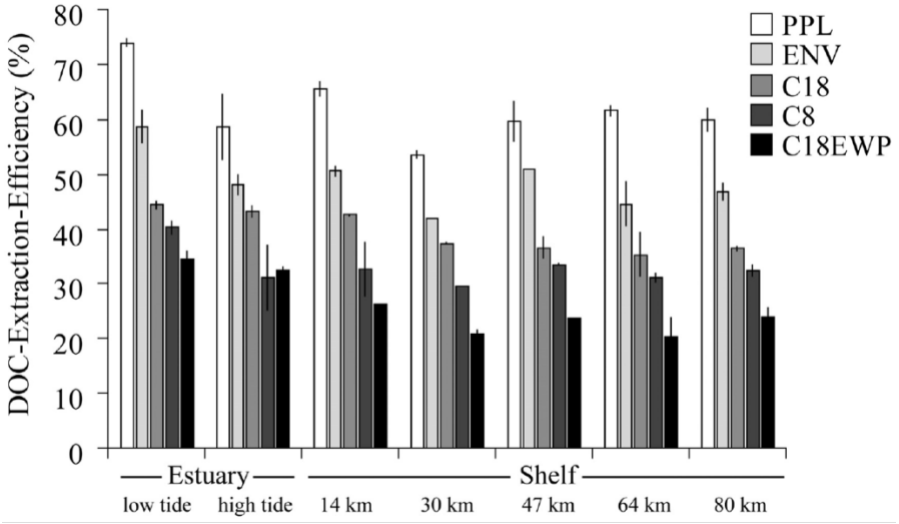

Figure 2.3: Solid phase extraction efficiencies for the isolation of DOM at 1°S in the Maracaçumé Estuary (low and high tide) and on the adjacent North Brazil shelf (distance offshore, km) using different sorbents. Image reproduced with permission from Dittmar *et al*. 2008.[19]

Ultimately, SPE is an applicable method to extract dissolved organic matter from various types of water samples. As mentioned above, PPL® cartridges are very efficient in providing large DOM recoveries when compared to other SPE cartridges. After completing the SPE step on the water samples of interest, the next step of DOM analysis is choosing the appropriate the analytical method(s) to further study the DOM sample under investigation.

2.1.2 DOM Characterization Methods

Following SPE extraction and collection, various analytical techniques are applied in an attempt to examine, fractionate, and separate the extracted DOM into its many different classes of compounds.[8] Figure 2.4 demonstrates the range of methods used in the isolation and separation of DOM, which usually involves three to five separation steps. The need for these additional steps is quite clear because non-selective analytical methods only describe bulk properties, or limited fractions of the total DOM pool; for example, total organic carbon (TOC) measurements, C:N ratios, or bulk fluorescence. Such approaches reduce DOM to an average theoretical material, with a characteristic fingerprint, which is often used for identification of the source, bulk transport, and comparative studies of water bodies. For molecular level information, only mass spectrometry (MS) and nuclear magnetic resonance (NMR) can begin to approach the level of selectivity required, although the complexity of the unfractionated material often results in extensive spectral overlap. Thus, the challenge currently sits in finding the right chromatographic approach to achieve DOM fractionation/separation prior to MS and NMR analyses.

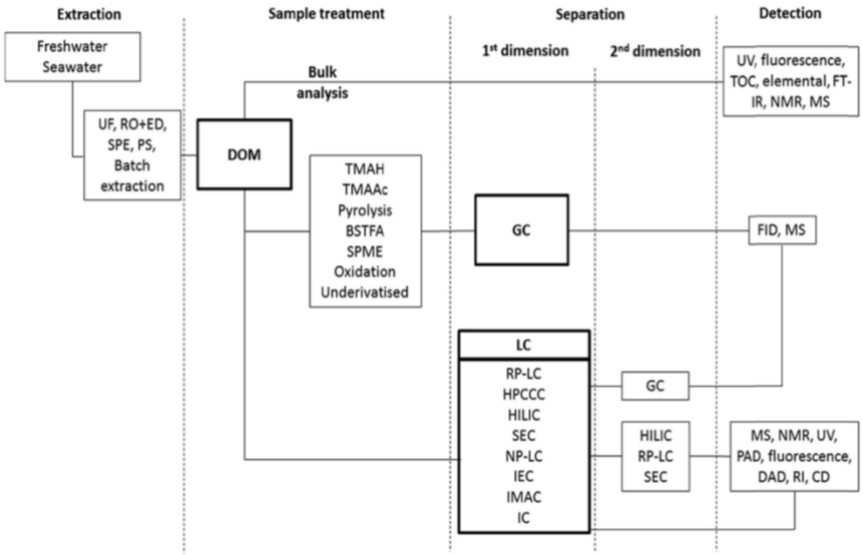

Figure 2.4: Analytical approaches to DOM isolation and separation. Image reproduced with permission from Sandron *et al*. 2005.[8]

2.1.3 Chromatographic Techniques to Analyse DOM

Liquid chromatographic methods that have been applied to the separation of DOM include reverse-phase liquid chromatography (RP-LC), normal-phase liquid chromatography (NP-LC), size exclusion chromatography (SEC), hydrophilic interaction liquid chromatography (HILIC), and ion exchange chromatography.[8] These various methods have been used to separate DOM by numerous characteristics, such as hydrophobic or hydrophilic polarity, molecular weight, charge, and degree of unsaturation.

When performing RP-LC on DOM there are some issues that might arise during the chromatographic separation that can be easily avoided. It is known that DOM often exhibits strong retention, which requires relatively strong mobile phase gradients for elution because of the large complex organic structures present.[8] These DOM compounds have a 'sticky' nature, which demands frequent blank runs between samples to eliminate any carryover and fully regenerate the column.[8] However, despite this limitation, RP-LC remains a very popular approach for DOM separation.

Mills *et al*. were among the very first to use RP-LC with UV detection and a water/acetonitrile mobile phase for analyzing DOM samples.[24] The reported chromatogram did not provide the best results as there were several clusters of largely unresolved peaks referred to as a 'hump' that dominated the chromatogram. The largest of these peaks eluted when acetonitrile was introduced to the chromatographic run, suggesting intermediate polarity of the sample. Mills *et al*. later attempted using this RP-LC method again with minor improvements such as the use of a phosphate buffer mobile phase.[24] However, once again most of the detectable DOM components eluted in a similar way as before with the unresolved 'hump' observed.[24] With their minor improvements,

however, large peaks eluted in the beginning of the chromatograms which indicated the presence of highly polar organic material.[24]

Koch *et al*. investigated the impact of pH and the use of mobile phase buffers in a RP-LC separation of DOM, and proposed using a neutral pH water/methanol gradient with a phosphate buffer additive (pH 6.8).[25] Methanol exhibits both polar and hydrogen bonding interactions with the analyte, particularly when the pH of the mobile phase is neutral. Koch *et al*. found that not using a buffer, and instead, a mobile phase with a neutral pH resulted in more resolved peaks of the water-soluble components.[19] When a lower pH mobile phase was used, this caused extensive coelution of the water-soluble components. Despite the partial success of this approach, Koch *et al*. mentioned the necessity to decrease the complexity of DOM samples prior to RP-LC as much as possible, and proposed using multi-dimensional chromatography involving SEC.[19]

RP-LC with MS detection is potentially applicable for the analysis of DOM because of the molecular fingerprinting that MS provides which is essential for such complex mixtures.[8] However, despite MS detection providing additional information with achievable resolution, there are still challenges that remain in the interpretation of the resulting MS spectra, which are derived from the thousands of compounds discovered in DOM.[8] Additionally, it is often difficult to identify and isolate signals derived from artifacts, which can originate from the extraction or chromatographic stage and also from the ion source in MS.[8]

In 2007, Dittmar *et al.* applied RP-LC-MS to the mapping of terrestrially derived DOM along a river transect.[26] The RP-LC chromatograms resulted in an unresolved 'hump' being present and no resolution of individual molecules in the beginning of the run. Dittmar *et al.*, found that the peak maximum of this 'hump' would have higher retention times for samples collected further offshore. Moreover, in this study, MS detection was able to further emphasize how DOM also

showed considerable variations due to photochemical alterations.[26] The average MS spectra was used to establish that the estuarine DOM displayed a bimodal mass distribution with a weighted average of 0.895 kDa, whereas 1.13 kDa was calculated for terrigenous DOM.[26] After irradiation, terrigenous DOM resembled more the composition of estuarine DOM, since its weighted mass distribution decreased to 0.885 kDa. Furthermore, a large fraction of UV-absorbing compounds was not being detected after photodegradation.[26]

Although the resolving power of MS detection is significant, there are potential biases originating from the ionization source. One ionization source can be more efficient for certain classes of compounds than others. For example, the most popular ionization source in DOM analysis is electrospray ionization (ESI), which is particularly appropriate for ionic, high polarity compounds.[8,27] The number of charges retained by a particular sample depends on molecular size and chemical composition of that sample, as well as the solvent composition and the instrument parameters.[8] When attempting to focus on low polarity compounds, atmospheric pressure chemical ionization (APCI) is also used.[8] Lastly, matrix assisted laser desorption ionization (MALDI), which is considered a soft ionization technique mainly targets large molecules with masses up to 300 kDa, such as proteins and peptides; thus, not providing information on the bulk of DOM.[8] Hence, there is no universal ionization technique capable of analyzing all the classes of compounds within DOM. The chosen ion source commonly represents the best compromise in attempting to target the vast majority of DOM compounds.

In 2012, two distinct comprehensive online 2D-LC approaches were explored by Duarte *et al.* for the first time, providing new information on molecular weight distributions of humic and fulvic acids.[7] With the first method, RP-LC was used in isocratic mode using a mobile phase containing 20% acetonitrile in water in the first-dimension.[7] The second-dimension utilized a SEC separation

also in isocratic mode and a 11% acetonitrile in 20 mM ammonium bicarbonate buffer at pH 8.0 as the mobile phase.[7] In the second method, the first-dimension included the use of a HILIC column and a 10% acetonitrile in 20 mM ammonium acetate at pH 6.0.[7] SEC was used in the second-dimension with the same parameters used in the RP-LCXSEC method.[7] Three different online detectors were used in both methods, which were ultraviolet spectroscopy monitored at 254 nm, fluorescence using a 240 nm excitation wavelength and an emission wavelength at 450 nm, as well as an evaporative light scattering detector (ELSD).[7] The two 2D-LC methods reported comparable results, with 2D chromatograms still showing fractions that were not completely resolved.[7] However, the authors discovered that compounds eluting at higher retention times within the second-dimension seemed to be related to more hydrophobic moieties.[7] Duarte *et al.* also emphasized the importance of method optimization, such as mobile phase compatibility, modulation period, and separation time.[7] In addition, they found that within SEC, acetonitrile contents higher than 20% provided poorer resolution and a move towards higher retention times.[7] These comprehensive 2D-LC methods proved to be promising in resolving the chemical heterogeneity of complex organic mixtures such as DOM, compared to conventional one-dimensional chromatographic methods.

2.1.4 Spectroscopic Techniques to Analyse DOM

Ultraviolet-visible (UV-Vis) and fluorescence spectroscopies are the most common spectroscopic techniques used to provide information on DOM concentrations and composition in aqueous systems, primarily due to their ease of use, fast response, low cost, and high sensitivity.[28,29] Both approaches, however, require absorption of ultraviolet or visible light by certain DOM fractions; chromophoric DOM (CDOM) is the only fraction that is able to absorb this type of light and thus be monitored.[29]

Light absorption in the ultraviolet and visible range occurs when using 254, 350, and 440 nm wavelengths, which is linearly correlated with DOC concentration, delivering a method for rapid and inexpensive in-lab or *in situ* optical determinations of DOC concentrations.[18] Conversely, the linear correlation of light absorption and DOC concentration fails in various water systems because of two reasons. The first reason is due to the strong anthropogenic inputs of DOC in ocean waters. Secondly, DOC has been extensively photodegraded which occurs in most ocean waters where autochthonous and photodegraded DOC are both predominant and thus not providing a necessarily accurate representation of the original DOM composition.[18]

UV-Visible absorption data are also combined with DOC concentration data to provide a specific UV absorption parameter (SUVA).[18] The wavelength used for this parameter varies but 254 nm is the most often used.[18] Thus, $SUVA_{254}$ is the ratio of the ultraviolet light absorption intensity at a wavelength of 254 nm to the DOM concentration sample in mg/L, and has been shown to correlate to the aromatic content per unit of organic carbon concentration.[30,31]

Reader *et al.* wanted to achieve a better understanding of the molecular and optical characteristics of DOM through the use of absorbance spectroscopy (UV-Vis) and mass spectrometry.[32] The authors' approach was the first of its kind to associate the mass spectra and absorbance spectra of DOM in one analysis. These researchers sampled from three boreal rivers in Sweden every month over a period of one year. Subsequently, some of the samples were then exposed to both photochemical and biological degradation.[32] The technique provided by Reader *et al.* gave insight into the cycling of DOM, as well as sources and reactivity in aquatic systems, such as the most dominant transformation that DOM undergoes is photochemical degradation

Fluorescence spectroscopy has been used for both DOC quantification and characterization.[18] A fraction of CDOM that emits fluorescence when excited by light at certain wavelengths is called

fluorescent DOM (FDOM).[29] Analyses of DOM using fluorescence spectroscopy uses an excitation wavelength in the UVA range at approximately 370 nm, and the emission wavelength used is in the range of 440 to 460 nm. In addition to being used as a quantification tool, fluorescence spectroscopy is also used to provide insights into the chemical composition and size of DOM; this can be done using a technique called excitation emission matrix (EEM).[18] Early EEMs work used fluorescence ratios of excitation maxima and minima to define peak types and to develop a fluorescence index. The fluorescence index is the ratio of emission intensity at 450 nm or 500 nm over the excitation intensity at 370 nm to estimate microbial vs. higher-land-plant contributions to the DOM pool.[18]

Advances in spectroscopic techniques such as absorbance and fluorescence spectroscopy have led to an increase of information gained about the composition and sources of DOM.[33] Nevertheless there remains a need for expansion of the spectroscopic methods used to analyse DOM, and a potential option is surface-enhanced Raman spectroscopy (SERS). SERS is a powerful spectroscopy technique that has not yet been used for analyzing DOM. However, SERS could potentially be quite useful in detecting and identifying the various separated compounds in DOM.

2.2 Surface-Enhanced Raman Spectroscopy (SERS)

SERS was first established in the 1970's when it was revealed that introducing a nanostructured coinage metal surface increased the Raman spectral intensity of the analyte by a million fold.[34,35] SERS has emerged over the past few decades as a promising analytical technique for the sensitive detection of analytes. In addition, the noble metal surfaces used in SERS also quench fluorescence, which can normally obscure the much weaker Raman signal.[36,37] This spectroscopic technique has been used in various applications such as trace analysis of pesticides,

pigments and dyes, identification of bacteria, genetic diagnostics, and nuclear waste analysis.[38] In addition, SERS is applicable in fields where there are great consequences for inaccurate results, including drug discovery, forensic analysis, and homeland security.[39] As a result of these advantages, and the lack of spectral interference from water and glass, several studies have used SERS as a detection modality for different chromatographic techniques.[39,40]

A major drawback of SERS is that it is not an ideal technique for samples that are very complex because typically only one or a few components within the sample are detected due to their dominant Raman scattering cross section. In 1977, Henzel *et al.* found a way to avoid this issue by having SERS used as a detection modality in conjunction with thin-layer chromatography (TLC).[37] Since then, TLC coupled with SERS has been used to detect synthetic dyes, drugs in botanical dietary supplements, and tobacco-related biomarkers in urine.[37,41,42] In these studies, silver colloids are added to the TLC plate onto which the various components in the sample have been separated, after which SERS can be conducted directly on the TLC plate.[37,41]

It has been shown that SERS is a useful detector when coupled to gas chromatography (GC). One study deposited fractions of benzene, toluene, ethylbenzene, and *o,m,p*-xylenes from the GC-column onto a TLC plate that had been previously pre-treated with Ag colloid.[43] Heaps *et al.* used another method wherein the already separated molecules from the GC were condensed onto a moving, liquid-nitrogen-cooled ZnSe window, which had a 5 nm layer of Ag deposited onto it using physical vapour deposition.[39] In this study, detection limits were determined to be lower than those of GC coupled with mass spectrometry (GC-MS).[39] In all of these studies, SERS in combination with GC was successful in providing sensitive molecular detection.

Many studies have reported the use of SERS as an online and offline detector for HPLC and ultra-high performance liquid chromatography (UHPLC).[44] UHPLC uses columns that contain

particles with diameters below two μm which requires higher mobile phase pumping pressures. Online detection means SERS detection is directly occurring in real time when the HPLC system is analyzing the sample whereas offline detection indicates that fractions are collected from the HPLC system and are then further analysed. Some of the main methods to accomplish online HPLC-SERS have been to incorporate metal colloids into the mobile phase flow, or the use of a roughened metal substrate placed at the end of the column to detect the separated molecules.[44] Online SERS detection of analytes as they elute from the column can be problematic. For example, adding colloid to the mobile phase and allowing it to aggregate can cause some risk of the colloid attaching to the inside of the flow cells and/or tubing used.[44] Additionally, there are also memory effects that occur when using the metal substrates and hence they must be cleaned between samples to ensure accurate and reproducible SERS signals. One way to overcome the memory effect has been to apply sheath-flow SERS. Sheath-flow SERS uses hydrodynamic focusing to confine analyte molecules eluting out of a column onto a planar SERS substrate, where the molecules are detected by their unique SERS signal.[45] However, sheath-flow SERS requires a fairly complex home-built setup which can be costly and troublesome.[45,46]

Offline SERS detection involves the separation and detection elements occurring individually, with the separation process happening first. Subsequently, the effluent fractions are collected during the HPLC run. These fractions are then analysed using a separate Raman instrument. Therefore, offline analysis is more labour-intensive compared to online analysis. Offline analysis removes the time-critical element of the identification; thus, the optimization of the SERS conditions can be taken into account for each fraction independently.[44,47] As a result, this means not needing to compromise the SERS response for separation efficiency. Therefore, in this thesis work, offline SERS detection will be used to detect various components of DOM that have been

previously separated by the 2D-LC. This thesis research will focus first on green tea as a model of DOM, and then will move on to a study of a local DOM source, the Sackville River in Nova Scotia, Canada.

2.3 Sackville River

Sackville is the fastest growing suburban community in Halifax, Nova Scotia, Canada, and is located along the Sackville River.[48] This 40 km urban river begins in Mount Uniacke and makes its way through highly developed commercial and residential areas in Sackville and Bedford, as shown in Figure 2.5.[49] There are parts of the river that branch out into the communities of Beaverbank and Hammonds Plains.[48] This water system has fifteen large lakes surrounding it and several tributaries leading into the Sackville River, with the Little Sackville River being the largest tributary. Many highways are somewhat parallel throughout the length of Sackville River including Highway 1, known as Sackville Dr. and Highway 101. The Sackville River is the largest source of fresh water to the Halifax Harbour through the Bedford Basin, providing a suitable habitat for fish and other aquatic organisms, while providing an uninterrupted sequence of rivers, lakes, and streams.[48,49]

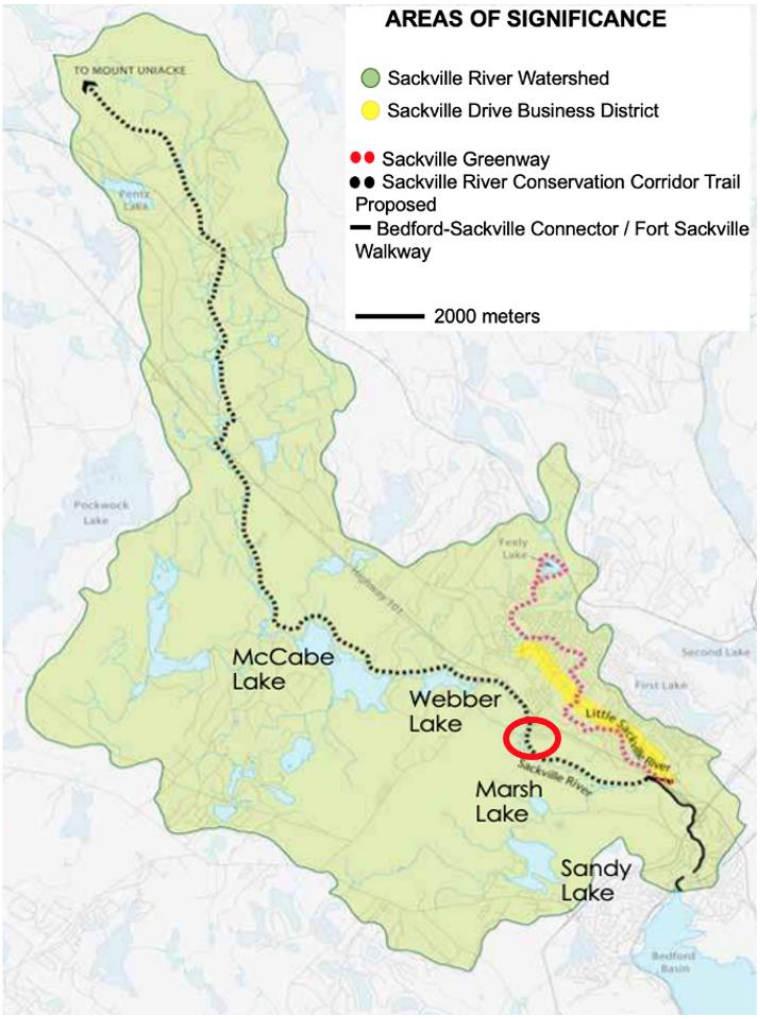

Figure 2.5: Map of the Sackville River. Adapted from reference [46]. Sampling site circled in red.

This fast run-off river flows through a valley of granite and glacial till, and in some areas the river is very rough with boulders dispersed throughout. Between these rough areas, there are long, deep, quiet waters flowing through swamps. The water in the Sackville River is dark brown in colour due to frequent heavy rains, or when construction work in the area is too close to the river.[48] Siltation has been a particular problem in the beginning of the Sackville River and in Sandy Lake.[49] Siltation is water pollution caused by terrestrial clastic material, with the size of the particles being dominated by silt or clay.

The Sackville River was used to collect water samples to analyse DOM for this thesis and was chosen because of its proximity to Saint Mary's University. One sampling site was chosen in the

Lower Sackville area (see Figure 2.5), to develop a method for DOM collection, extraction and analysis for this thesis work, with a particular emphasis on exploring 2D-LC-EC-SERS for DOM analysis, for the first time. To establish an appropriate method for DOM analysis, green tea was used as a model of DOM, as it represents a complex matrix with chemically similar components.

2.4 Green Tea

Understanding the composition of dissolved organic matter is important, however, DOM contains thousands of compounds which are challenging to separate and identify.[50] Therefore, for method development a much simpler but still complex mixture such as green tea can be used as a model of organic matter. Green tea has been used as a model for soil hot water extracts (HWE) for studying the transformation of labile soil organic matter (SOM).[50] SOM is the fraction of the soil that is formed through the partial decomposition of animal or plant debris by microorganisms.[50,51] Bell *et al.* investigated HWE buried green tea by NMR and Fourier transform ion cyclotron resonance mass spectrometry (FT-ICR-MS), as an alternative for labile SOM.[50]

Green tea is produced from the same tea leaves as black tea (*Camellia sinensis*) with the only difference being the lack of an oxidation step in the manufacturing process.[50] The composition of green tea has been studied extensively. Green tea contains a mixture of phenolics, terpenoids, xanthines, alkaloids, flavones, flavonoids, fatty acids, amino acids, and sugars, with each compound class containing many different molecules.[10,50,52,53] For example, Hooft *et al.* provided the most wide-ranging list to date of phenolics found in green tea identifying a total of 177 compounds.[50] Catechins exist in the highest concentration dominated by (-)-epigallocatechin-3-gallate (EGCG) followed by (-)-epigallocatechin (EGC).[10,50,52,53] Figure 2.6 comprises of the chemical structures of five major catechins found in green tea such as (+)-catechin, (-)-

epigallocatechin-3-gallate (EGCG), (-)-epigallocatechin (EGC), (-)-epicatechin-3-gallate (ECG) and (-)-epicatechin (EC) as well as caffeine.

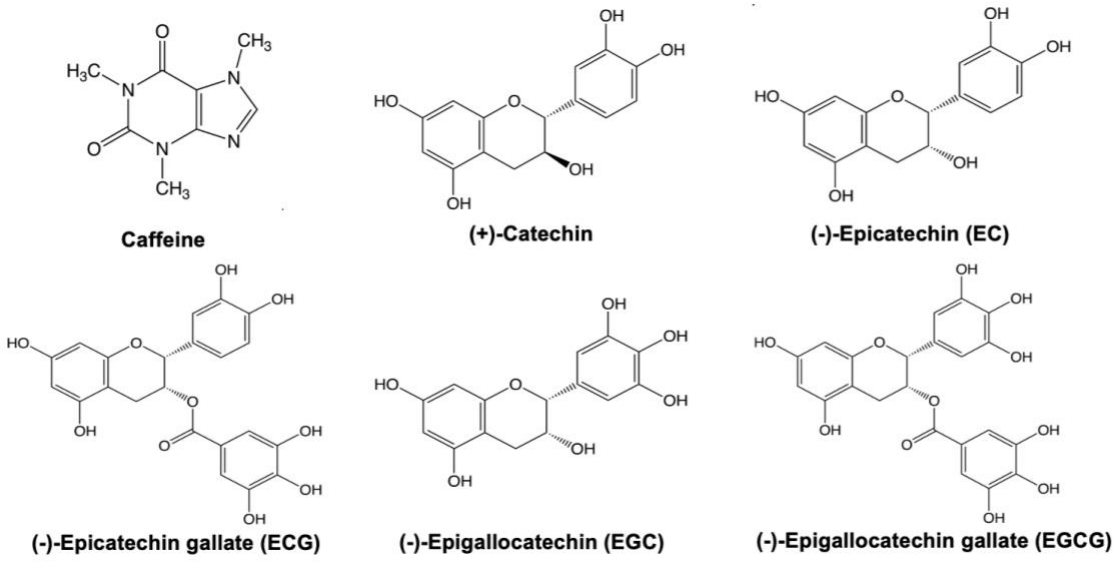

Figure 2.6: Chemical structures of five catechins and caffeine.

2.4.1 Chromatographic Techniques to Analyse Green Tea

A large variety of chromatographic techniques have been reported for the analysis of green tea, including high performance thin-layer chromatography (HPTLC), UHPLC, gas chromatography, capillary electrophoresis, and micellar electrokinetic capillary chromatography.[54,55,56] However, high performance liquid chromatography (HPLC) is by far the most widely used chromatographic for the analysis of green tea.[54,57,58] HPLC is often combined with mass spectrometry such as time of flight MS (TOF-MS) in order to gain a more comprehensive understanding of the various compounds found in green tea.[54,55] In general, reverse phase liquid chromatography (RP-LC) is the main method for the separation of green tea phenolic compounds.[59]

One limitation of using HPLC to analyze green tea is that it can be time consuming due to the complexity of the sample, with run-times of >30 minutes.[60] To help overcome this problem,

UHPLC utilizing smaller stationary phase particle diameters offers a decreased analysis time and increased resolution. Theppakorn *et al.* developed a fast and reliable isocratic HPLC method for simultaneous separation, identification and quantification of various compounds in green tea such as gallic acid, (+)-catechin, (-)-epicatechin, (-)-epicatechin-3-gallate, (-)-epigallocatechin, and (-)-epigallocatechin-3-gallate.[60] In this work, a C-18 reversed phase column with dimensions of 3 μm x 7 mm x 53 mm was used. Various mobile phases and compositions were used, and ultimately water and acetonitrile (87:13) containing 0.05% trifluoroacetic acid (TFA) were found to provide the best results, providing a final run-time of seven minutes to separate majority of components of interest components of the green tea sample.[60]

Wangkarn *et al.* tried three columns that were monomeric, end capped and deactivated C-18 column (5.0 μm x 3.0 mm x 150 mm) with high purity and inert silica present.[58] Various different solvents and different compositions were tried such as water combined with methanol or acetonitrile. The presence of an acid such as acetic acid is crucial for achieving a complete separation, especially between (-)-epigallocatechin and gallic acid.[58] Gradient elution and isocratic elution methods using a variety of flow rates were evaluated. Gradient elution was found to provide a better separation and was ultimately used for the analysis of *Miang*, a traditional Lanna fermented tea leaf originating from Northern Thailand.[58]

Even though HPLC has been extensively used for the detection of catechins found in green tea, there are notable limitations regarding sample matrices and their complexity.[58] For example, Kanpiengjai *et al.* found that during the fermentation process, tannin-tolerant lactic acid bacteria and yeasts produce various phenolic compounds, organic acids, and volatile acids which interfere with the matrix of green tea, making the analysis and identification of the original compounds more difficult.[58] Therefore, new methodologies and techniques have to be established to overcome

this limitation such as using two-dimensional liquid chromatography. Both offline and online 2D-LC has been used for the analysis of green tea.[59,61] Even though some RP-LC methods have been successful for separating the various compounds in green tea, it has been mentioned that RP-LC in some cases does not provide sufficient resolving power to enable complete resolution of the diverse amount of phenolics found in green tea.[59] Therefore, hydrophilic interaction chromatography (HILIC) is useful in the analysis of the polar compounds found in green tea.[59]

A HILICXRP-LC method was developed by Kalili *et al.* that has been successfully used for the analysis of procyanidins in cocoa and apple extracts before utilizing the method for the separation of green tea phenolics.[59] Several types of detectors such as photodiode array, fluorescence, and ESI-MS were used, allowing for the selective detection of the various phenolics.[59] For the first-dimension, the mobile phase used was acetonitrile mixed with acetic acid (99:1% v/v) and methanol mixed with water and acetic acid (94.05: 4.95: 1% v/v/v). For the second-dimension, the mobile phase consists of 0.1% (v/v) formic acid in both water and acetonitrile. Gradient elution was used in both dimensions. Using this offline comprehensive HILICXRP-LC method provided an effective approach to improve the resolving power of a 1D-LC method for the complicated phenolic compounds known to be in green tea.

Scoparo *et al.* developed an offline SECXRP-LC method for the analysis of green tea.[61] SEC used in the first-dimension proved to have other interactions with the green tea than simple permeation based on molecular masses.[61] The compounds eluted in order of decreasing molecular weight.[61] Flavonoids and their corresponding glycosides had notable interactions with the SEC column. The analysis time in the second-dimension was only eight minutes with the main compounds eluting within the first three minutes.[61] The combination of SEC in the first-dimension and RP-LC in the second provided the orthogonality required for a 2D method.

Online comprehensive RP-LCXRP-LC was established to provide a thorough analysis and quantification of purine alkaloids and catechins in green tea.[62] This was a significant finding because the predominant compounds found in green tea are catechins with (-)-epigallocatechin-3-gallate being the most abundant.[62] Krieger *et al.* found a coelution between caffeine and (-)-epigallocatechin-3-gallate in the first-dimension which was resolved in the second-dimension.[62] The mobile phases used were water and methanol in the first-dimension with 0.05% trifluoroacetic acid present and then water and acetonitrile in the second-dimension with 0.05% trifluoroacetic acid present.[62] Due to the feasibility and easy pairing of reverse phase chromatography in both dimensions, this method was chosen as a starting point for this thesis work.[62]

2.4.2 Spectroscopic Techniques to Analyse Green Tea

Although the above techniques are used for the analysis of green tea, they are laborious, destructive, and sometimes not suitable for online monitoring of green tea.[63] Presently, techniques that are accurate, environmentally friendly, cost effective, non-invasive, rapid, and feasible have provoked much interest amongst researchers for classifying tea varieties and identifying and quantifying total polyphenol content (TPC) in green tea.[63,9] Particularly, vibrational spectroscopy involving ultraviolet-visible (UV-Vis), near-infrared (NIR), mid-infrared (MIR), Raman, SERS, NMR and hyperspectral imaging (HSI) have been explored.[63]

NMR spectroscopy has been criticized for its low sensitivity; however, it is a non-destructive technique which provides detailed sample insight and offers rapid analysis times.[64] It is also an appropriate technique for metabolite fingerprinting when coupled with multivariate tools such as principal component analysis (PCA).[64] Jeong *et al*. obtained ^{1}H NMR spectra of green and black tea which were then analyzed by PCA.[64] The spectra of the three teas, Woojeon, Jaksul, and Daejak, were quite similar except for the flavonoid region at 8.39 ppm.[64] The flavonoid content

was increased depending on the cultivated time since Jaksul, and Daejak grew under strong sunlight on summer solstice as compared to Woojeon. The region between 6.45 to 7.02 ppm in the ^{1}H NMR spectra is correlated to catechins.[64] The PCA analysis determined that the catechin content in green tea is higher than in black tea.[64]

NIR and UV-Vis are two very common analytical techniques due to their cost-effectiveness and ease of use.[9] Both techniques coupled with chemometric algorithms have been widely applied to identify tea varieties and quantify the content of caffeine and total polyphenols in tea.[9] NIR offers information based on the absorbance of the vibration frequencies of chemical bonds, such as O–H, N–H, C–H functional groups in the region 750-2500 nm.[9] UV-Vis provides some useful information in the 200-800 nm if the compound contains double or triple bonds, and/or is conjugated or cyclic.[9] The information obtained from the two techniques is complementary due to the differences in principle and range of spectra.[9] Wang *et al*. used NIR and UV-Vis for the identification of five green tea varieties (Longjing, Maojian, Biluochun, Maofeng and Yunwu) and their total polyphenol content.[9] NIR was helpful for the fast quantitative determination of the total polyphenol content.[9] However, it was very difficult to distinguish tea varieties using NIR and UV-Vis data.[9] Therefore, Wang *et al*. also used data fusion to help with their work.[9] Data fusion is the process of integrating data matrices from different instruments into a single model.[9] The authors used PCA and the random forest pattern recognition technique on their data fusion set which had better potential to successfully differentiate the five varieties of green tea.[9]

Surface-enhanced Raman spectroscopy (SERS) is a well-established vibrational fingerprinting technique which offers advantages of rapid analysis time, field portability, ease of use and little to no sample preparation.[65] SERS has become a useful analytical method for many chemical and biological applications.[65] Recently, SERS has been explored for polyphenolic

mixtures, as well as tea samples. Zeiri *et al.* used various plants including green tea to reduce gold and silver salts to perform SERS.[66] A 785 nm excitation wavelength was used that produced a good SERS spectrum.[66] Both gold and silver colloids were used but the gold nanoparticles produced better results; the silver colloids provided spectra with weaker signal and the silver aggregates were less stable.[66] The peaks found in the SERS spectra of the green tea in this work were 730, 965, 1010, 1117, 1235, 1313, 1348, 1465 and 1605 cm^{-1}.[66] SERS proved to be useful to analyse these plant materials including green tea because the presence of the colloids quenches the strong fluorescence that would be produced if normal Raman was performed on the pure material of these plant samples.[66]

Zareef *et al.* used SERS coupled with multivariate analysis to analyze caffeine from black tea.[67] Gold nanoparticles were used for SERS substrates and caffeine exhibited several SERS characteristic peaks after adsorption on the nanoparticles owing to electromagnetic enhancement while excited by 785 nm laser excitation.[67] Buyukgoz *et al*. used SERS to specify the predominant ingredient in the tea content and construct spectral fingerprints of seven tea samples.[65] PCA was used for the discrimination of each tea variety.[65] This study was performed under ordinary conditions with little sample preparation and a very short analysis time of twenty seconds.[65] The other advantages of this system include its simplicity and on-site detection ability.[65] Buyukgoz *et al*. used silver colloids as their SERS substrate and when combined with tea samples, this provided a characteristic spectrum of tea varieties and an optimized signal enhancement.[65] The authors were able to provide some vibrational mode assignments for green tea, such as a specific band at 482 cm^{-1} which was identified as a C=O out of plane bending mode, specific to green tea.[65] A second band at 487 cm^{-1} was reported to most likely arise from C–C–O deformations.[65]

Chapter 3: Theory

3.1 Liquid Chromatography

Liquid chromatography is a common and powerful separation technique in which the analyte is distributed between a stationary and mobile phase in the chromatographic column.[68] The stationary phase is made of solid, porous, or surface-active materials in small-particle form or a thin film of liquid coated on a solid support or a column wall.[68] Depending on the type of chromatography, the mobile phase is typically a gas (gas chromatography, GC) or a liquid (liquid chromatography, LC), transporting the analyte through the column. For this thesis work, high performance liquid chromatography (HPLC) is used, thus, the mobile phase is a liquid. HPLC is the most versatile and extensively used type of chromatography.[69] The objective of this separation technique is to entirely separate the majority of the components in a sample in the shortest amount of time.[70] To accomplish this objective, different chromatographic parameters can be adjusted, including many parameters of the column, as well as the composition and flow rate of the mobile phase.

Figure 3.1 is a theoretical chromatogram to help explain chromatographic concepts. In this example, the sample is injected onto the chromatograph at zero seconds, and the unretained species will elute at a retention time of t_0, which provides the flow rate of the mobile phase. Components A and B interact with the column differently and, thus, elute at different times, called retention times (t_R). The width of each peak (w) is obtained by drawing tangents to the sides of the Gaussian peak at the inflection points and extrapolating the tangents to intercept the baseline as shown in Figure 3.1.[70] Retention time and peak width can be used to derive other parameters such as the column resolution and number of theoretical plates. Column resolution and number of theoretical

plates are used to determine the quality of the column. In addition, retention time and peak area are valuable for determining the identity and concentration of an analyte, respectively.

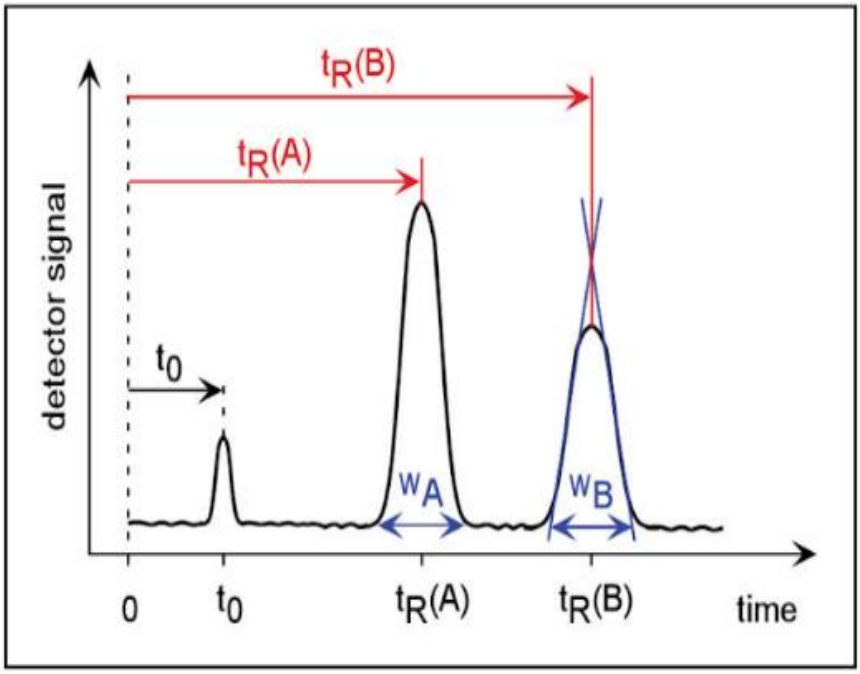

Figure 3.1: Chromatogram illustrating retention time (t_R) and peak width (w). Image reproduced with permission from Manz *et al.* 2015.[70]

A few of the most important concepts in chromatography include the retention factor (*k*), the selectivity factor (α), and band broadening. The retention factor compares the migration rates of solutes through the column which can be defined by Equation 3.1. If *k* is less than 1, the solute moves very fast through the column, and therefore it is hard to determine the correct retention time for that compound.[70]

$$k_A = \frac{t_R - t_M}{t_0} = \frac{t_s}{t_0} \qquad (3.1)$$

The selectivity factor provides a measure of how well the column will separate two different solutes, A and B, and is a ratio of their retention factors as shown in Equation 3.2.

$$\alpha = \frac{k_B}{k_A} \qquad (3.2)$$

A chromatographic separation is strongly affected by band broadening.[69] The slower the rate of mass-transfer processes between the mobile and stationary phases as a solute migrates through the column, the broader the peak for that solute.[69] If the amount of band broadening is significant, this could lead to peak overlap, known as coelution, and the resolution will be reduced. Some of the various ways of reducing band broadening include selecting well packed, short, and narrow columns (< 0.12 mm inner diameter is ideal), using smaller size stationary phase particles, heating the column, and lastly using higher or possibly lower flow rates of the mobile phase (depending on which term is being reduced i.e., longitudinal diffusion or mass transfer).[71]

One way to determine column efficiency is using plate theory which includes the column length (L), plate height (H or HETP, height equivalent to theoretical plate), or theoretical number of plates (N). The larger the number of plates and the smaller the plate height, the greater the column efficiency.[69,70] However, plate theory does not accurately account for band broadening because it assumes there is an equilibrium continuously established between both the stationary and mobile phases with the analyte throughout the separation.[69] Rate theory considers band broadening more precisely. The van Deemter equation for high velocities in packed columns outlines three parameters that influence band broadening as shown in Equation 3.3:

$$H = A + \frac{B}{u} + C\mu \qquad (3.3)$$

A is the Eddy diffusion term, which describes the influence of column packing on band broadening.[69] Eddy diffusion is constant for a given column and is independent of solvent velocity, u.[69] The longitudinal diffusion term, $\frac{B}{u}$, explains analyte movement from an area of high concentration to low concentration. Lastly, the third term, Cu, describes the resistance to mass transfer between the stationary phase and mobile phase since it takes time for a solute to establish

an equilibrium between the stationary and mobile phase.[69] By plotting the theoretical plate height as a function of mobile phase flow rate (u), one can determine the optimum flow rate for a chromatographic separation as demonstrated in Figure 3.2.[69]

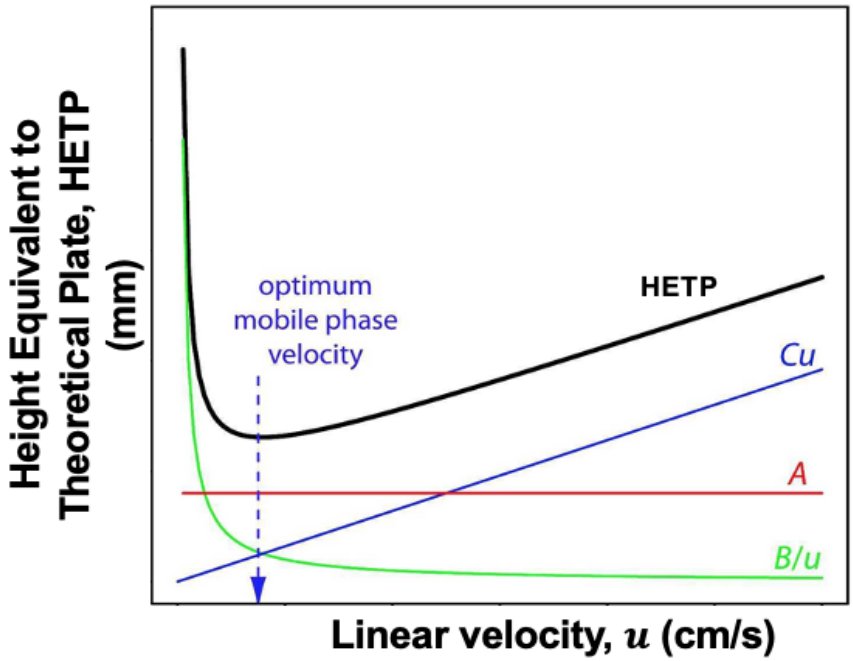

Figure 3.2: A van Deemter plot for the determination of optimum chromatographic flow rate (u). Adapted from reference [68].

3.2 Multidimensional Liquid Chromatography (2D-LC)

Multidimensional liquid chromatography was introduced to overcome the limitations of HPLC when analyzing samples that demand higher separation power. The limitations that arise in HPLC result from complex samples that contain compounds that are challenging to separate.[72,73] Examples of these highly complex samples include biological cells, blood, urine, and environmental samples.[3] These samples are too complex to be sufficiently separated in one dimension such as in a traditional HPLC experiment and coelution often occurs.[3] Multidimensional chromatography is a valuable separation technique in these circumstances because of the increased peak capacity and consequently, superior separation power.[3] 2D-LC contains two separations as

shown in Figure 3.3, therefore, the instrumentation and processing becomes much more sophisticated, expensive, time consuming and requires additional training and knowledge.[3]

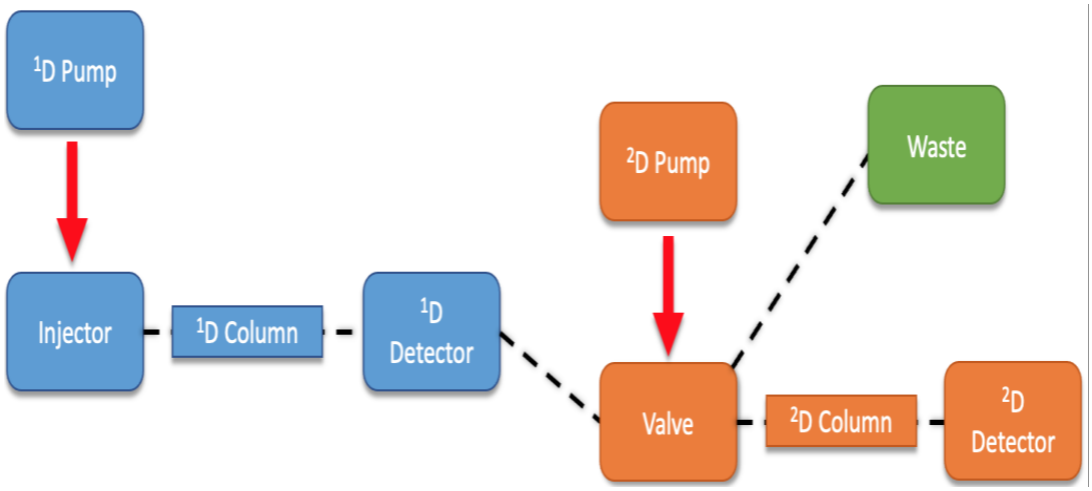

Figure 3.3: Box diagram of a 2D-LC system. Adapted from reference [2].

There are two main modes that can be chosen for the second-dimension (^{2}D) which are comprehensive mode and heart-cutting mode.[3] In comprehensive two-dimensional liquid chromatography (LCXLC), all the eluent from the first-dimension (^{1}D) column is transferred online onto the ^{2}D column.[3] For heart-cutting 2D-LC (LC-LC), only selected fractions of the ^{1}D peaks are transferred onto the ^{2}D column for additional separation.[3] Figure 3.4 is a schematic diagram of the comprehensive and heart-cutting 2D-LC. LC-LC is usually less complicated and has lower operation costs when compared to LCXLC. Furthermore, multiple heart cuts can be examined if there is no significant time limit of the ^{2}D analysis and a sampling loop is present.[3] Additionally, the second-dimension run-time can be longer, resulting in improved resolution. Comprehensive 2D-LC occasionally takes longer than 1D-LC separations, with analysis times typically ranging from thirty minutes to several hours.[74] There have been several sub modes created such as selective two-dimensional chromatography (sLCXLC) and multiple heart-cutting 2D-LC (mLC-LC). Multiple heart-cutting 2D-LC is different from LC-LC because fractions of

several [1]D peaks are transferred one at a time to the second-dimension for [2]D analysis after being stored in a sample loop.[3] For this research thesis project, multiple heart-cutting 2D-LC was used.

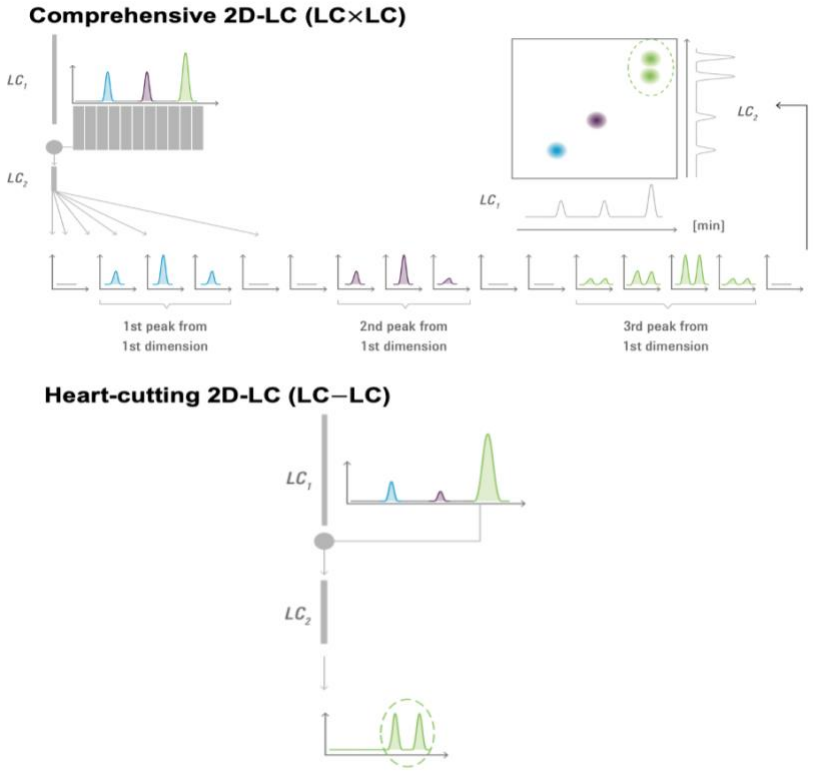

Figure 3.4: Schematic diagram of the comprehensive (LCXLC) and heart-cutting (LC-LC) modes in 2D-LC. Image reproduced with permission from Carr *et al*. 2015.[3]

The heart of the 2D-LC is the [2]D switching valve which is very sophisticated as shown in Figure 3.5. The desired [1]D effluent(s) (also known as cuts) is/are captured and stored in a sample loop within the valve until being transferred onto the [2]D column for further separation. In Figure 3.5, the blue line indicates the tubing that connects the [1]D column to the valve and then to waste, and the red line represents the tubing connecting the [2]D pump to the valve and then onto the [2]D column. Between ports 4 and 5 there is a sample loop present, where the [1]D effluent is stored until being transferred onto the [2]D column. Multiple heart-cutting separations contain many sample loops for temporary storage of desired cuts. The 2D-LC used for this thesis research is equipped with two decks containing five sample loops each. The top valve image of Figure 3.5 illustrates

the position that allows for the storage of ^{1}D effluent in the loop. The bottom image displays the valve position for the effluent to be transferred to the ^{2}D column.

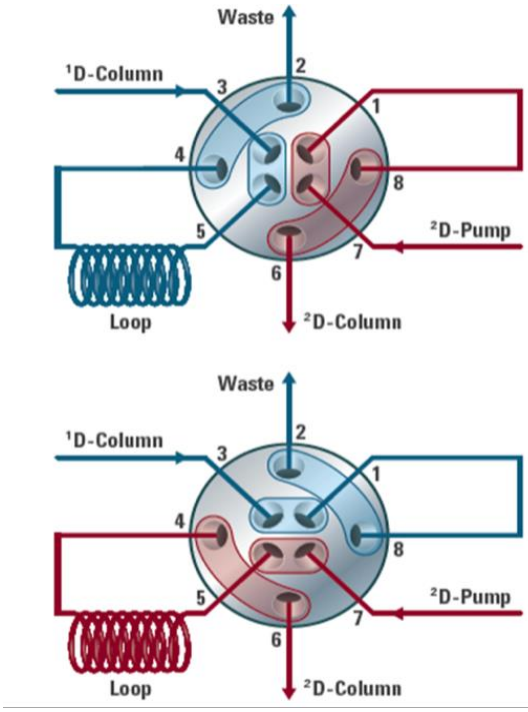

Figure 3.5: Configurations of an 8-port/2-position valve needed for LC-LC separation. Image reproduced with permission from Carr *et al*. 2015.[3]

The real power of multidimensional chromatography is the increase in peak capacity that the second-dimension provides without significantly increasing analysis time.[3] Peak capacity (n_c) is a theoretical concept that estimates the maximum number of peaks that can be resolved in the separation window, which is the time difference between the first and last eluting peak.[3,72] Therefore, it is suitable to choose peak capacity as the measure of resolving power in chromatography. The peak capacity is limited for 1D-LC when separating very complex samples containing hundreds of compounds.[3] 2D-LC can achieve peak capacities of over one thousand.[3] In contrast, the maximum peak capacity accomplished by 1D-LC is a few hundred depending on the analysis.[72,74] Figure 3.6 helps to illustrate the difference in peak capacities of 1D-LC and 2D-LC.

The product rule is used to measure the resolving power of each of the two dimensions. Equation 3.4 highlights how peak capacity is calculated for 2D-LC:

$$n_{c,tot} = {}^{1}n_c \; x \; {}^{2}n_c \qquad (3.4)$$

The total peak capacity obtained for a 2D-LC system ($n_{c,tot}$) is the product of the peak capacity achieved in the first ($^{1}n_c$) and second ($^{2}n_c$) dimension. If $^{1}n_c$ were fifty and $^{2}n_c$ were twenty, then $n_{c,tot}$ for a 2D-LC system would be one thousand. However, it must be understood that the product rule only provides an estimate of the theoretical maximum peak capacity and applies only under certain ideal conditions.[3] First, the retention of the sample must be controlled by two or more different (orthogonal) physicochemical properties.[3] Second, the separated compounds must be spread across the entire two dimensional separation space.[3] Lastly, when the compounds are separated in the first-dimension, there must be no remixing, which adds to peak broadening.[3] Of particular significance, the peak capacity found in 2D-LC is greatly superior than when tandem columns are used, as in offline LC-LC, which at best only results in the addition of the peak capacities of the two columns.[3]

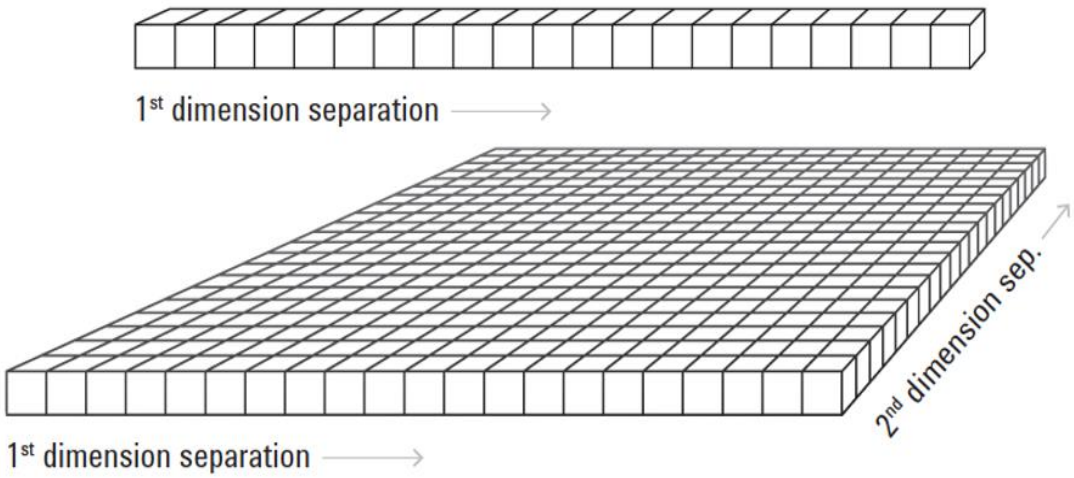

Figure 3.6: Schematic illustrations of peak capacity in 1D-LC and 2D-LC systems. Image reproduced with permission from Carr *et al*. 2015.[3]

Orthogonality is an important concept to understand when seeking to optimize separations using 2D-LC.[2] To achieve the best 2D-LC separation, the second-dimension separation conditions should be as different from the first-dimension as possible. Completely different separation conditions for the two dimensions will result in complete orthogonality, as shown in Figure 3.7(a).[75] An example of a 2D-LC system that would provide complete orthogonality would be using either normal phase (NP-LC) or reverse phase (RP-LC) liquid chromatography in the first-dimension followed by the other for the second-dimension.[3] However, this combination is difficult to realize because of solvent miscibility issues for the mobile phases between the two dimensions, which could result in emulsion formation. Another example would be size exclusion chromatography (SEC) used in the first-dimension and RP-LC in the second-dimension.[3] Figure 3.7(f) is the poorest example of orthogonality suggesting that both dimensions in the separation are highly complementary and lead to coelution in both dimensions, rendering the ^{2}D separation unnecessary.[75] Figure 3.7(b) to (e) demonstrate various ways orthogonality is affected in a 2D-LC separation and provides non-desirable separations.[75] Figure 3.7(b) displays excessive interactions between the analyte and stationary phase in the second-dimension.[75] Figure 3.7(c) demonstrates low interaction between the analyte and the stationary phase in the second-dimension.[75] Figures 3.7(d) and (e) display poor choice of the first-dimension column, therefore affecting the orthogonality and offering an unsuccessful 2D-LC separation.[75] Figure 3.7(a) a is an example of complete orthogonality in separation, which is ideal but rarely obtained experimentally.

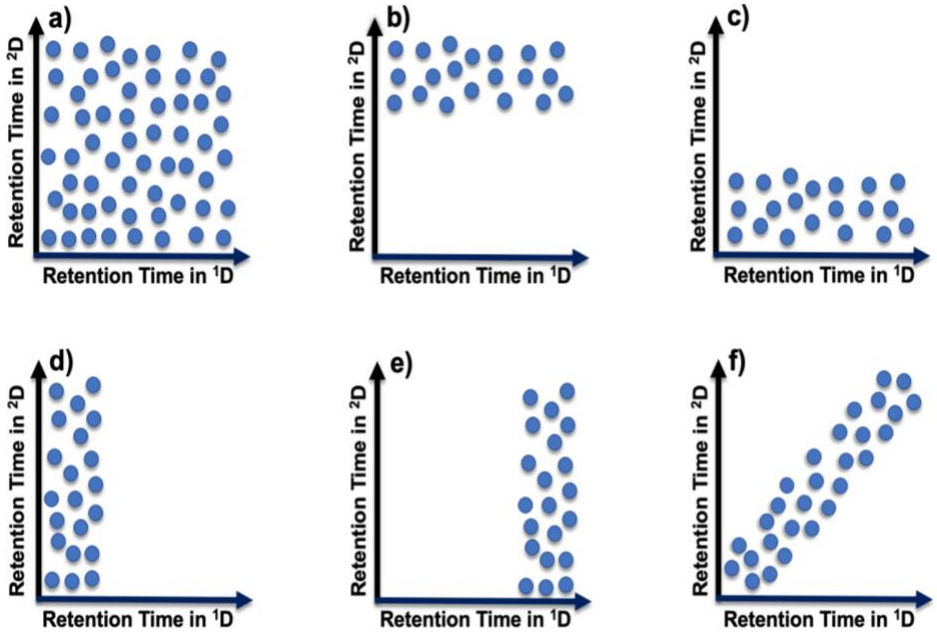

Figure 3.7: Schematic diagram exhibiting various levels of orthogonality in 2D-LC. Adapted from reference [75].

It was mentioned that to obtain the best orthogonality, one would want to choose separations that are uncorrelated to one another such as NP-LCXRP-LC. However, Carr *et al.* discovered when they scored several different combinations based on a variety of important operational characteristics including orthogonality, NP-LCXRP-LC did not score the highest as shown in Table 3.1.[3] RP-LCXRP-LC was the combination that scored the highest with orthogonality being its lowest score. For this project, reverse phase chromatography was chosen for both dimensions (RP-LCXRP-LC) since it is rated well for other 2D-LC chromatographic metrics, such as applicability and solvent compatibility.[3]

Mode	IECxRP [45]	SECxRP [46]	NPxRP [47]	RPxRP [2]	HILICxRP [48]	HILICxHILIC [43]	ACxRP [49]	SECxNP [50]	SECxIEC [7]	LCCCxRP [51]
Orthogonality	++	++	++	+	+	-	++	+	+	++
Peak capacity	+	+	+	++	+	+	-	-	--	+
Peak capacity/ time	-	--	+	++	+	+	-	--	--	+
Solvent compatibility	+	+	--	++	+	++	+	+	+	-
Applicability	+	+	-	++	+	-	+	-	-	-
Score	4	3	1	9	5	2	2	-2	-3	2

Table 3.1: Comparison of different combinations of 2D-LC separations. Image reproduced with permission from Carr *et al*. 2015.[3]

It is very important to utilize as much of the 2D space as possible to capitalize on the potential benefit of the product rule. Nevertheless, when using highly complementary modes such as RP-LCXRP-LC, substantial portions of the 2D space are unoccupied as indicated by the two triangles labeled A and B in Figure 3.8a) when the full gradient is used. Full gradient covers a wide range of mobile phase compositions in a very short amount of time, and is programmed to be the same during the whole ^{2}D run.[76] However, when shift-gradient is introduced in the comprehensive 2D-LC system, the 2D space is further utilized as displayed in Figure 3.8b). Shift-gradient uses a narrower range of mobile phase composition and continuously varies the concentration range according to retention time as shown in Figure 3.9d).[76] Shift-gradient is a mixture of full and parallel gradient.[76] Full gradient covers a wide range of mobile-phase compositions in a very short time. The second-dimension gradient program is the same during the whole run-time. Whereas parallel gradient uses a program independent of the second-dimension run-time. Parallel gradient is a quasi-isocratic elution, however, offers a much shallower gradient in the second-dimension. Subsequently, to optimize the second-dimension of the 2D-LC method in this thesis, shift-gradient was explored.

the gradient covers a wide range of mobile-phase compositions in a very short time. The second-dimension gradient program is the same during the whole run.

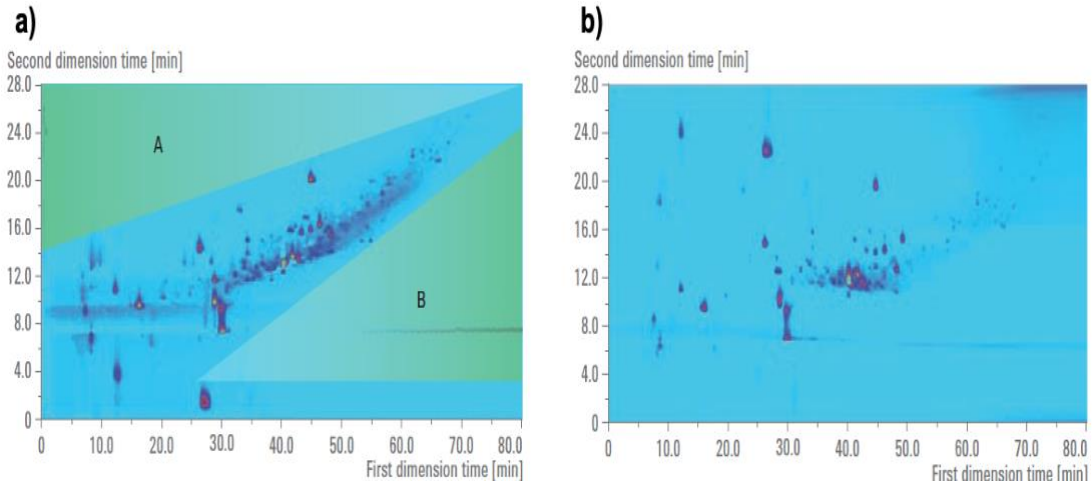

Figure 3.8: Comprehensive 2D-LC separation of a traditional Chinese medicine extract (a) using full gradient and (b) using shift gradient in the ^{2}D. A and B indicate unused 2D separation space Image reproduced with permission from Carr *et al.* 2015.[3]

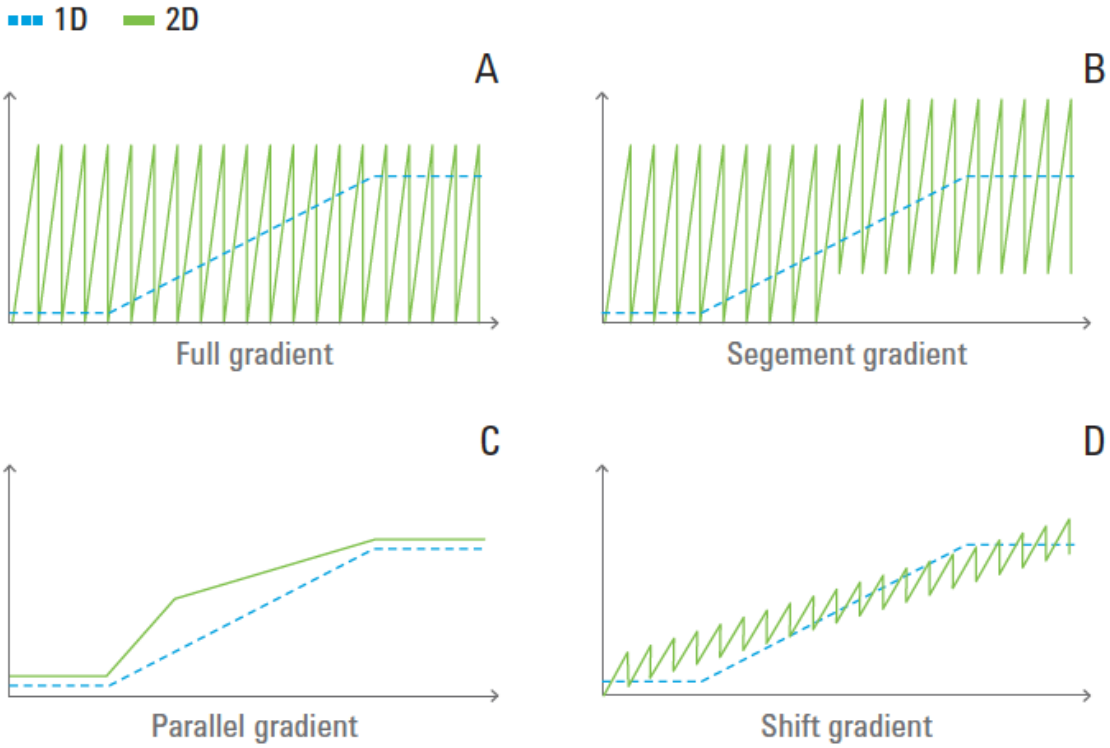

Figure 3.9: Different types of gradient programs used in the first- and second-dimension of a 2D-LC separation. Image reproduced with permission from Carr *et al.* 2015.[3]

3.3 Raman Spectroscopy

Raman spectroscopy is a vibrational spectroscopic technique defined by the interaction between a molecular species and incident photons of monochromatic light. Raman scattering was discovered in 1928 by Sir Chandrasekhara Venkata Raman, assisted by his student Kariamanikkam Srinivasa Krishman.[77,78] When a monochromatic beam of light impinges onto a sample, much of the light passes through the sample unchanged or can be absorbed.[78] Additionally, when light is interacting with the sample, the incident photons can be scattered either elastically or inelastically.[79] The light source has the ability to disturb the electron cloud of a sample which can be determined from the electron cloud polarizability.[77] The electron cloud in a chemical bond can oscillate due to electromagnetic radiation and cause light to be emitted, also called scattering. The energy of the incident light used to oscillate the electron cloud is completely given back in the emitted light.

About 0.1% of the incident light is elastically scattered, meaning that the energy of the incident photon does not change after collision with a molecule of the sample and the scattered photons have the same frequency and wavelength as the incident photon, otherwise known as Rayleigh scattering.[77,78,80] Rayleigh scattering does not offer any vibrational information about the molecule since there is no net gain or loss of energy.[81,82] An even smaller fraction of the incident light, about 1 in a million photons, will be scattered inelastically, otherwise known as Raman scattering.[78,83] Particularly, Raman spectroscopy is centered on inelastic scattering of incident monochromatic light. There are two types of Raman scattering referred to as Stokes and anti-Stokes scattering. Stokes scattering provides useful vibrational information about the analyte molecule.[81,82] Stokes scattering occurs when energy is transferred via the incident photons to the molecule in the ground state which is then excited to a virtual energy state. A virtual energy state represents simply the

distortion of the electron distribution of a covalent bond and is not a stationary energy state.[79] After the molecule is excited, it will relax back to a vibrational state that is higher than the ground state and the scattered photons will have lower frequencies, and therefore, a longer wavelength, than the initial photon.[78] On the contrary, anti-Stokes scattering occurs if energy is transferred to the molecule which is initially at an excited vibrational state, and then reaches a virtual energy state and proceeds to relax back to the ground state. In this case, the scattered photons have higher frequencies and shorter wavelengths than the incident photon.[78] Stokes scattering occurs more frequently than anti-Stokes scattering because most molecules are excited to a virtual state from the ground state, rather than from a vibrational state and hence, Stokes scattering is typically what is measured in Raman spectroscopy.[84] The energy diagrams of Rayleigh, Stokes, and anti-Stokes scattering are shown in Figure 3.10.

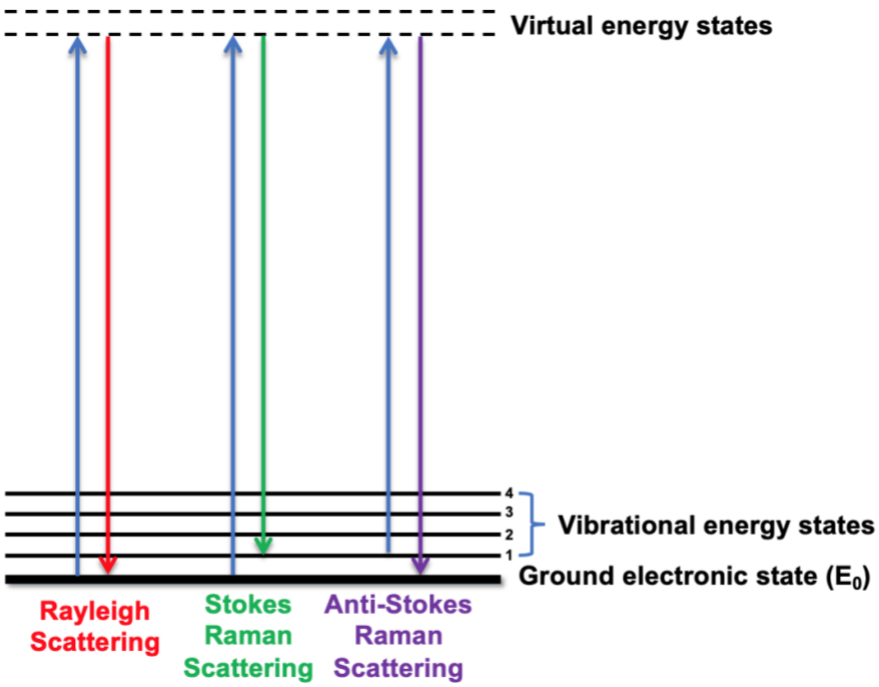

Figure 3.10: Energy level diagrams for Rayleigh, Stokes, and anti-Stokes scattering. Adapted from reference [81].

The intensity of the Raman scattering is not comparable in all directions; consequently, a certain angle should be present between the incident light source and the detector.[79] Effective

Raman scattering can be obtained at 90° (right angle scattering) or 180° (backscattering).[79] Most modern systems employ a backscattering set-up, although initially 90° was used.[78] Figure 3.11 depicts the basic components of a Raman spectrometer with a backscattering set-up.

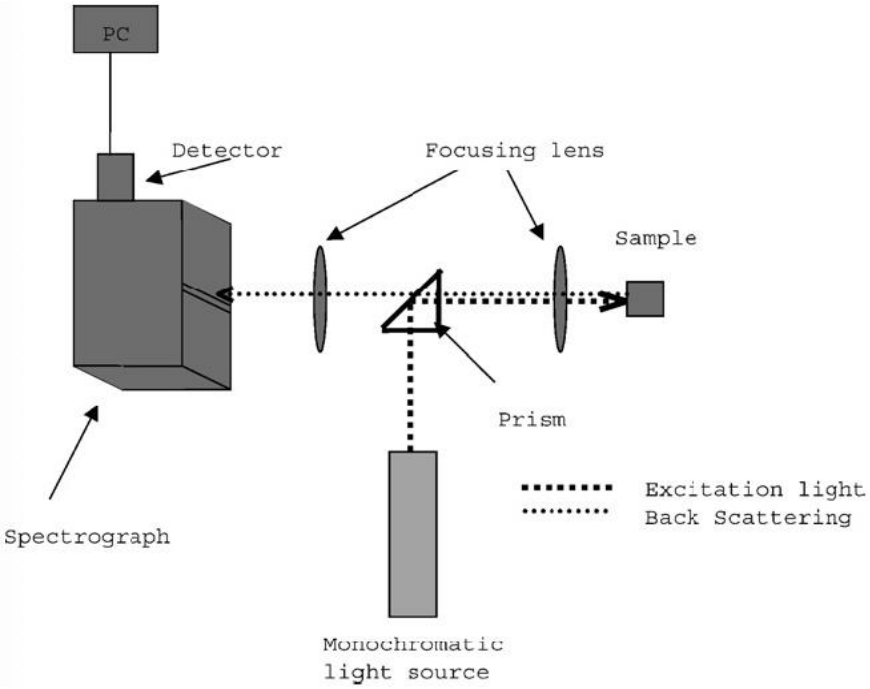

Figure 3.11: A Raman spectrometer with is basic components with backscattering geometry. Image reproduced with permission from Browne *et al.* 2007.[78]

The differences in energy between the incident photons and inelastically scattered photons correspond to vibrational frequencies of the scattering molecule and the intensity is proportional to the fourth power of the scattered radiation i.e. $(\bar{\upsilon} - \bar{\upsilon}_m)^4$ (Stokes) or $(\bar{\upsilon} + \bar{\upsilon}_m)^4$ (anti-Stokes).[78] Raman spectra are plots of Raman scattered intensity as a function of the energy difference between the incident and scattered photons, known as the Raman shift.[77,78] Raman shift is expressed in units of cm^{-1}, which is the inverse of wavelength ($\bar{\upsilon} = 1/\lambda$).[77] The relationship between wavenumbers and wavelength can be understood by Equation 3.5 where h is Planck's constant, v is frequency of light, c is the speed of light, λ is wavelength of light and $\bar{\upsilon}$ is the wavenumber of light.

$$E = h\nu = \frac{hc}{\lambda} = hc\bar{\upsilon} \qquad (3.5)$$

Raman peaks are spectrally narrow, and in many cases can be uniquely associated with the vibration of a particular chemical bond or a single functional group in the molecule.[77] Raman peaks are a result of the photon interacting with the molecular electron cloud, and consequently, causing a temporary change of the polarizability within the molecule, resulting in an induced dipole moment.[81] As shown in Figure 3.12, when a molecule is present in an electric field, there is a disturbance of the electron cloud such that the nuclei and electrons are attracted to opposite poles, becoming polarized, resulting in an induced electric dipole moment (μ).[78]

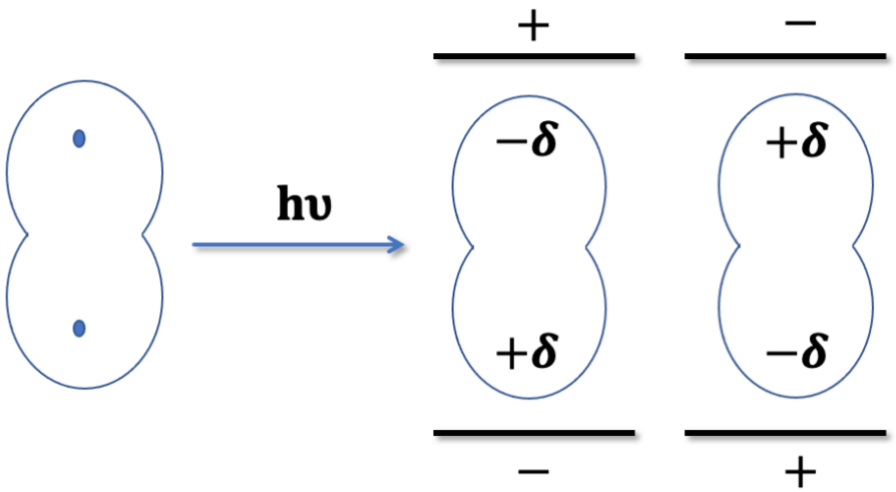

Figure 3.12: Polarization of a diatomic molecule in an electric field. Adapted from reference [81].

The size of the dipole moment produced by the incident electromagnetic field (E) is determined by the polarizability (α) of the molecule, as shown in Equation 3.6:

$$\mu = \alpha E \qquad (3.6)$$

The equation above is not representative for actual molecules because both the induced dipole moment and electric field are vectors and consist of three components in x, y, and z directions. For example, an electric field in the x direction not only induces a dipole in the x direction but also the

y and x directions.[82] Therefore, this is represented by making α a tensor, recognized as the polarizability tensor, as shown in Equation 3.7:

$$\begin{bmatrix}\mu_x\\ \mu_y\\ \mu_z\end{bmatrix} = \begin{bmatrix}\alpha_{xx} & \alpha_{xy} & \alpha_{xz}\\ \alpha_{yx} & \alpha_{yy} & \alpha_{yz}\\ \alpha_{zx} & \alpha_{zy} & \alpha_{zz}\end{bmatrix}\begin{bmatrix}E_z\\ E_y\\ E_z\end{bmatrix} \quad (3.7)$$

The main criterion for a molecule to have an allowed Raman vibrational mode is that any of the six components of the polarizability tensor change during the vibration or rotation, and that during that change, one or more of the quantities must not be zero.[82,85] Raman selection rules specify what types of vibrational transitions are allowed.[79] The selection rule is not exclusive to Raman spectroscopy; it can be applied to other spectroscopic techniques such as infrared spectroscopy (IR).[81]

Raman spectroscopy has many advantages as a vibrational spectroscopic technique. For example, water molecules are weak scatterers which is very advantageous when investigating biological samples prepared in aqueous solutions because water does not interfere much.[40] For IR spectroscopy, the strong absorption of infrared radiation by water is a common interference and can make analysis in aqueous samples challenging. Additionally, carbon dioxide, glass, and alcohols are also weak Raman scatterers. The diameter of the laser beam is typically less than 100 μm when focused onto the sample, which allows for small sample requirement.[40] Other advantages involve the ease of attaining a Raman spectrum, minimal sample preparation required, non-destructive nature, rapid analysis time, and Raman spectroscopy can be portable since hand-held instrumentation is widely available.[40,77,86] However, there are several disadvantages of Raman spectroscopy including the necessary requirement of a powerful laser source that can cause photodecomposition of the sample, however, lowering the laser power and/or acquisition time can generally resolve this issue.[81] Fluorescence can occur for some compounds when illuminated by

the energetic laser beam, resulting in a significant background that swamps the much weaker Raman signal, and no real information about the analyte can be gained.[79] This issue is often solved by using a less energetic excitation wavelength, for example in the near-IR. The main disadvantage of Raman spectroscopy is the inherent weakness of Raman Stokes scattering since only a minute amount of the light is inelastically scattered.[87] Consequently, only bulk solids, liquids, or gases exhibit useful normal Raman spectra. A variant of Raman spectroscopy that has been established which does not experience some of these disadvantages is called surface-enhanced Raman spectroscopy (SERS).

3.4 Surface-Enhanced Raman Spectroscopy (SERS)

In 1974, Martin Fleischmann *et al.* reported that pyridine and other molecules displayed an enhancement of their Raman signal when adsorbed onto an electrochemically roughened silver electrode.[34,88] Richard P. Van Duyne and David L. Jeanmarie subsequently explored several factors that can affect the Raman signal intensity, including surface roughness, effect of applied potential, solution analyte concentration, and electrolyte composition of the solution.[35] Van Duyne, Jeanmaire, Albrecht and Creighton simultaneously revealed that molecules present on the surface of a nanostructured coinage metal surface can exhibit an extraordinary enhancement of their Raman signal.[89,90] This phenomenon was established as surface-enhanced Raman spectroscopy (SERS). SERS is a very sensitive and selective technique, increasing the Raman signal by four to eleven orders of magnitude.[88,91] There are two mechanisms that are responsible for this enhancement, referred to as the chemical mechanism (CM) and the electromagnetic mechanism (EM).[91,92] These mechanisms result from the intensity of Raman scattering being directly proportional to the square of the induced dipole moment (μ).[92] The chemical mechanism of

enhancement is understood to be the minor contributor to the overall SERS enhancement, while the electromagnetic mechanism of enhancement is the main contributor.[91,92]

Chemical enhancement involves charge transfer mechanisms through the chemisorption of the molecule to the surface of the metal, allowing the electrons from the molecule to interact with the electrons from the metal surface and vice-versa.[88,91,92] The chemical enhancement occurs when the excitation wavelength is resonant with the metal-molecule charge transfer electronic states.[88] This mechanism contributes up to two to three orders of magnitude of the observed enhancement of the SERS signal and in order to achieve this enhancement the molecules should be directly adsorbed onto the metal surface.[38,88,91,93] The magnitude of the chemical enhancement is different based on the substrates and analyte involved as well as substrate adsorption sites.[91]

The electromagnetic enhancement arises from the amplification of the light by the excitation of localized surface plasmon resonances (LSPRs), and is therefore a wavelength-dependent effect.[88,92,94] This type of mechanism contributes up to five to eight orders of magnitude of the Raman signal enhancement.[92,94,95] LSPR primarily occurs in nanostructures that are smaller in all dimensions than the incident wavelength, such as a nanosphere, which will cause the conduction electrons in the metal to collectively oscillate in resonance with the oscillating electric field, as presented in Figure 3.13.[36,38,88,92,96,97] LSPR is reliant on many aspects of the nanostructure such as the size, shape, nanometric roughness, and the material used.[38]

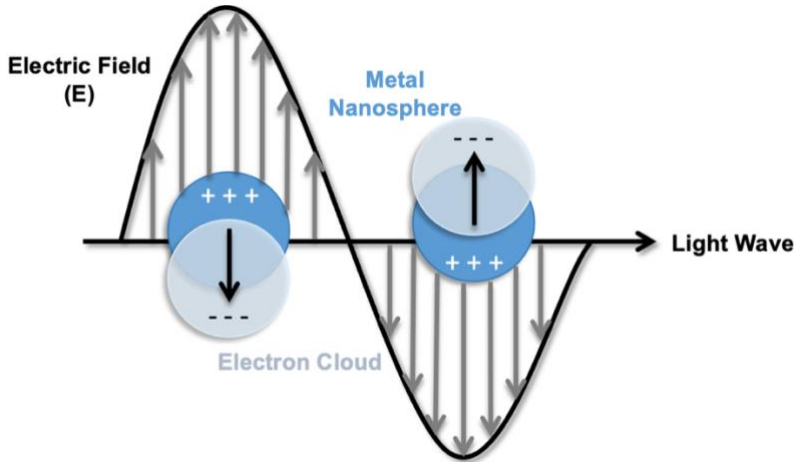

Figure 3.13: Illustration of the localized surface plasmon resonance effect. Adapted from reference [92].

Unlike with the former mechanism, the electromagnetic mechanism does not require the molecule to be in direct contact with the metal surface.[91] However, the molecule does have to be in close proximity to experience the enhancement since studies have shown that the electromagnetic enhancement reduces dramatically as the distance between the molecule and metal surface increases.[91,92] Therefore, the ideal distance for SERS detection is within four nanometers from the surface.[91]

In some cases, SERS studies of analytes of biological origin are facilitated when molecules containing a thiol or amine group are able to chemisorb onto the roughened metal SERS substrate, thereby achieving maximum SERS intensity.[91] Additionally, the SERS intensity can change depending on the orientation of the analyte and the tensor symmetry with respect to the metal surface.[91] Moskovits developed surface selection rules that consider the polarizations and correlation of a molecule and its effect on the SERS intensity.[98] This work determined that the local field polarizations should be perpendicular to the metal substrate to achieve the maximum SERS intensity because the electric field of the incident light is enhanced in the direction of the surface normal.[99,100] In contrast, when the local field polarizations are parallel to the metal surface, the SERS intensity is attenuated.

Crucial aspects to consider regarding SERS enhancement is choosing the appropriate nanoscale metal substrate and its optimal size and shape. Nanoparticles (NPs) have been used in a variety of different fields such as nanotechnology, biology, chemistry, physics, material science, medicine, computer science, and engineering.[101] Different metals such as aluminium, gold, silver, copper, palladium, and platinum have been used for different applications depending on their plasmonic properties.[95] The most used metals for SERS are gold and silver because of their optimal plasmonic properties in the visible region, their relative inertness, and ease of production of various nanostructures with controllable size and shape.[95] Gold NPs (AuNPs) are very stable, are biocompatible and have distinct optical properties. However, they are fairly expensive to produce and interband interference limits their plasmonic application to excitation wavelengths longer than 600 nm.[95] Silver NPs (AgNPs) offer many advantages over gold and other metals such as providing a strong surface plasmon at wavelengths between 300-1200 nm, high electrical and thermal conductivity, and they are relatively cheap to produce.[95] However, AgNPs have biocompatibility issues and can be prone to oxidation.[95]

The ability of a metal nanoparticle to support surface plasmons is dependent on its complex dielectric function ε, which includes a real component (ε_r) and an imaginary component (ε_i), both of which vary with excitation wavelength, λ.[95] The dielectric function of a material reflects the unique interaction between its electrons and incident light. Mie theory is used to describe LSPR in SERS and for calculating the absorption and scattering (known as extinction) cross section (C_{ext}) of a metal nanosphere:

$$C_{ext} = \frac{24\pi^2 R^3 \varepsilon_m^{3/2}}{\lambda} \left[\frac{\varepsilon_i}{(\varepsilon_r + 2\varepsilon_m)^2 + \varepsilon_i^2}\right] \quad (3.8)$$

where R is the radius, and ε_m is the relative dielectric constant of the medium surrounding the nanosphere.[95] The interaction between a metal nanoparticle and light depends strongly on ε_r and ε_i. Figure 3.14 demonstrates ε_r and ε_i for silver, gold, and silicon.[95] Silicon has large positive values for ε_r, unlike for gold and silver. Additionally, Equation 3.8 indicates that ε_i should be close to zero to support a strong resonance, a condition that only silver is able to meet between 300 and 600 nm as shown in Figure 3.14.[95]

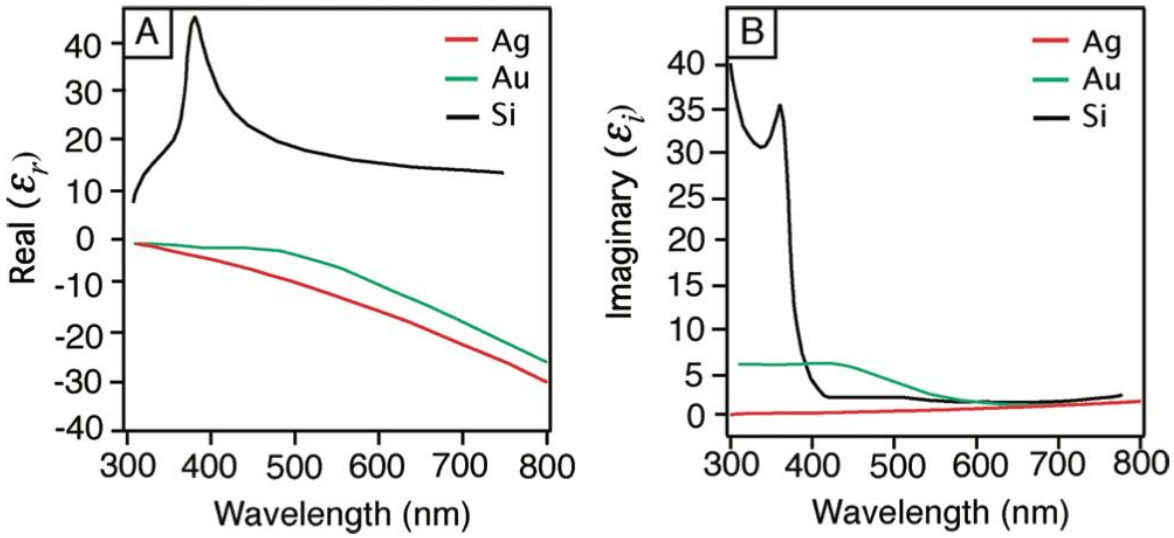

Figure 3.14: Plot of: A the real, ε_r, and B, the imaginary, ε_i, components of the complex dielectric function of Ag, Au, and Si as a function of wavelength. Image reproduced with permission from Rycenga *et al.* 2011.[95]

Many methods have been established to prepare different shapes of nanoparticles such as spheres, cubes, triangles, rods, and hollow structures.[102,103] However, these methods might not provide optimal SERS-active nanostructures due to the requirement of various capping agents and these structures may also not be stable over time. In this research, spherical AgNPs were used for all experiments. The first SERS experiment performed on spherical AgNPs was conducted by Creighton in 1979.[102] One of the simplest procedures for spherical AgNPs synthesis that does not require a large amount laboratory reagents or equipment is the citrate reduction method reported by Lee and Meisel in 1982.[104] This chemical reduction method involves the use of citrate to reduce

Ag^+ to metallic Ag colloids.[104,105] However, this bottom-up synthesis provides a polydisperse sample with a variety of colloidal sizes ranging between 20-600 nm with reasonably poor shape control. Consequently, seed-mediated growth strategies can be used to produce more monodisperse nanoparticles.[95] The seed-mediated growth used in this thesis work was a modified Lee and Meisel method which proved to provide nanoparticles that were more uniform in size and shape than the standard Lee and Meisel method.[106]

The AgNPs used in this work are lyophobic colloids which are thermodynamically unstable, meaning that these colloidal particles have low affinity towards the dispersion medium (in this case water), and will eventually coagulate.[107] Lyophobic colloidal dispersion stability can be explained by DLVO theory, named for the four scientists who developed it, Boris Derjaguin, Lev Landau, Evert Verwey and Theodoor Overbeek.[107] DLVO theory combines the interactions of attractive van der Waals forces and repulsive electric double-layer forces between colloidal particles.[107] The primary force that stabilizes lyophobic colloidal dispersions is the electrostatic repulsive force which arises due to the presence of an electric double-layer of charge on the particles.[107] The double-layer of charge consists of an inner layer of charge and a counter ion layer of charge.[107] However, the counter ions will fall off over time leading to aggregation and destabilization of the colloids.[107] In some applications such as SERS, aggregation is encouraged because interparticle junctions of nanoparticles can be created, called a "hot spot".[108,109] In a hot spot, the SERS enhancement is the highest because the electromagnetic field is amplified with the nanoparticles being so close to one another. However, the positioning of the analyte near a hot spot is important since it can provide ten times higher signal than if the hot spot is a few nm away. There are ways to destabilize these colloidal dispersions through heating, centrifuging, adjusting pH and stirring which all reduce the double-layer of charge.[107]

SERS is a very sensitive and powerful technique; in fact single molecule detection has been reported using SERS.[110] Another advantage of SERS is that the noble metal surface effectively quenches interfering fluorescence that often occurs in Raman spectroscopy, swamping the much weaker Raman signal. SERS analysis can be done very quickly and is non-destructive and has gained in popularity over the past several decades, finding application in polymer and materials science, biochemistry, biosensing, catalysis, and electrochemistry.[88]

3.5 Electrochemistry

Electrochemistry involves the analysis of chemical effects through electrical measurements conducted at the interface between an electrode and a solution. Various processes can be monitored, including oxidation-reduction reactions as well as adsorption and desorption phenomena. Current, potential, or charge are typically used to monitor the chemical effects in various systems. Electrolyte and electrodes are required to conduct electrochemical measurements. The supporting electrolyte is a solution of high ionic strength that allows current to flow and should not react with the analyte or undergo any Faradaic electron transfer processes.[111] An ideal electrolyte solution should have an ionic strength between 0.01-1.0 M using highly purified reagents.[111] Problems arise while performing electrochemistry if oxygen is present in the electrolyte solution such as a large background current created when oxygen is reduced, interfering with the measurement of the analyte. The products produced from oxygen reduction may also affect the electrochemical process under investigation. To avoid the reduction of oxygen, the supporting electrolyte is purged with an inert gas such as argon or nitrogen prior to use.[111]

The reference electrode (RE), counter electrode (CE), and working electrode (WE) are the three electrodes typically present in an electrochemical cell.[112] The RE maintains a constant potential that is not affected by the applied potential and serves as a reference for the measurement

of the cell potential. Common REs include the silver-silver chloride electrode (Ag / AgCl) and the saturated calomel electrode (Hg / Hg_2Cl_2, SCE).[111,112] The CE is made from an inert conductive material, such as a platinum or graphite, and its function is to help pass current and complete the circuit in the electrochemical cell.[113] The WE is where the reaction under investigation takes place. The material of the WE affects the electrochemistry and some characteristics such as reproducibility, cost, availability, toxicity, potential window, and electrical conductivity need to be considered beforehand.[111] Carbon is one of the most widely used WEs for many reasons, including its suitability for various types of analyses, chemical inertness, a broad potential window, a low background current and affordability.[111]

Potentiometric and potentiostatic measurements are the two distinctive types of electroanalytical techniques, measuring the electrochemical process occurring at the electrode-solution interface. The difference between the two is the type of electrical signal used for quantification. In this research, potentiostatic measurements are used which focus on the charge-transfer processes occurring at the interface between the electrolyte and electrode. When a voltage is applied, charged molecules will move and orient themselves depending on their charge. For example, a negatively charged molecule will be attracted to a positively charged electrode, enabling electron transfer or surface adsorption, both of which are ideal processes for optimized analyte detection via SERS.[114]

The electrical double-layer model is used to visualize the array of ionic species at the electrode surface. A positively charged electrode will attract a layer of negative ions, and vice-versa, resulting the formation of an electrical double-layer. Many different models have been proposed to explain the electrical double-layer at a charged interface.[114] The simplest model is the Helmholtz model. As demonstrated in Figure 3.15(a) and (b), when ions of opposite charge to the solid surface

adsorb onto the electrode, this completely neutralizes the surface of the solid. Consequently, the potential reduces to zero rapidly.[107] The Helmholtz model is unrealistic due to its disregard of thermal motion of the ions and participation of solvent molecules. Gouy-Chapman developed a model that describes a diffuse layer of ions where the charge on the surface is gradually neutralized by an excess of oppositely charged ions further away from the surface as shown in Figure 3.15(c) and (d).[107] However, the model does not treat ions as point charges.[107] For example, for conditions of high surface electrical potential (ψ_0) and ionic strength, the estimated concentration of real ions occupying volume near the surface is greater than can be accommodated in the volume available.[107] A solution to this problem with the Gouy-Chapman model is presented in the Stern model. This model proposed that the size of the ions should be considered for only the first layer of adsorbed ions, with ions further away being treated as point charges as in the previous model.[107] Therefore, the Stern model suggests two regions as displayed in Figure 3.15(e), the layer closest to the surface is called the Stern layer where ion size is important.[107] The region outside of the Stern layer is called the diffuse layer and this is where the Gouy-Chapman treatment of ions still applies.[107]

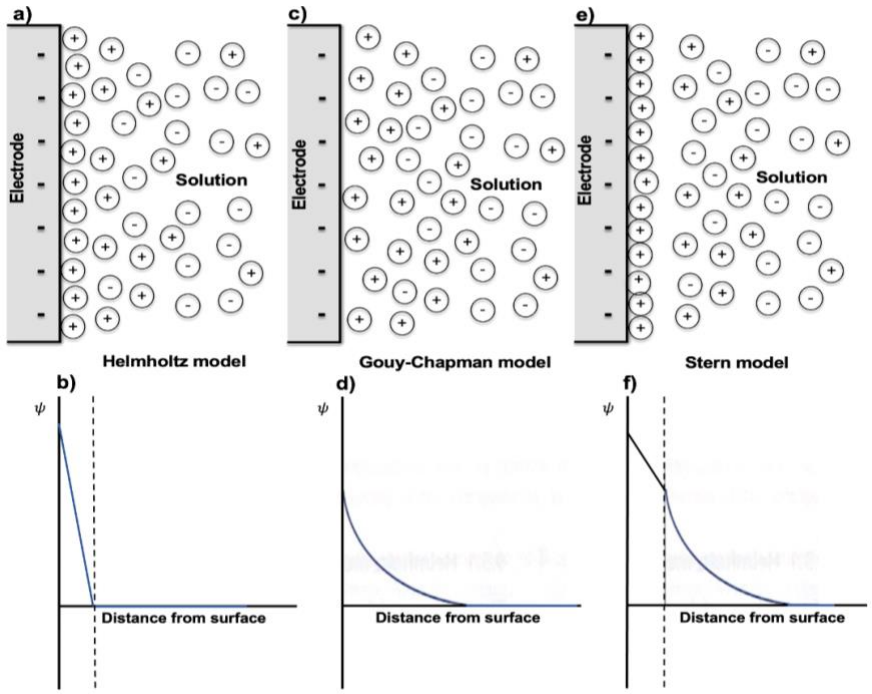

Figure 3.15: Schematics of the Helmholtz, Gouy-Chapman, and Stern models of the interface (a), (c), (e) the distribution of ions and (b), (d), (e) the graph of the electrical potential. Adapted from reference [97].

The most recent model, and the model used by most researchers in the field was described by Bockris, Devanthan, and Muller (BDM) in 1963.[115,116] The BDM model describes the specific adsorption of ions and the role of solvent at the interface, taking into consideration the interaction between the electrode and dipolar solvents.[116] The BDM model has three distinctive regions as shown in Figure 3.16. The first region is the inner layer close to the electrode surface called the inner Helmholtz plane (IHP) which contains solvent molecules and desolvated, adsorbed ions.[116] The next region is the outer Helmholtz plane (OHP) which is an imagined plane that passes through the center of solvated ions that are non-specifically adsorbed.[111,116] The last region is beyond these layers named the diffuse layer which is a three-dimensional region of diffused solvated ions and solvent molecules.[111,116] Depending on the ionic strength of the electrolyte, the thickness of the double-layer may range from 0.1 to 10 nm from the surface.[111,116]

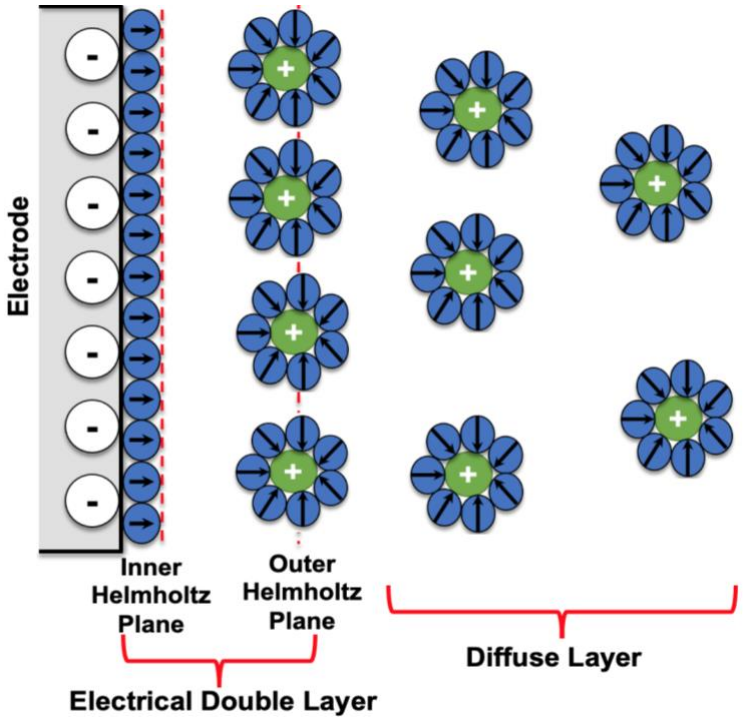

Figure 3.16: Illustration of the electrical double-layer according to Bockris / Devanthan / Mueller model. Adapted from reference [116].

The charge can be changed through altering various parameters such as the electrode potential, the charge density and polarity of the surface. The potential of zero charge (pzc) refers to the potential at which the overall surface charge density is equal to zero.[117] Negatively charged ions will interact preferentially with the surface when it is positively charged if the electrode potential is more positive than the pzc.[117] Conversely, if the electrode potential is more negative than the pzc, the surface will have weaker affinity for anions.[117]

3.6 Electrochemical Surface-Enhanced Raman Spectroscopy (EC-SERS)

SERS substrates can easily be used as electrodes in electrochemistry because they are metallic. The combination of SERS and electrochemistry is named electrochemical SERS (EC-SERS) and can detect and monitor analytes present on the metallic surface of the working electrode wherein voltage is applied and electrolyte is present.[118,119,120] Changing the applied voltage can alter the SERS signal in many ways, including through the reductive desorption of the interfering matrix

species at more negative potentials, electrostatic interactions between the metal and analyte, and potential-induced re-orientation of the analyte.[121] Additionally, the Fermi level of the metal can be changed through variation of the applied voltage resulting in an increase of charge transfer between the analyte and modified metallic surface of the working electrode, thus, enhancing the chemical enhancement.[116,121] Hence, EC-SERS is a very sensitive technique and improves the SERS intensity for various molecules.[40,122,123,124] Furthermore, through adjusting the voltage of the nanostructured working electrode, different molecules of a complex mixture can adhere to the electrode surface at different voltages, thus greatly improving the selectivity of SERS for complex analytes.[121] The selectivity that EC-SERS provides occurs because of the differences in molecular charge, shape and functional groups of each analyte.[121]

EC-SERS is one of the most complex SERS techniques because of the changes occurring on the electrode surface with the application of voltage. However, EC-SERS can provide a great deal of valuable information about the conformation, orientation, and the behaviour of analyte at the interface between the metal and electrolyte. In addition, application of a voltage to the SERS substrate often results in a further enhancement of the SERS signal of typically 1-2 orders of magnitude. EC-SERS provides many advantages such as being sensitive, selective, portable and cost-effective.[118] This spectroelectrochemical technique has been useful in many studies such as detecting and characterizing DNA aptamers, bovine insulin, bilayer lipid membranes, bacteria, polyphenols, organic pigments and drug metabolites and to monitor surface redox systems.[36,121,122,123,125,126,127]

Chapter 4: Experimental

4.1 Reagents and Materials

President's Choice® green tea was purchased from the Atlantic Superstore (Halifax, NS). Bond Elut PPL® SPE cartridges (bed mass:1 g, volume: 6 mL and particle size: 125 μm) and Bond Elut luer locks were purchased from Agilent Technologies. Silicone (inner diameter: 4.8 mm) and Teflon® (inner diameter: 2 mm) tubing for SPE extraction were purchased from MasterFlex and Amazon, respectively. Ammonium acetate (99.0%), acetonitrile (99.8%, HPLC grade), hydrochloric acid (37.0%), methanol (99.9%, HPLC grade) and sulfuric acid (98.0%) were purchased from Fisher Scientific (Ottawa, Ontario). 0.7 μm inline glass fiber filters (GF/F), Corning square 250 mL polycarbonate bottles, one-liter glass bottles, $AgNO_3$ (99.9999%), $NaBH_4$ (≥96%), NaF (99%), and KCl (≥99%) were all purchased from Sigma Aldrich (St, Louis, MO, USA). Citric acid (>99%) and caffeine (99%) were purchased from Alfa Aesar (Tewksbury, MA, USA). Acetic acid (99.5%) and sodium citrate (>99%) were purchased from ACP (Montreal, Quebec, Canada). Carbon screen printed electrodes (SPEs) (15 x 61 x 0.36 mm) were purchased from Pine Research Instrumentation (Durham, NC, USA). Argon (99.999%) was purchased from Air Liquide Canada Inc. (Montreal, Quebec, Canada). All glassware was placed in an acid bath composed of neat sulfuric acid overnight and was then thoroughly rinsed with Millipore water (≥18.2 MΩ cm) from a Milli-Q plus system (Millipore, California, USA) prior to use. Millipore water was used to prepare all solutions. All chemicals were used without further purification.

4.2 Procedures

4.2.1 Preparation of Green Tea

In this thesis research, green tea was used as a model of a complex sample for method development for eventual analysis of DOM. A volume of 80 mL of Milli-Q water was brought to boiling in a beaker. Subsequently, the contents of a green tea bag were poured into another beaker. A volume of 25 or 50 mL of the boiling Milli-Q water was then poured into the beaker with the green tea. The green tea was allowed to steep for five minutes, and then an aliquot of the steeped tea was filtered through a 0.45 μm syringe filter for 2D-LC analysis or was filtered through a 0.7 μm inline glass fiber filter for EC-SERS analysis.

4.2.2 Sackville River Water Collection

Before water sample collection, 250 mL and 1 L bottles were rinsed with HPLC grade methanol and Milli-Q water three times each before being sonicated with Milli-Q water for 30 minutes. During sample collection, a rope was tied around the rim of the bottles which were then lowered into the river from the bridge and were kept in place until the bottle was filled. Water collection was completed in January and March.

4.2.3 Solid Phase Extraction (SPE) of DOM

It was crucial to extract the dissolved organic matter (DOM) from the water samples using solid phase extraction (SPE) on the same day of water collection to avoid any further microbial degradation from occurring. Before SPE, the water samples were vacuum filtered using 0.7 μm inline GF/F filters that were previously combusted at 450°C for 4 hours using a muffle furnace. For the first set of water samples, the filtrate was then used for SPE. However, the second set of samples, the filtrate was acidified to pH 2 using hydrochloric acid before doing SPE. The first step of the SPE method established by Dr. Heather Reader was to clean the silicon and Teflon® tubing

with pH 2 Milli-Q water that was acidified using hydrochloric acid, for roughly thirty minutes with the help of a variable flow peristaltic pump (Fisherbrand™ Variable-Flow Peristaltic Pump) which was purchased from Fisher Scientific (Ottawa, Ontario).[32] The night before extraction, the PPL® cartridge was soaked in HPLC grade methanol.[32] The cartridge was filled completely with methanol to ensure the bed was wetted.[32] On the day of extraction, the methanol was drained from the cartridge and then rinsed with 250-300 mL of pH 2 Mill-Q water to remove any methanol left in the sorbent and to reduce the risk of sample contamination.[32] During this step, the flow rate was set using a small graduated cylinder and a stopwatch to adjust the setting of the peristaltic pump to obtain an appropriate flow rate of 10-12 mL/min. After passing the sample through the cartridge it was necessary to wash any salts and impurities from the sample that may be in the resin bed; this was accomplished by passing 150-200 mL of pH 2 Milli-Q water through the column. Lastly, the column was then dried using a vacuum. At this point, the DOM captured from the sorbent is semi-stable and can be stored in the freezer for up to 12 weeks without significant changes in DOC concentrations, as found through the work done by Cook *et al.*[128] To extract and collect the captured DOM, 20 mL of HPLC methanol was passed through the cartridge at a flow rate of 1-2 mL/min.[32] Figure 4.1 is an image of the solid phase extraction set-up.

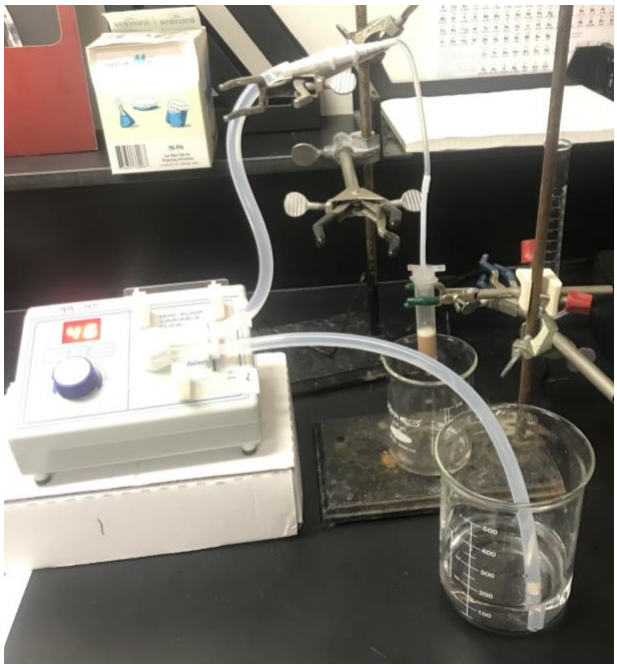

Figure 4.1: Solid phase extraction set-up

4.2.4 Spectroscopy

4.2.4.1 UV-Vis Spectroscopy

UV-visible measurements were obtained using a Cary 60 UV-visible spectrometer (Agilent, Santa Clara, CA). This instrument was used to record UV-Vis extinction measurements for the colloidal sol, and of the DOM extract from the Sackville River. Samples were placed in a quartz cuvette and were diluted with Milli-Q water. Spectra were collected over the spectral range from 200 – 800 nm. The instrument resolution was 1.5 nm. For data analysis, the software program Origin 8.1 (OriginLab Corporation, Northampton, MA, U.S.A.) was used on a standard PC.

4.2.4.2 Raman Spectroscopy

Normal Raman spectroscopy conducted in this work was completed using a DeltaNu Advantage 785 Raman spectrometer (SciAps, Woburn, MA). This spectrometer is fitted with a 785 nm diode laser, an air-cooled CCD detector, and has a resolution of 4.0 cm^{-1}. The spectrometer was operated with NuSpec software for signal acquisition and processing. The samples were

placed onto a glass slide for Raman analysis. For spectral processing and data analysis, the software program Origin 9.75 (OriginLab Corporation, Northampton, MA, U.S.A.) was used on a standard PC. All data measured were corrected for acquisition time and laser power, and also smoothed using the adjacent-averaging smoothing method of eight data points.

4.2.4.3 Electrochemical Surface-Enhanced Raman Spectroscopy

4.2.4.3.1 Silver Nanoparticle (AgNP) Synthesis

A literature procedure for a modified Lee-Meisel synthesis of silver nanoparticles was followed for this thesis work.[106] Briefly, 1.0 mL of silver nitrate solution (0.1 M), 3.4 mL of aqueous sodium citrate (5%), and 0.6 mL of citric acid (0.17 M) were added into a 250 mL three-neck flat-bottom flask with 95.0 mL of water. A volume of 0.2 mL of freshly prepared sodium borohydride solution (0.1 mM) was then added into the flask at room temperature under magnetic stirring. The mixture was allowed to stand at room temperature for 1 minute and then brought to boil under reflux within 20 minutes under magnetic stirring. After boiling for 1 hour, the murky yellow-green solution was allowed to cool to room temperature. Two 715 μL aliquots of colloidal suspension were added to each of the 56 tubes of Eppendorf tubes, which were then centrifuged at 8 000 rpm for 20 minutes (Labnet PRISM microcentrifuge, Edison, NJ, USA). The supernatant was then removed and discarded, and the paste of 14 Eppendorf tubes was put into one tube and centrifuged again. The final paste was adjusted to a final volume of 50 μL with water.

4.2.4.3.2 Preparation of EC-SERS Substrates

Screen printed electrodes (SPE) were purchased from Pine Research Instrumentation and the carbon working electrode was modified with nanoparticles for use in EC-SERS detection. Three layers of the AgNP paste were drop coated onto the working electrode surface of a carbon screen printed electrode in 5 μL aliquots, drying fully between layers. Using three layers of the AgNP

paste was found to be the ideal amount to ensure uniform surface coverage. The electrodes were then immersed in 0.5 M KCl for 30 minutes to remove citrate, rinsed with ultrapure water, and dried prior to application. This treatment is useful for the removal of adsorbed citrate, which poses a significant interference for SERS measurements.[123]

4.2.4.3.3 EC-SERS Analysis

EC-SERS work was completed using a DXR Smart Raman Spectrometer (Thermo Fisher Scientific, Mississauga, ON, Canada). This spectrometer can use two different laser excitation wavelengths: 532 nm and 780 nm and can be fitted with two different gratings: a full range, low resolution (5 cm^{-1}) grating, and a shorter range, high resolution (3 cm^{-1}) grating. The 780 nm laser line with the high-resolution grating was used for this thesis research, as using a lower energy wavelength will result in reduced background fluorescence. A Pine Research Instrumentation portable USB Wavenow potentiostat/galvanostat (Durham, NC, U.S.A.) was used for conducting electrochemical measurements with the electrochemical software, Aftermath Data Organizer (version 1.2.4361), also produced by Pine Research Instrumentation. Modified SPEs were placed in the electrochemical cell, which was a modified glass vial (2 x 4.5 x 0.6 cm) and a special mini USB adapter that is made to fit the SPEs. The electrodes were then analysed before the electrolyte was added using the Raman spectrometer, termed the "in air' signal to ensure that the working electrode surface was at the focal point of the laser. The "in air" spectrum also represents the normal SERS spectrum that could be collected in the absence of electrochemistry. The open circuit potential (OCP) spectrum could then be collected when the 0.1 M NaF supporting electrolyte (purged with argon for 30 minutes prior to use) was added to the electrochemical cell containing the SPE. The system was first stepped in the cathodic direction (0.0 V to -1.0 V) and then in the anodic direction (-1.0 V to 0.0 V), both in increments of 0.1 V. Positive voltages were avoided in order to prevent

oxidation of the silver surface. At each applied potential a SERS spectrum was collected. All potentials are reported versus the Ag/AgCl reference electrode. For spectral processing and data analysis, the software program Origin 9.75 (OriginLab Corporation, Northampton, MA, U.S.A.) was used on a standard PC. All data measured were corrected for acquisition time and laser power, and also smoothed using the adjacent-averaging smoothing method of 10 points.

4.2.5 Liquid Chromatography

Single-dimension and multidimensional liquid chromatographic analysis were carried out on an Agilent 1290 Infinity II series 2D-UHPLC system (Agilent Technologies, Santa Clara, CA). For chromatography processing and data analysis, the software program Origin 9.75 (OriginLab Corporation, Northampton, MA, U.S.A.) was used on a standard PC.

4.2.5.1 Green Tea

4.2.5.1.1 First-Dimension Parameters

The parameters of the first-dimension are outlined in Table 4.1.

Table 4.1: 1D-LC Parameters for the Separation of Green Tea.

First-Dimension Column	Agilent ZORBAX SB-C18 (2.1 x 100 mm x 1.8 μm)
Injection Amount	2.5 μL
Solvent A	Water
Solvent B	Methanol
Flow Rate	0.2 mL/min
Gradient	5% B at 0 min 60% B at 10 min 95% B at 11 min
Column Temperature	30 °C
Run-time	15 minutes
Post Run-time	10 minutes
Wavelengths	254 nm & 280 nm

4.2.5.1.2 Second-Dimension Parameters

The first-dimension separation was exactly as outlined above in Table 4.1. The parameters of the second-dimension are outlined in Table 4.2. Peaks of interest from the first-dimension were further investigated in the second-dimension by heart-cut mode. The threshold was chosen based on the intensity of peaks in the first-dimension which sometimes varied between runs.

Table 4.2: 2D-LC Parameters for the Separation of Green Tea.

Mode	Heart-Cut mode (300 mAU Threshold)
Second-Dimension Column	Agilent ZORBAX Bonus-RP (2.18 x 50 mm x 1.8 μm)
Injection Amount	2.5-5.0 μL
Solvent A	5 mM ammonium acetate in 1:9 water: acetonitrile (v/v)
Solvent B	5 mM ammonium acetate in 0.5:9.5 water: acetonitrile (v/v)
Flow Rate	0.5 mL/min
^{1}D Gradient	5% B at 0 min 60% B at 10 min 95% B at 11 min
^{2}D Gradient	10% B at 0 min 10% B at 0.10 min 90% B at 1.40 min 90% B at 1.50 min 10% B at 1.6 min 10% B at 2.00 min
^{2}D Gradient Stop Time	1.6 minutes
^{2}D Cycle Time	2.0 minutes
Column Temperature	30 °C
Run-time	20 minutes
Post Run-time	10 minutes
Wavelengths	254 nm & 280 nm

4.2.5.1.3 Second-Dimension with Fraction Collection Parameters

The first-dimension separation was exactly as outlined above in Table 4.1. The parameters of the second-dimension with fraction collection are stated in Table 4.3. Peaks of interest in the second-dimension were collected as fractions by selecting the retention time to collect the whole

peak. Fractions were collected into an Agilent 96-well plate and then were transferred to vials for spectroscopic studies.

Table 4.3: 2D-LC with Fraction Collection Parameters for the Separation of Green Tea.

Mode	Heart-Cut mode (300 mAU Threshold)
Second-Dimension Column	Agilent ZORBAX Bonus-RP (2.18 x 50 mm x 1.8 μm)
Injection Amount	2.5-5.0 μL
Solvent A	5 mM ammonium acetate in 1:9 water: acetonitrile (v/v)
Solvent B	5 mM ammonium acetate in 0.5:9.5 water: acetonitrile (v/v)
Flow Rate	0.5 mL/min
^{1}D Gradient	5% B at 0 min 60% B at 10 min 95% B at 11 min
^{2}D Gradient	10% B at 0 min 10% B at 0.10 min 90% B at 1.40 min 90% B at 1.50 min 10% B at 1.6 min 10% B at 2.00 min
^{2}D Gradient Stop Time	1.6 minutes
^{2}D Cycle Time	2.0 minutes
Column Temperature	30 °C
Run-time	20 minutes
Post Run-time	10 minutes
Wavelengths	254 nm & 280 nm

4.2.5.2 Dissolved Organic Matter without Acidifcation Prior to SPE

4.2.5.2.1 First-Dimension Parameters

The parameters of the first-dimension are outlined in Table 4.4 which are quite different than the parameters established for green tea analysis. One of the reasons the parameters among the green tea and DOM are different is because it was more difficult to separate the components in DOM than it was for the green tea. Methanol was replaced by acetonitrile for the first-dimension separation mobile phase. The gradient was modified to have the organic phase introduced sooner in the run because the compounds in the DOM extract elute out in the organic phase. Lastly, the injection volume was larger than it was for the green tea (5 μL versus 2.5 μL).

Table 4.4: 1D-LC Parameters for the Separation of DOM.

First-Dimension Column	Agilent ZORBAX SB-C18 (2.1 x 100 mm x 1.8 μm)
Injection Amount	5.0 μL
Solvent A	Water & 0.1% formic acid
Solvent B	Acetonitrile & 0.1% formic acid
Flow Rate	0.2 mL/min
Gradient	20% B at 0 min 50% B at 1 min 70% B at 4 min 95% B at 15 min
Column Temperature	30 °C
Run-time	15 minutes
Post Run-time	10 minutes
Wavelengths	254 nm & 280 nm

4.2.5.2.2 Second-Dimension Parameters

The first-dimension separation was carried out exactly as outlined above in Table 4.4. The parameters of the second-dimension are outlined in Table 4.5. Peaks of interest from the first-dimension were further investigated in the second-dimension by the heart-cut mode. The threshold was chosen based on the intensity of peaks in the first-dimension which occasionally varied.

Table 4.5: 2D-LC Parameters for the Separation of DOM.

Mode	Heart-Cut mode (50 mAU Threshold)
Second-Dimension Column	Agilent ZORBAX Bonus-RP (2.18 x 50 mm x 1.8 μm)
Injection Amount	5.0 μL
Solvent A	5 mM ammonium acetate in 1:9 water: acetonitrile (v/v)
Solvent B	5 mM ammonium acetate in 0.5:9.5 water: acetonitrile (v/v)
Flow Rate	0.5 mL/min
^{1}D Gradient	20% B at 0 min 50% B at 1 min 70% B at 4 min 95% B at 15 min
^{2}D Gradient	10% B at 0 min 10% B at 0.10 min 90% B at 1.40 min 90% B at 1.50 min 10% B at 1.6 min 10% B at 2.00 min
^{2}D Gradient Stop Time	1.6 minutes
^{2}D Cycle Time	2.0 minutes
Column Temperature	30 °C
Run-time	15 minutes
Post Run-time	10 minutes
Wavelengths	254 nm & 280 nm

4.2.5.3 Dissolved Organic Matter with Acidification Prior to SPE

4.2.5.3.1 First-Dimension

The method established for the first DOM extract in the first-dimension after some further method development was used for the second DOM extract obtained as outlined in Table 4.6. Peaks of interest from the first-dimension were further investigated in the second-dimension by

the heart-cut mode. The threshold was chosen based on the intensity of peaks in the first-dimension which occasionally varied.

Table 4.6: 1D-LC Parameters for the Separation of DOM with Acidification.

First-Dimension Column	Agilent ZORBAX SB-C18 (2.1 x 100 mm x 1.8 μm)
Injection Amount	5.0 μL
Solvent A	Water & 0.1% formic acid
Solvent B	Acetonitrile & 0.1% formic acid
Flow Rate	0.2 mL/min
Gradient	20% B at 0 min 50% B at 1 min 70% B at 4 min 95% B at 15 min
Column Temperature	30 °C
Run-time	15 minutes
Post Run-time	10 minutes
Wavelengths	254 nm & 280 nm

4.2.5.3.2 Second-Dimension

The parameters of the second-dimension are outlined in Table 4.7 which are different than the parameters established for green tea and the original DOM extract analysis. The run-time was increased to 2.5 minutes and the gradient was modified to have the organic phase introduced sooner in the run because the compounds in the DOM extract elute out in the organic phase.

Table 4.7: 2D-LC Parameters for the Separation of DOM with Acidification.

Mode	Heart-Cut mode (150 mAU Threshold)
Second-Dimension Column	Agilent ZORBAX Bonus-RP (2.18 x 50 mm x 1.8 μm)
Injection Amount	5.0 μL
Solvent A	5 mM ammonium acetate in 1:9 water: acetonitrile (v/v)
Solvent B	5 mM ammonium acetate in 0.5:9.5 water: acetonitrile (v/v)
Flow Rate	0.5 mL/min
^{1}D Gradient	20% B at 0 min 50% at 1 min 70% B at 4 min 95% B at 15 min
^{2}D Gradient	10% B at 0 min 90% B at 0.50 min 90% B at 1.40 min 90% B at 1.50 min 10% B at 1.6 min 10% B at 2.00 min 10% B at 2.50 min
^{2}D Gradient Stop Time	2.2 minutes
^{2}D Cycle Time	2.5 minutes
Column Temperature	30 °C
Run-time	15 minutes
Post Run-time	10 minutes
Wavelengths	254 nm & 280 nm

4.2.5.3.3 Second-Dimension with Fraction Collection Parameters

Table 4.8: 2D-LC with Fraction Collection Parameters for the Separation of DOM with Acidification.

Mode	Heart-Cut mode (150 mAU Threshold)
Second-Dimension Column	Agilent ZORBAX Bonus-RP (2.18 x 50 mm x 1.8 μm)
Injection Amount	5.0 μL
Solvent A	5 mM ammonium acetate in 1:9 water: acetonitrile (v/v)
Solvent B	5 mM ammonium acetate in 0.5:9.5 water: acetonitrile (v/v)
Flow Rate	0.5 mL/min
^{1}D Gradient	20% B at 0 min 50% at 1 min 70% B at 4 min 95% B at 15 min
^{2}D Gradient	10% B at 0 min 90% B at 0.50 min 90% B at 1.40 min 90% B at 1.50 min 10% B at 1.60 min 10% B at 2.00 min 10% B at 2.50 min
^{2}D Gradient Stop Time	2.2 minutes
^{2}D Cycle Time	2.5 minutes
Column Temperature	30 °C
Run-time	15 minutes
Post Run-time	10 minutes
Wavelengths	254 nm & 280 nm

4.2.6 Mass Spectrometry

An Agilent 6530 quadrupole time of flight (Q-TOF) mass analyzer equipped with electrospray ionization (ESI) was used. Direct injection was completed with a syringe pump with a flow of 90 μL/h. Software used for analysis was MassHunter (Agilent Technologies, Santa Clara, CA). Table 4.9 provides the MS parameters used for the cuts of green tea.

Table 4.9: Q-TOF MS Parameters

Ionization mode	Positive and negative electrospray
Acquisition rate	3 spectra/s
Time	333.3 ms/spectra
Mass range	30 – 700 m/z
Drying gas temperature	350 °C
Drying gas flow rate	8 L/min
Nebulizer gas	30 psi
Skimmer voltage	65 V
Fragmentor	0 sec 120 V 30 sec 100 V 60 sec 80 V
Capillary Voltage	3000 V
Collision energy	0 V

4.2.7 Attenuated Total Reflectance-Fourier Transform Infrared Spectroscopy (ATR-FTIR)

An attenuated total internal reflection Fourier transform infrared (ATR-FTIR) spectrometer (Bruker Alpha, Bruker, Massachusetts) was used to collect all IR spectra. The ATR-FTIR contains a ZnSe window and 32 or 60 scans were taken for each measurement depending on the sample

being analysed. For spectroscopic processing and data analysis, the software program Origin 9.75 (OriginLab Corporation, Northampton, MA, U.S.A.) was used on a standard PC.

4.2.8 Scanning Electron Microscopy-Energy-Dispersive X-ray Spectroscopy (SEM-EDX)

Scanning electron microscopy (SEM) images were obtained using a Tescan Mira3 LMU field emission microscope (Warrendale, PA, U.S.A.). The SEM is equipped with a high brightness Schottky emitter electron gun and backscattered and secondary electron detectors. The maximum resolution of the SEM is 1.2 nm at 30 kV. This SEM is paired with an INCA X-max 80 mm 2 EDX system to identify elements present in a selected SEM area delivering both qualitative and semi-quantitative information. The EDX system uses a silicon drift detector (SDD). Carbon tape and/or a silicon wafer was used as the substrate depending on the sample being analysed. Image J (National Institutes of Health, Bethesda, MD, USA) was used to determine the diameter of the AgNPs that were used in EC-SERS experiments.

Chapter 5: Results and Discussion

5.1 Green Tea

5.1.1 2D-LC

Green tea was used to develop the chromatographic and spectroscopic methods used in this thesis work before analyzing the DOM extracted from the Sackville River. Green tea was chosen because it is a good example of a complex sample with DOM components. Krieger developed a 2D-LC method for separating green tea using reverse phase chromatography in both the first and second-dimensions.[62] An optimized version of this 2D-LC method was used for the separation of green tea components in this thesis work.

5.1.1.1 First-Dimension Optimization

The column used in the first-dimension was a Zorbax Eclipse Plus C-18 (1.8 μm x 2.1 mm x 50 mm). This reverse phase column contains a dense monolayer of dimethyl-n-octadecylsilane bonded to an ultra-high purity silica support as the stationary phase. The number of theoretical plates found in this column is 10,902. The plate height is 0.00459 mm. The selectivity and linear velocity are 1.88 and 0.446 cm/s, respectively. These parameters were determined by the manufacturer based on data collected for naphthalene. The first-dimension separation utilizes a gradient elution, meaning that the mobile phase is not at a constant composition during the run-time. The parameters of the gradient elution are listed in Table 5.1. Solvent A is water and solvent B is methanol.

Table 5.1: Gradient Parameters for the First-Dimension Separation.

Time	Composition of Methanol
0 min	5%
10 min	60%
11 min	95%

5.1.1.1.1 Mobile Phase Additives

The mobile phase that was used in the first-dimension of the method established by Krieger was water with 0.05% trifluoracetic acid (Solvent A) and methanol with 0.05% trifluoracetic acid (Solvent B). Acidic mobile phase additives are commonly used to facilitate mass spectrometry measurements after separation.[129] Trifluoracetic acid was not available at the time our experiments were conducted and formic acid was suggested as a replacement. Figure 5.1 is a chromatogram showing the separation of green tea with the modified mobile phase. The chromatogram demonstrates the complexity of the green tea as there are many different components and some are not well resolved. For example, the peaks between 5 and 6 minutes and between 6 and 7.5 minutes (each indicated by an asterisk in Figure 5.1) are not completely resolved. The resolution of these peaks is below 1.5, the value that is the optimum resolution to attain complete separation. The second-dimension separation using the 2D-LC is ideally suited for peaks such as these, where coelution is evident.

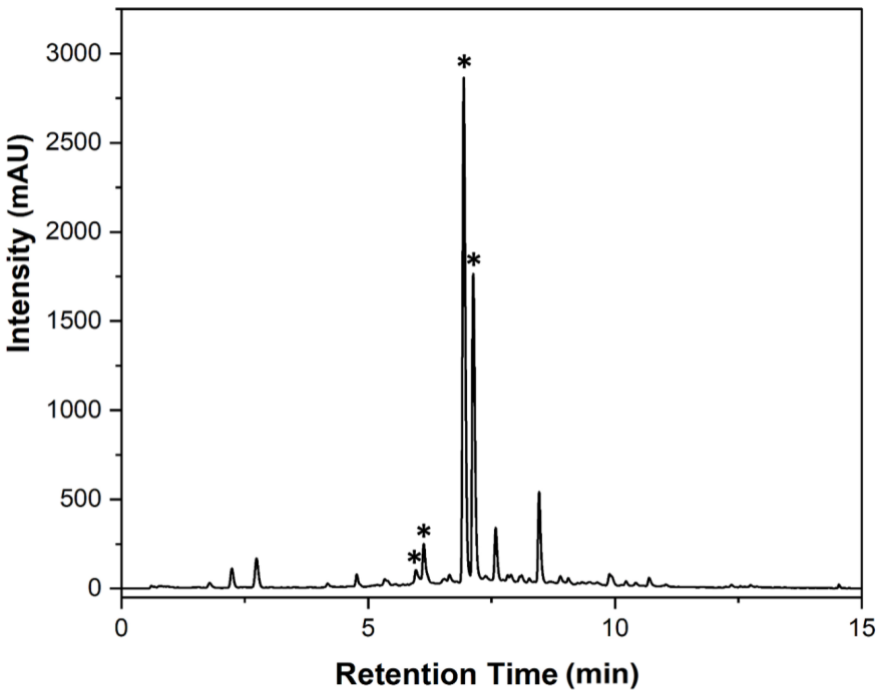

Figure 5.1: [1]D chromatogram of green tea at 280 nm. Milli-Q water with 0.1% formic acid and methanol with 0.1% formic acid used for the mobile phase. Injection volume was 2.5 μL.

Formic acid was removed from the mobile phase and the separation was attempted once more as shown in Figure 5.2. This was done as formic acid was not considered an essential additive, as mass spectrometry was not a major component of this work, and also because prior work had indicated that formic acid can interfere with SERS spectra collection.[130] The peak resolution is improved when the formic acid is removed, when Figures 5.1 and 5.2 are compared. Additionally, the baseline is smoother leading to a better separation. Therefore, water and methanol without formic acid as an additive were used for all future separations of green tea in the first-dimension. The intensities between the two chromatograms are different because the injection volumes were different.

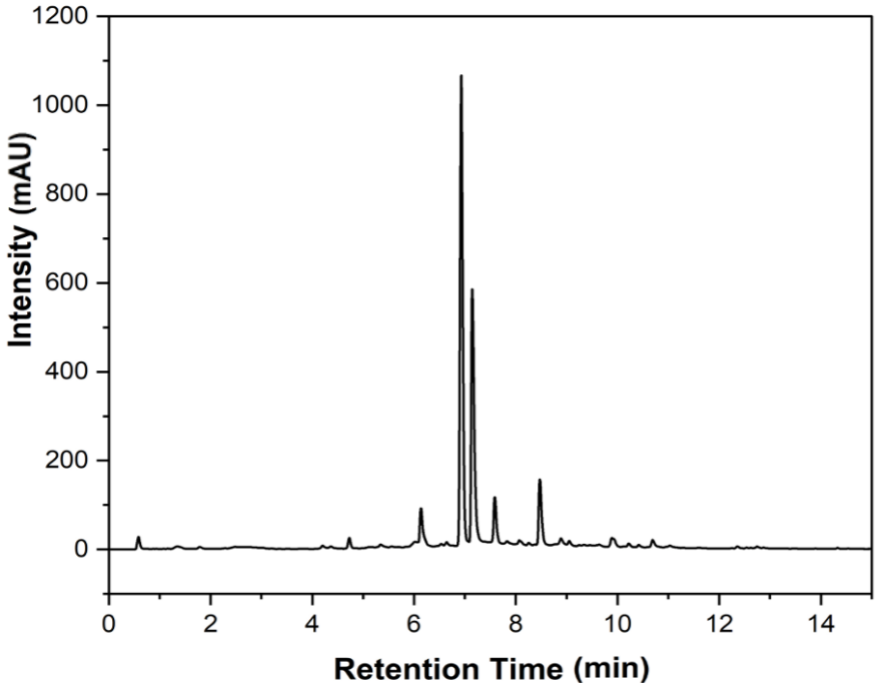

Figure 5.2: [1]D chromatogram of green tea at 280 nm. Milli-Q water and methanol used for the mobile phase. Injection volume was 1 μL.

5.1.1.2 Second-Dimension Optimization

The column used in the second-dimension was a Zorbax Bonus RP (2.1 mm x 50 mm x 1.8 μm) column. The stationary phase material found in this column contains diisopropyl-C14 groups covalently bonded through an embedded amide functionality to an ultra-pure silica support. The number of theoretical plates found in this column is 10,045. The plate height is 0.00498 mm. The selectivity and linear velocity are 1.81 and 0.390 cm/s respectively. These parameters were determined by the manufacturer using data collected for naphthalene. The run-time for each heart cut chromatogram in the second-dimension was two minutes.

5.1.1.2.1 Mobile Phase

The mobile phase in the second-dimension consisted of water and acetonitrile and the gradient elution parameters are listed in Table 5.2. It is important to note that the [2]D separations are poor

as shown in Figure 5.3 and there is not much of a separation occurring. Therefore, part of this thesis research explored ways in which to optimize the second-dimension separation.

Table 5.2: Gradient Parameters for the Second-Dimension Separation.

Time	Composition of Acetonitrile
0 min	5%
1.4 min	95%

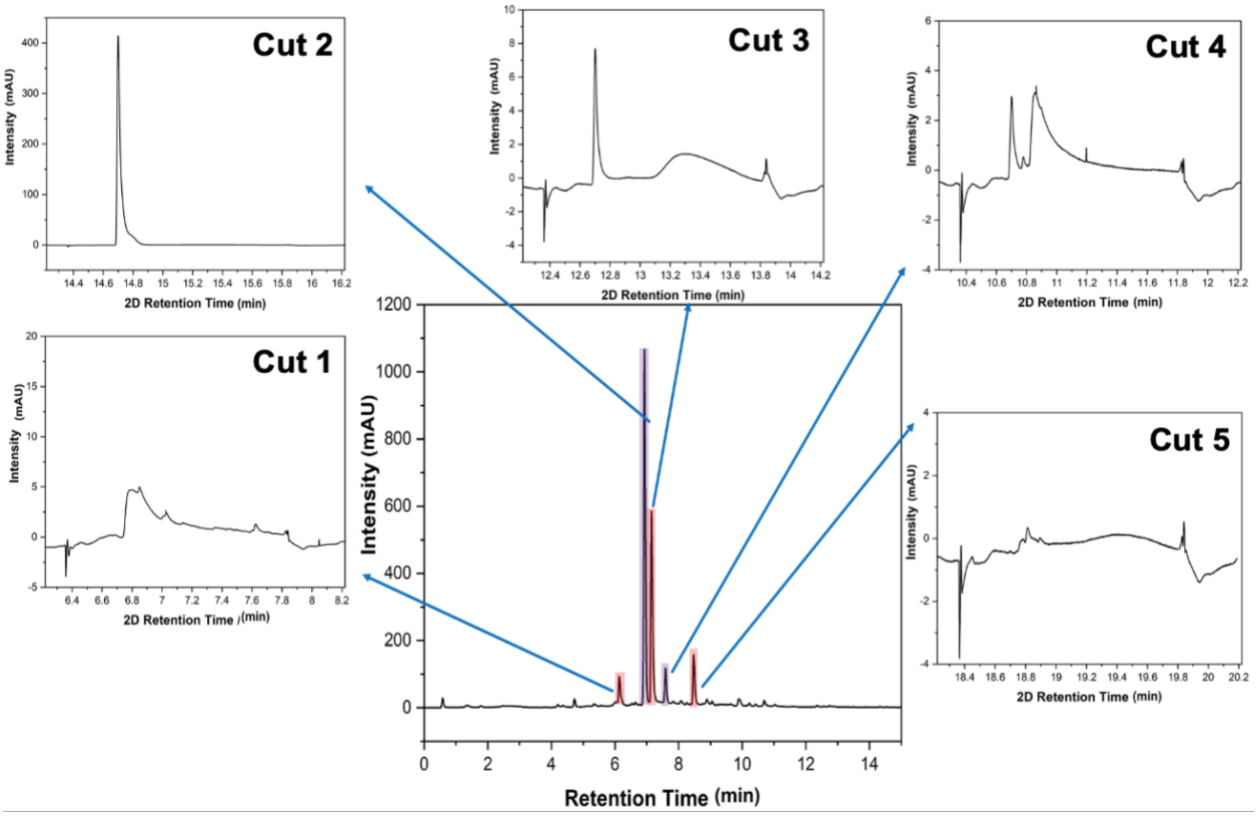

Figure 5.3: Chromatogram of green tea in the first-dimension (centre) and chromatograms in the second-dimension of heart cuts highlighted from the first-dimension at 280 nm. Milli-Q water (Solvent A) and acetonitrile (Solvent B) were used for the mobile phase. Injection volume was 2.5 μL.

Additives are extensively used in chromatographic mobile phases when separating DOM and it was found in the literature that buffers present in the mobile phase resulted in better resolution for water-soluble components present in a DOM sample.[23] Many DOM researchers using

chromatography have used ammonium acetate in their mobile phases and this additive was chosen for use in the second-dimension mobile phase to improve the separation for this thesis work. Clyde *et al*. used 5 mM ammonium acetate in their water and acetonitrile mobile phases to analyze drugs and were successful in their UHPLC separation.[131] In this thesis research, when a 1:9 acetonitrile: water (v/v) with 5 mM ammonium acetate (Solvent A) and a 9.5:0.5 acetonitrile: water (v/v) with 5 mM ammonium acetate (Solvent B) mobile phase was used in the second-dimension, it led to a more successful result than when no additive was present, as shown in Figure 5.4 because using high organic/low aqueous buffered mobile phase with a polar stationary phase helps with the separation of many of the charged solutes.[131]

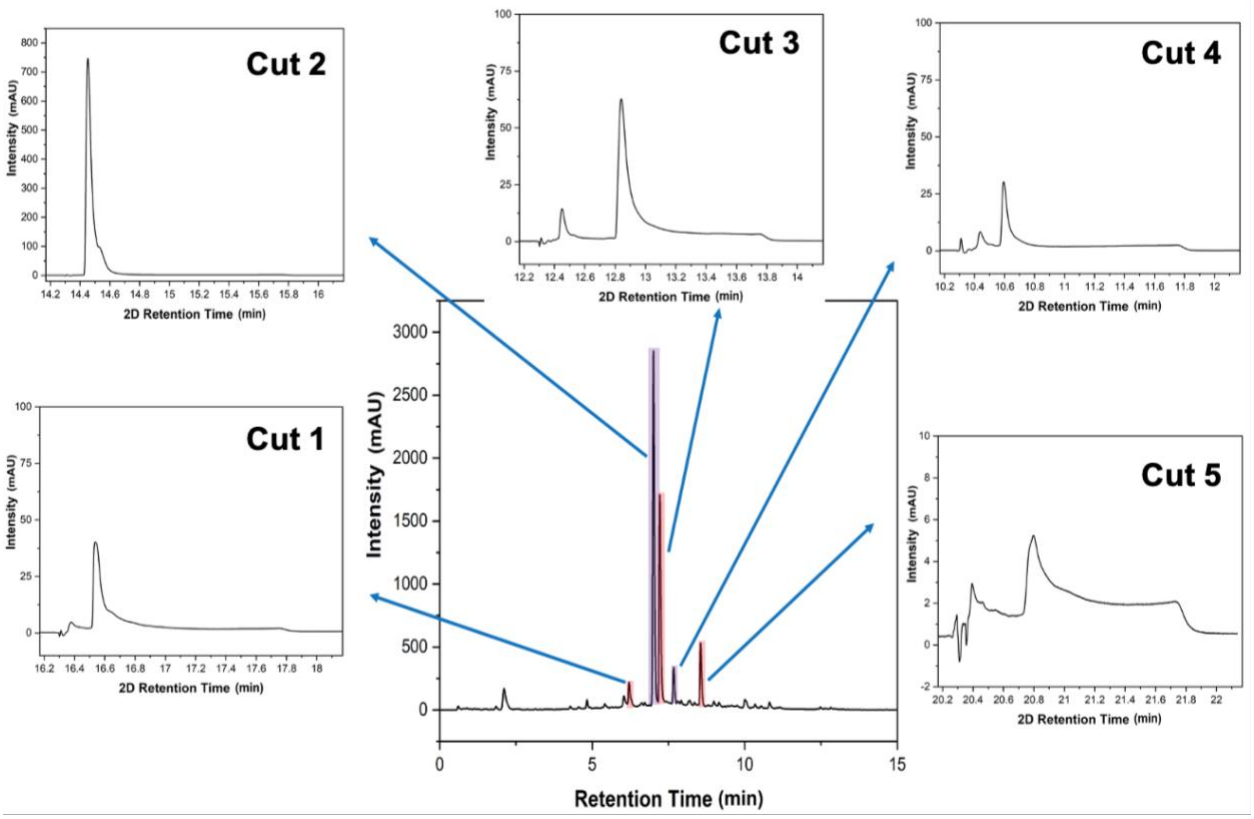

Figure 5.4: Chromatogram of green tea in the first-dimension (centre) and chromatograms in the second-dimension for cuts highlighted from the first-dimension at 280 nm. 1:9 acetonitrile/Milli-Q water (v/v) with 5 mM ammonium acetate buffer and 9.5:0.5 acetonitrile/Milli-Q water (v/v) with 5 mM ammonium acetate buffer used for the second-dimension mobile phase. Injection volume was 5 μL.

5.1.1.2.2 Reduced Flow Rate in Second-Dimension

Another parameter that can be optimized to achieve a better separation is to change the flow rate of the mobile phase. Originally, the mobile phase flow rate used in the second-dimension was 1 mL/min which did provide a sufficient separation as shown above. However, reducing the flow rate could provide a better separation because it would allow the components in the heart cut to interact with the column for a longer amount of time. Therefore, the flow rate was reduced to 0.5 mL/min and, in addition, the run-time was extended to two minutes. Figure 5.5 includes the second-dimension chromatograms obtained with a flow rate of 0.5 mL/min. For cut 1, there are two peaks now observed, compared to a single peak observed previously, meaning that with the higher flow rate used earlier was too fast and was not able to separate these two components. However, with the other cuts, the separation in the second-dimension is comparable to when the higher flow rate was used.

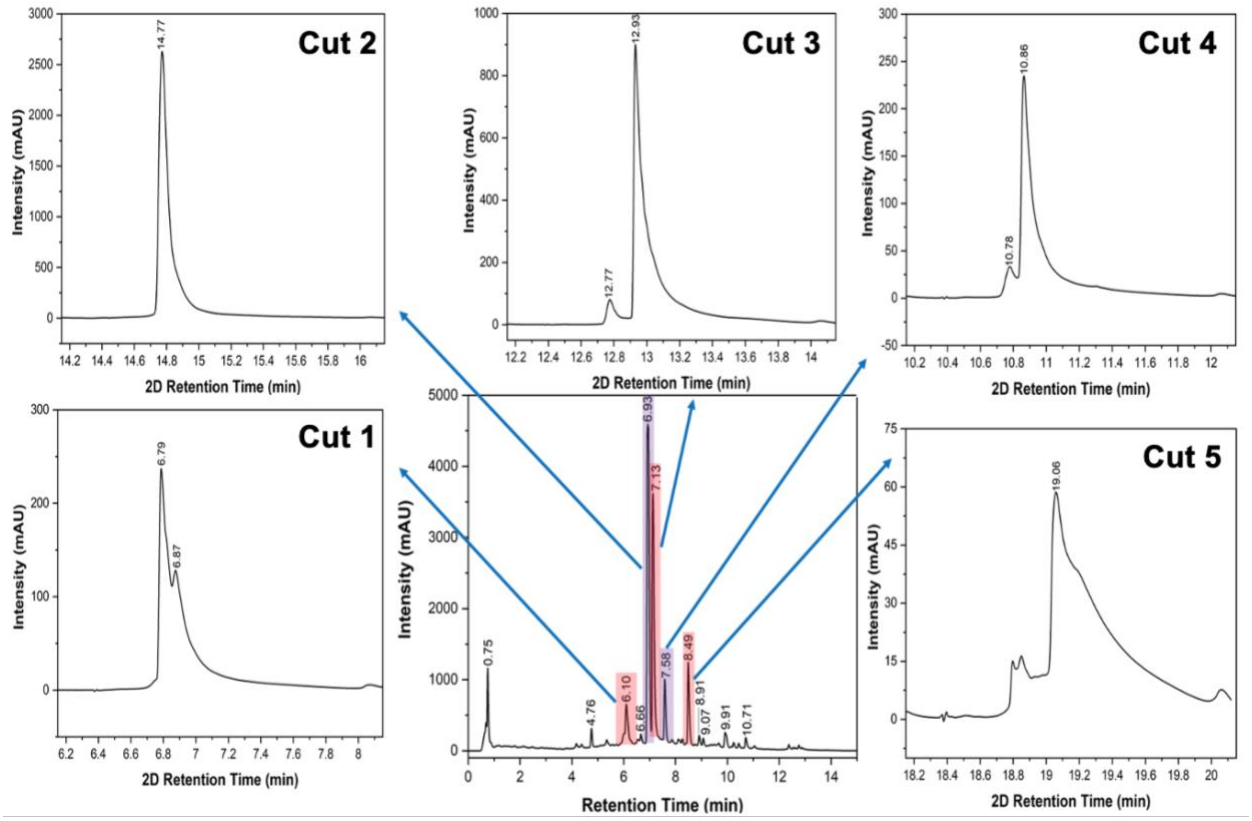

Figure 5.5: Chromatogram of green tea in the first-dimension (centre) and chromatograms in the second-dimension of cuts highlighted from the first-dimension at 280 nm. 1:9 acetonitrile/Milli-Q water (v/v) with 5 mM ammonium acetate and 9.5:0.5 acetonitrile/Milli-Q water (v/v) with 5 mM ammonium acetate used for the second-dimension mobile phase. Retention times stated above each peak. Injection volume was 5 μL.

For clarity for this thesis work, Table 5.3 lists the cut assignments of the peaks that were further analysed in the second-dimension using the heart-cutting mode.

Table 5.3: Cut Number Assignment of Peaks in the First-Dimension.

^{1}D Retention Time (min)	Cut #
6.10	1
6.93	2
7.13	3
7.58	4
8.49	5

5.1.1.3 2D-LC of Caffeine Standard

Since caffeine is known to be a major component in green tea, a 1 mM aqueous caffeine standard was prepared and analysed by 2D-LC with the same parameters noted above. Figure 5.6 compares the chromatograms of the green tea and the 1 mM caffeine standard with retention times noted. Since there is only 0.01 minute difference between the retention times recorded for the caffeine standard and the major peak observed for green tea, it can be concluded that cut 2 contains caffeine as the major component.

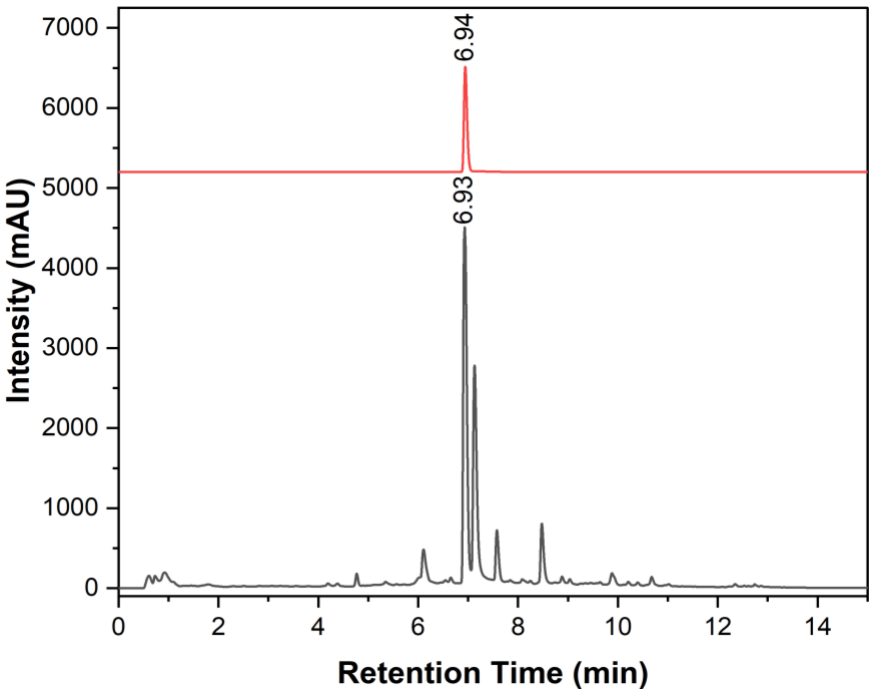

Figure 5.6 Comparison of [1]D chromatogram of green tea (lower) and 1 mM caffeine (upper) at 280 nm.

In conclusion, for the 2D-LC analysis of green tea many parameters were optimized for both the first and second-dimension to try and achieve a successful separation of green tea. It was determined that mobile phase additives were useful in the second-dimension separation but not the first-dimension separation and, in addition, a reduced mobile phase flow rate and a longer run-time was beneficial for the second-dimension separation. At this point, the 2D-LC separation was considered optimized for the green tea and therefore, the research could move forward to proof-of-concept EC-SERS detection of green tea fractions, and then onto the DOM sample extracted from the Sackville River.

5.1.2 EC-SERS

5.1.2.1 Nanoparticle synthesis

It was important to characterize the AgNPs after their synthesis to ensure that they were near-monodisperse and the correct size (~20 to 30 nm in diameter). The initial characterization of the AgNP colloidal sol was completed by measuring the extinction spectrum using a UV-Vis

spectrophotometer. The spectrum is shown in Figure 5.7, which shows the LSPR response of the colloidal particles. The extinction maximum was observed to be at 393 nm, which is consistent with spherical AgNPs made from this modified Lee and Meisel method.[106] The full width at half max (FWHM) of this LSPR peak was 44 nm, an indication that the colloidal nanoparticles were near-monodisperse. This observation was then confirmed using scanning electron microscopy (SEM). Figure 5.8 shows an SEM image of the AgNPs which coat the surface of the carbon working electrode of the screen printed electrode. Image J analysis of Figure 5.8 for n = 20 particles provided a nanoparticle diameter of 21.7 nm ± 2.2 nm.

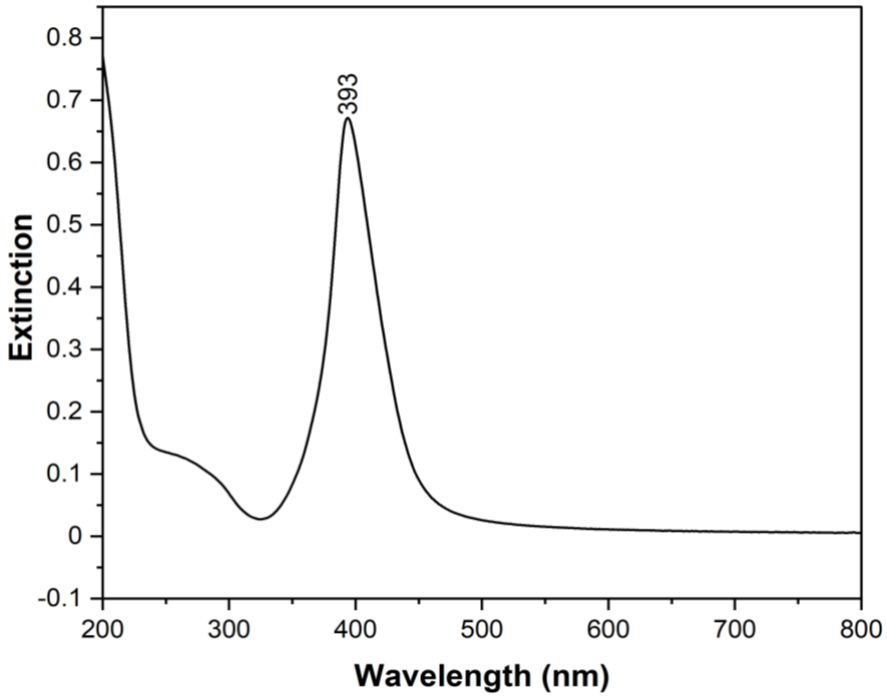

Figure 5.7: UV-Vis extinction spectrum of AgNPs.

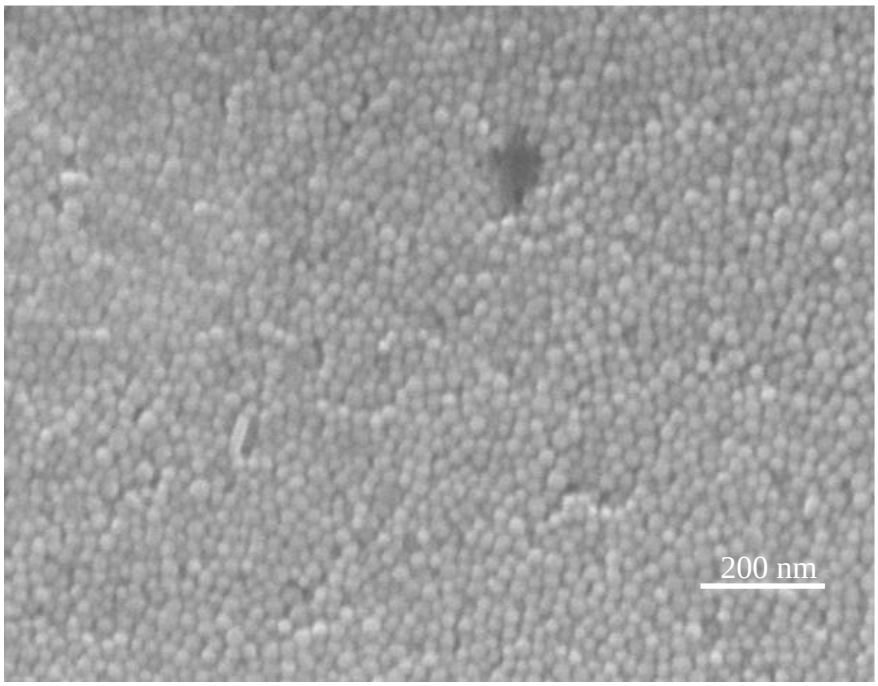

Figure 5.8: Scanning electron microscopy (SEM) of AgNPs. SEM image was obtained using a Tescan MIRA3 LMU field emission under high vacuum mode at 20.0 kV and secondary electron detection used.

5.1.2.2 EC-SERS Studies of the Second-Dimension Mobile Phase

The goal of this thesis work is to assess whether electrochemical surface-enhanced Raman spectroscopy (EC-SERS) can be a useful offline detection modality for 2D-LC. As a result, this research will require the collection of fractions from the second-dimension separation followed by EC-SERS analysis of these fractions. Hence, before collecting fractions of the cuts of green tea and analyzing them through EC-SERS, it was important to observe if the components of the second-dimension mobile phase would interfere with the detection of the compounds of interest since this was recognized as a problem in previous work by our research group.[130] Figures 5.9 and 5.10 are the EC-SERS plots for one milliliter of 1:9 acetonitrile: water (v/v) with 5 mM ammonium acetate and 9.5:0.5 acetonitrile: water (v/v) with 5 mM ammonium acetate mobile phases added to the electrochemical cell. One milliliter of supporting electrolyte is then added to the electrochemical cell (0.1 M NaF) and the SERS signal is collected in the absence of any applied

potential; this is termed the open circuit potential (OCP) spectrum. The potential is then stepped in 100 mV increments from 0.0 V to -1.0 V (cathodic progression) and the SERS signal is collected at each applied voltage. The potential is then stepped back in the anodic direction (anodic progression) from -1.0 V to 0.0 V and the signal is again collected at each potential. Finally, the OCP spectrum is collected again after the anodic progression. It can be observed that only noise is present in the signal from the 1:9 acetonitrile: water (v/v) with 5 mM ammonium acetate in Figure 5.9. However, in Figure 5.10, when 9.5:0.5 acetonitrile: water (v/v) with 5 mM ammonium acetate was analysed, there are a few peaks present that are characteristic for acetonitrile. Table 5.4 provides the peak assignment of acetonitrile.[132,133] This finding suggests that when the second-dimension fractions are analyzed, acetonitrile can potentially interfere in the EC-SERS analysis.

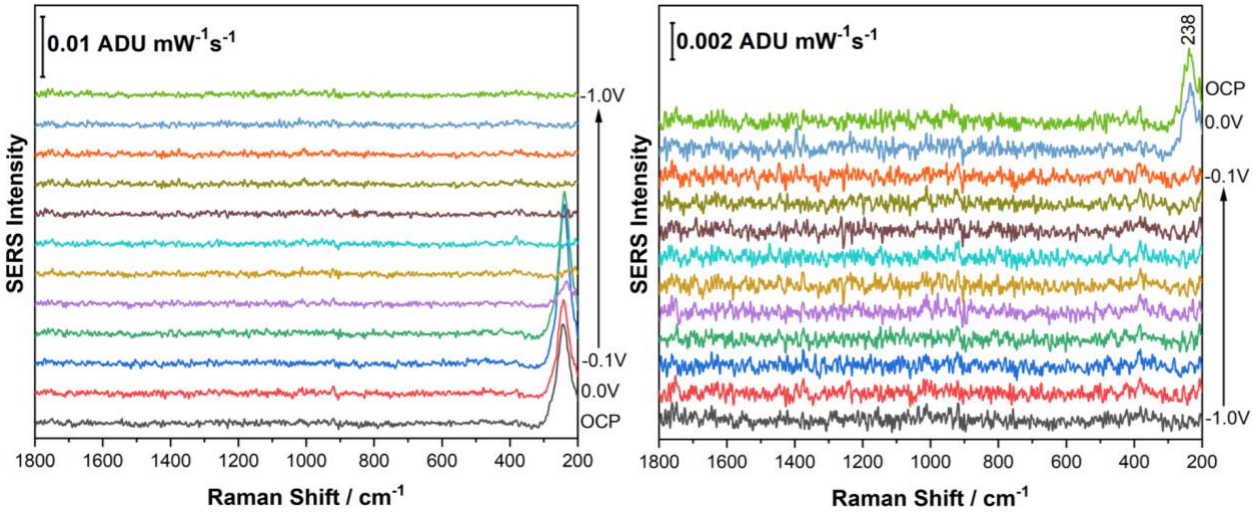

Figure 5.9: EC-SERS analysis of 1 mL of 5mM ammonium acetate in 1:9 acetonitrile: water (v/v) electrode mixed with 1 mL of 0.1 M NaF electrolyte (Cathodic, 0.1 V stepwise progression from 0 V to -1.0 V and Anodic, 0.1 V step-wise progression from 0 V to -1.0 V) using an excitation wavelength of 780 nm with a laser power of 80 mW and acquisition time of 30 seconds.

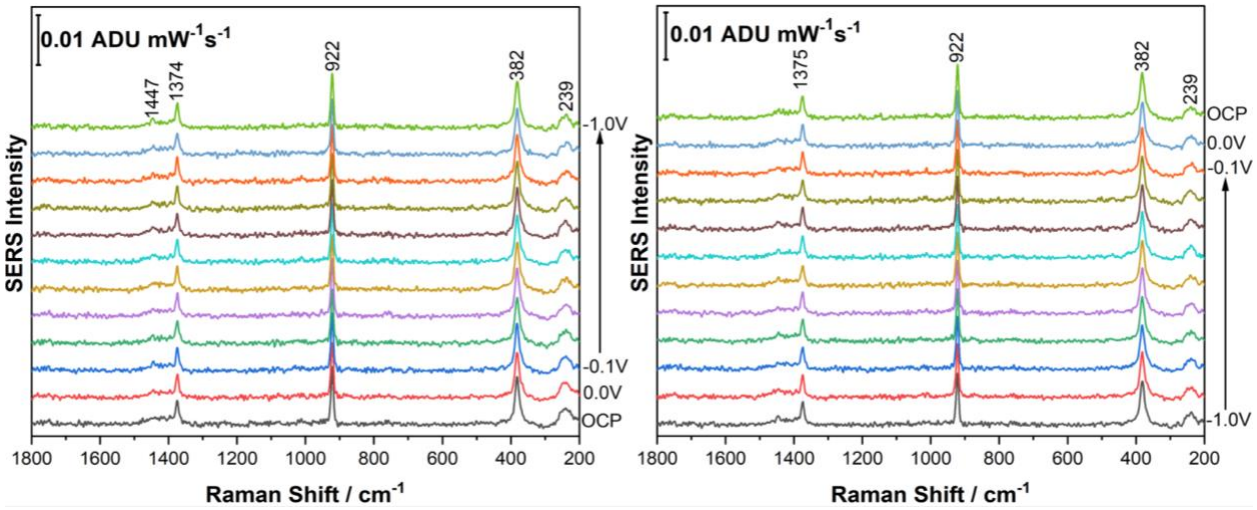

Figure 5.10: EC-SERS analysis of 1 mL of 5mM ammonium acetate in 9.5:0.5 acetonitrile: water (v/v) mixed with 1 mL of 0.1 M NaF electrolyte (Cathodic, 0.1 V stepwise progression from 0 V to -1.0 V and Anodic, 0.1 V step-wise progression from 0 V to -1.0 V) using an excitation wavelength of 780 nm with a laser power of 80 mW and acquisition time of 30 seconds.

Table 5.4: SERS Peak Assignment of Acetonitrile. (δ = bending mode and υ = stretching mode)

Raman Shift (cm^{-1})	Peak assignments
382	C-C≡N bending
922	C-C Stretching
1374	CH_3 Deformation
1447	CH_3 Deformation

5.1.2.3 5 μL of 25 mL Green Tea dropped coated on working electrode

Green tea was measured directly in order to observe how green tea behaves during EC-SERS analysis. Typically for EC-SERS measurements, a small volume (5 μL) of the analyte solution is drop coated onto the modified working electrode and allowed to air dry before introducing the supporting electrolyte and beginning the experiment. Hence, this method was implemented initially for the green tea, prior to 2D-LC analysis. Figure 5.11 shows the cathodic EC-SERS spectra of the pure green tea measured this way; it can be noticed that no compounds were detected,

only noise was recorded. As these molecular components in green tea are water soluble, when the 0.1 M NaF is added to the electrochemical cell, it is likely that the green tea components that were previously dried onto the electrode simply diffuse into the bulk of solution, and thus cannot be detected using SERS. Additionally, since the sample size of green tea deposited onto the electrode is very small (5 µL), the concentration of compounds is low. Thus, it was decided to prepare the electrolyte solution using the green tea directly to reduce diffusion from the surface.

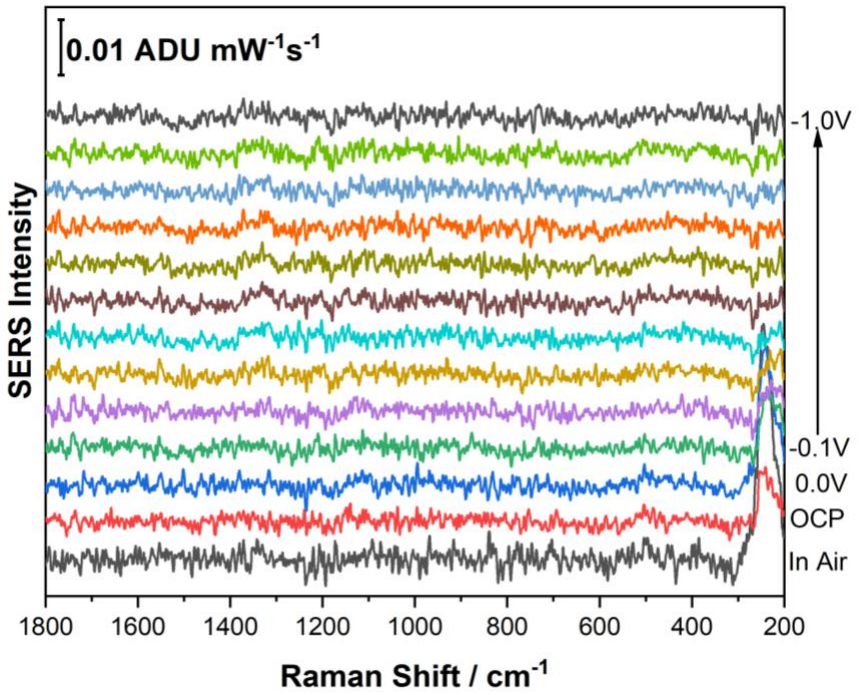

Figure 5.11: EC-SERS analysis of 5 microliters of green tea on the surface of AgNP coated screen-printed electrode (Cathodic, 0.1 V stepwise progression from 0 V to -1.0 V and Anodic, 0.1 V step-wise progression from 0 V to -1.0 V) using an excitation wavelength of 780 nm with a laser power of 80 mW and acquisition time of 30 seconds.

5.1.2.4 25 mL Green Tea + 0.1 M Sodium Fluoride Electrolyte

To improve the likelihood of collecting an EC-SERS signal for the green tea, the supporting electrolyte was prepared as followed: enough solid NaF was added a 25 mL solution of green tea to make 0.1 M NaF electrolyte. This would ensure that the solution concentration was high in green tea components while also ensuring that the ionic strength of the solution was high enough

for electrochemical studies. This solution was then purged with argon to remove any dissolved oxygen. Roughly two milliliters of this solution were then added into the electrochemical cell containing the modified SPE and EC-SERS was performed. Figure 5.12 shows the cathodic and anodic plot of the analysis of green tea mixed with 0.1 M sodium fluoride. Throughout the analysis during both cathodic and anodic progressions, signal is successfully observed. Compounds found in the green tea solution can adhere to the working electrode through electrostatic interactions. The change in peak intensity occurs because either there is an increase in surface concentration of the detected compound or there is a reorientation of the compound on the surface due to the applied potential. Additionally, there are new peaks being introduced while others are disappearing, indicating possibly compounds are adsorbing or desorbing from the surface and/or there is some redox chemistry taking place. Table 5.5 lists many of the peaks produced in the EC-SERS analysis of green tea and their tentative assignments, which are consistent with the SERS analysis of green tea.[65] Peaks found in the region of 1430-1625 cm^{-1} are ring carbon-carbon stretching vibrations attributed from benzene compounds which can be strong. There are many compounds found in green tea including catechins and polyphenols that contain benzene rings.[50] Since mixing the green tea with the electrolyte was successful, this method was tried for the remainder of EC-SERS analysis for this thesis research, including for the 2D-LC fractions from the green tea as well as the DOM extract sample.

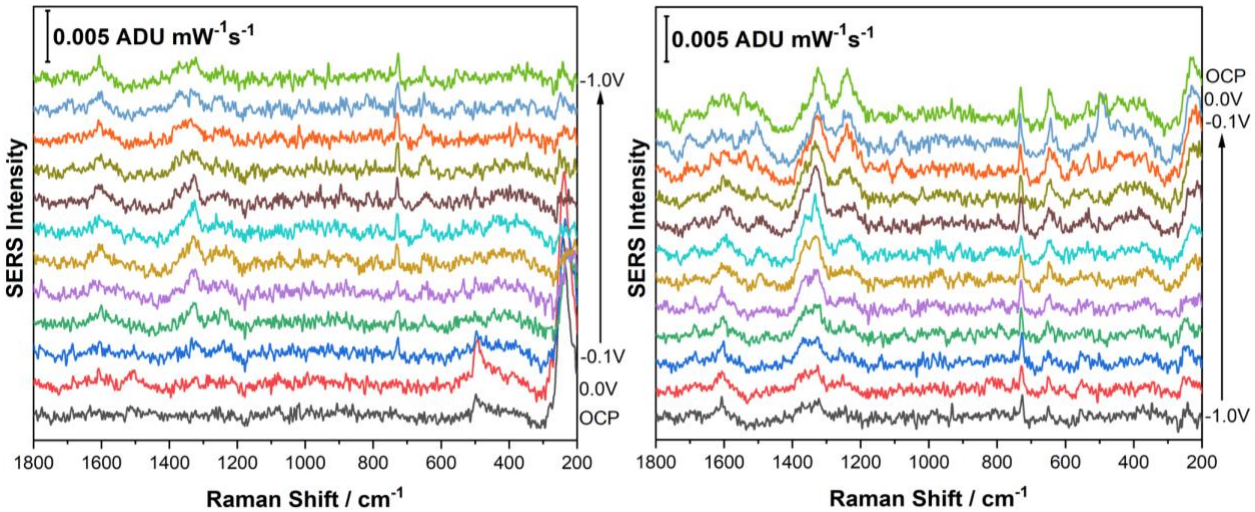

Figure 5.12: EC-SERS analysis of green tea / 0.1 M NaF mixed electrolyte (Cathodic, 0.1 V stepwise progression from 0 V to -1.0 V and Anodic, 0.1 V step-wise progression from 0 V to -1.0 V) using an excitation wavelength of 780 nm with a laser power of 80 mW and acquisition time of 30 seconds.

Table 5.5: SERS Peak Assignment of Green Tea. (δ = bending mode and υ = stretching mode)

Raman Shift (cm^{-1})	**Peak assignments[134]**
229	-
248 & 384	δ(CC) aliphatic chains
495	δ(C–C–O) deformations
532	C–H stretching
650 & 726	C–H stretching, υ(CC) alicyclic, aliphatic chains vibrations
932	υ(C-O-C)
1020	υ(CC) aromatic ring chain vibrations
1231, 1245, 1323 & 1330	υ(CC) alicyclic, aliphatic chains vibrations
1393	$\delta(CH_2, CH_3)$ asymmetric
1494, 1595 & 1607	υ(CC) aromatic ring chain vibrations, υ(C=C)

5.1.2.5 Optimization of EC-SERS Detection of Compounds in 2D-LC Fractions for Green Tea

5.1.2.5.1 5 μL of Cut 2 Dropped Coated on Working Electrode

The collected fraction volumes from the second-dimension separation typically range from 50-250 μL. Ideally, for an EC-SERS offline detection tool, the fraction would be used directly, without the need for pre-concentration. To explore this, 5 μL of the cut 2 extract was applied directly to the modified working electrode of the SPE to see if signal could be detected. Cut 2 was chosen for the initial EC-SERS optimization studies because it had the highest intensity and therefore the highest concentration. After the deposited sample had air dried, EC-SERS was completed in 0.1 M NaF. Peaks appear throughout the EC-SERS spectra, as displayed in Figure 5.13. The detection of compounds is significant because the concentration of these compound(s) is quite low in 2D-LC fractions (~1 ppm[130]) and only five microliters are being drop coated onto the electrode. The peaks present can be from the compound(s) found in cut 2. There is no noticeable interference from the second-dimension mobile phase. However, the intensity of these peaks is weak, less than 0.0025 ADU $mW^{-1}s^{-1}$. This showcases the ultra-sensitivity of EC-SERS. Nevertheless, it would be better to achieve a stronger detection and for that reason further optimization was explored.

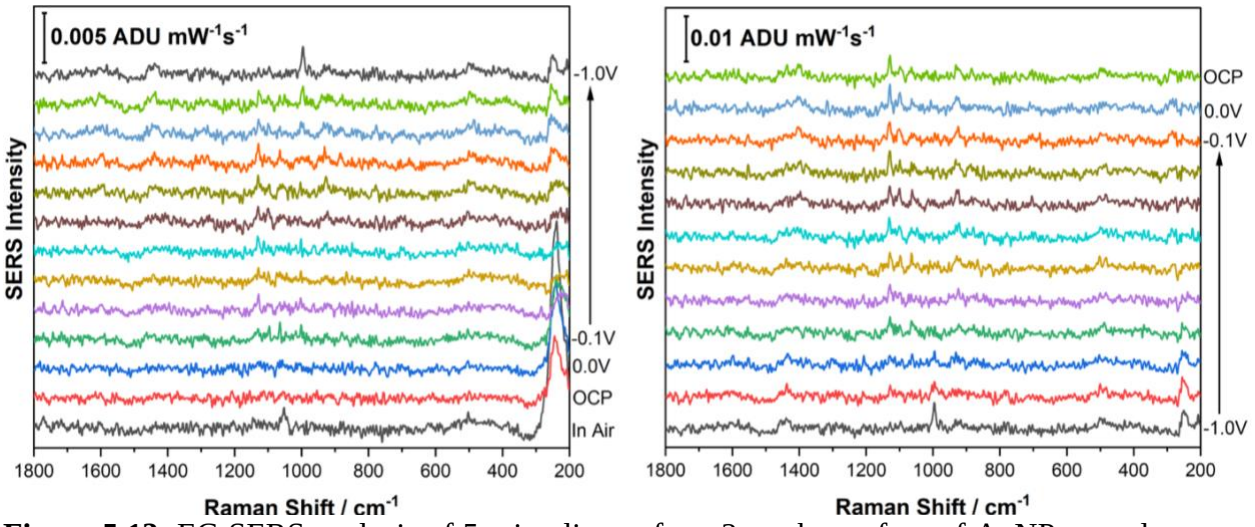

Figure 5.13: EC-SERS analysis of 5 microliters of cut 2 on the surface of AgNP coated screen-printed electrode (Cathodic, 0.1 V stepwise progression from 0 V to -1.0 V and Anodic, 0.1 V step-wise progression from 0 V to -1.0 V) using an excitation wavelength of 780 nm with a laser power of 80 mW and acquisition time of 30 seconds.

5.1.2.5.2 Removal of Solvent in Cut 2

In order to increase the observed signal, evaporating off a portion of the mobile phase was attempted, which would help increase the concentration of the compounds within the cut. To accomplish this, the vial that contained the cut was left in the fume hood overnight. The next day, there was a significant decrease of mobile phase. Afterwards, five microliters of the fraction were drop coated onto the electrode and left to dry. EC-SERS analysis was performed on the sample and, again regrettably, there was no signal produced, indicating that the concentration of the compounds was still too low or that drop-coating the cut onto the electrode and allowing it to dry is not optimal for SERS. It can be noted that for the in-air spectrum in Figure 5.14, some peaks were originally present, and in addition some background fluorescence is observed. This suggests that there are species on the surface initially. However, once the electrolyte is added, the signal is lost, a strong indication that diffusion of weakly bound surface species into the bulk of solution is taking place. Therefore, it was decided that the analyte should be present in the bulk of solution at

a constant concentration, and in order to do this, several cuts would need to be collected and combined as highlighted in the next section.

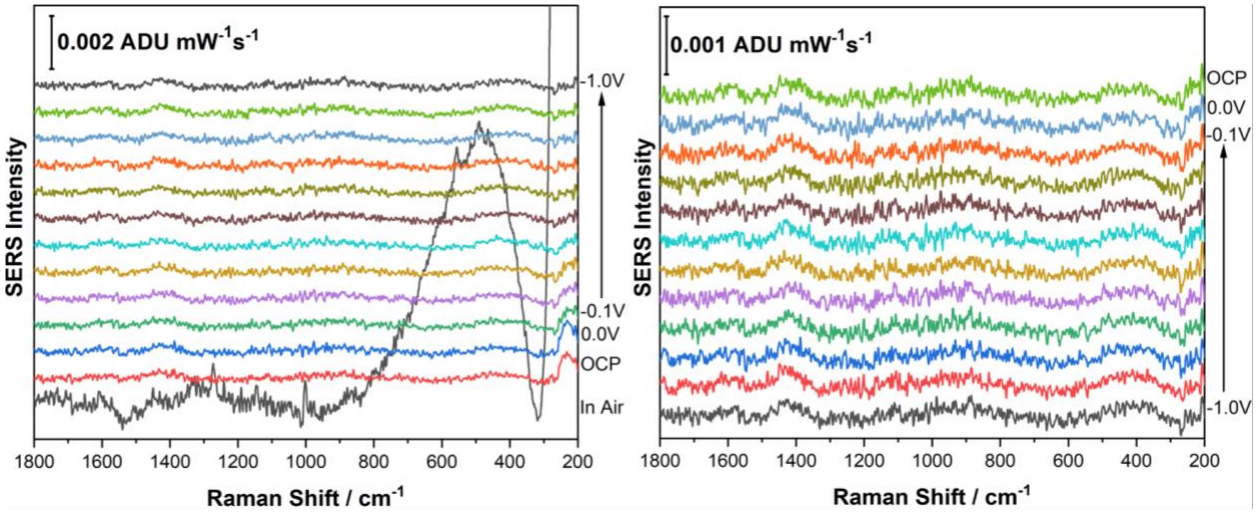

Figure 5.14: EC-SERS analysis of 5 microliters of cut 2 with solvent removed beforehand on the surface of AgNP coated screen-printed electrode (Cathodic, 0.1 V stepwise progression from 0 V to -1.0 V and Anodic, 0.1 V step-wise progression from 0 V to -1.0 V) using an excitation wavelength of 780 nm with a laser power of 80 mW and acquisition time of 30 seconds.

5.1.2.5.3 Collecting 10 Fractions of Green Tea Cuts

After performing a 2D-LC separation of the green tea, certain ^{1}D peaks were chosen as cuts for the second-dimension to collect as fractions. Cuts 1, 2, and 4 in the first-dimension (refer to Figure 5.5 and Table 5.3) were chosen to collect as fractions for EC-SERS analysis because of their high intensity in the second-dimension. Cut 3 in some cases would not be able to be further analysed in the second-dimension because it elutes out very soon after cut 2 in the first-dimension, and the valve would not be able to pick up the cut. Cut 5 was not collected as a fraction because the intensity of the peak was very low in the second-dimension (60 mAU in Figure 5.3) and consequently would not provide a successful EC-SERS analysis. For the EC-SERS analysis of the cuts, one milliliter of the cut and then one milliliter of 0.1 M NaF supporting electrolyte would be added to the electrochemical cell. As a result, in order to collect the required volume of the fraction, several runs were completed, and the fractions were combined.

Figure 5.15 shows the results of the EC-SERS analysis of cut 1. Table 5.6 lists the assignments of peaks observed in the EC-SERS spectra. Some peaks grow in intensity and disappear in the cathodic progression such as 1595 cm^{-1} and 1000 cm^{-1}. From the peak assignment, the compounds present likely contain aliphatic chains, aromatic rings and asymmetric CH_2 and CH_3 functional groups. The peaks found in the region 990-1290 cm^{-1} are due to C-H in-plane deformation vibrations. For example, a strong band at 1000 cm^{-1} may be attributed to mono-, 1,3 di, and 1,3,5 trisubstituted benzenes. It is known that there are many types of catechins present in green tea, however there is not much SERS work done on green tea and no available databases to help identify what compound(s) could be present in this cut. It would be important in the future to purchase catechin standards such as (-)-epicatechin-3-gallate (ECG) and catechin and analyse these standards under the same 2D-LC conditions in both dimensions to try and identify the compounds(s) present in this cut.

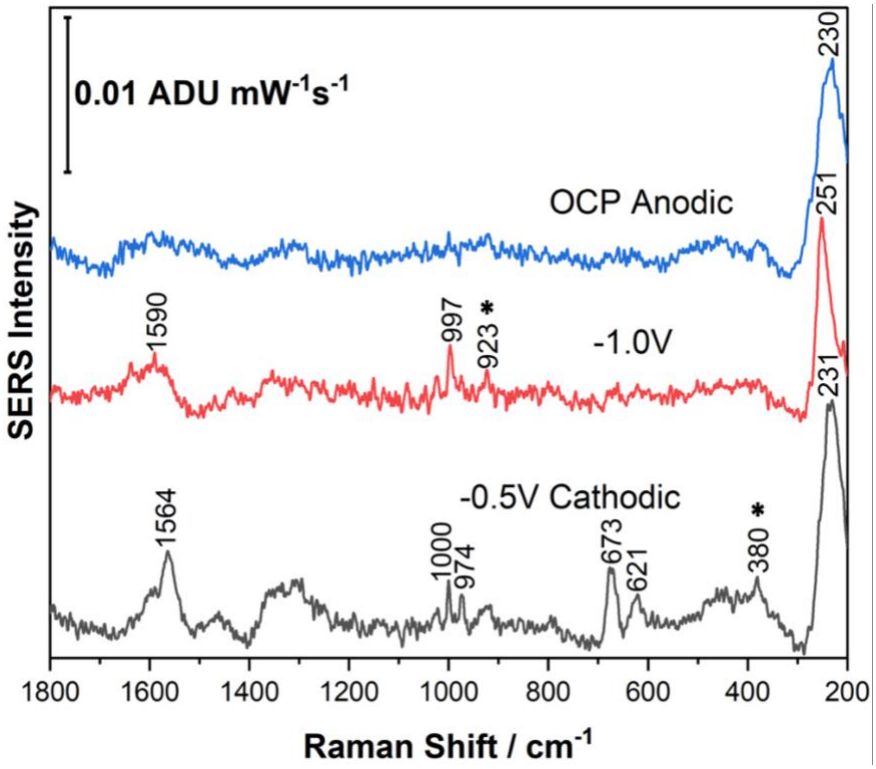

Figure 5.15: EC-SERS analysis of 1 mL of cut 1 mixed with 1 mL of 0.1 M NaF electrolyte (Cathodic, 0.1 V stepwise progression from 0 V to -1.0 V and Anodic, 0.1 V step-wise progression from 0 V to -1.0 V. Asterisks indicate peaks due to second-dimension mobile phase.) An excitation wavelength of 780 nm with a laser power of 80 mW and acquisition time of 30 seconds was used.

Table 5.6: SERS Peak Assignment of Cut 1. (δ = bending mode and υ = stretching mode)

Wavenumber (cm^{-1})	**Peak assignment[134]**
231 - 251	υ(CC) alicyclic, aliphatic chain vibrations
621 & 673	C-H stretching, υ(CC) alicyclic, aliphatic chain vibrations
974 - 1000	υ(CC) alicyclic, aliphatic chain vibrations
1564 - 1590	υ(C=C) & υ(CC) aromatic ring chain vibrations

Figure 5.16 shows the EC-SERS spectra of cut 2. The peak assignment of cut 2 can be found in Table 5.7. It was found that cut 2 indeed contains caffeine, as was highlighted above from the 2D-LC work. This was because the EC-SERS peak comparison with a caffeine standard at a voltage of -0.8 V is in very good spectral agreement, as highlighted in Figure 5.17. Normal Raman

was also performed on solid caffeine (Figure 9.1 in appendix) which contained peaks that were found in cut 2 when EC-SER was performed. However, caffeine is not the only compound in this cut; acetonitrile from the mobile phase is of course present with peaks at 380 cm^{-1} and 923 cm^{-1}, and 1475 cm^{-1} (as indicated with asterisks in Figure 5.16). Table 5.7 contains the peaks found in caffeine that are found in cut 2.[135]

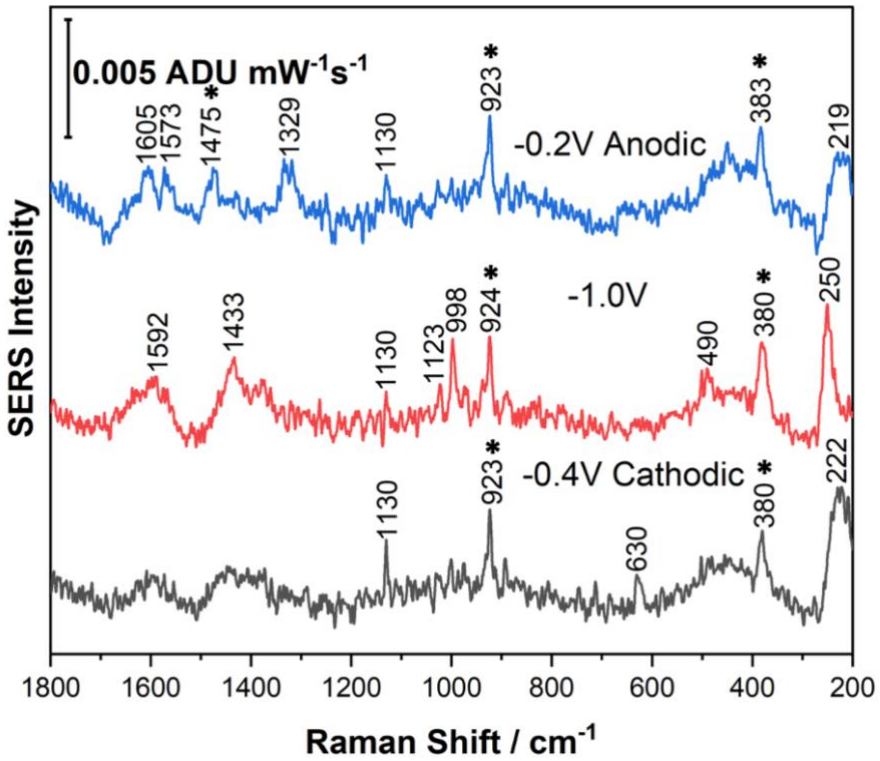

Figure 5.16: EC-SERS analysis of 1 mL of cut 2 mixed with 1 mL of 0.1 M NaF electrolyte (Cathodic, 0.1 V stepwise progression from 0 V to -1.0 V and Anodic, 0.1 V step-wise progression from 0 V to -1.0 V. Asterisks indicate peaks due to second-dimension mobile phase.) An excitation wavelength of 780 nm with a laser power of 80 mW and acquisition time of 30 seconds was used.

Table 5.7: SERS Peak Assignment of Cut 2. (δ = bending mode and υ = stretching mode)

Wavenumber (cm^{-1})	Peak assignment[134]
219 - 250	-
490	δ(C–C–O) deformations
630	υ(CC) alicyclic, aliphatic chain vibrations
998	υ(CC) alicyclic, aliphatic chain vibrations
1123 & 1130	υ(CC) alicyclic, aliphatic chain vibrations
1329	υ(CC) alicyclic, aliphatic chain vibrations
1433	δ(CH2) & δ(CH3) asymmetric
1574 - 1605	υ(C=C) & υ(CC) aromatic ring chain vibrations

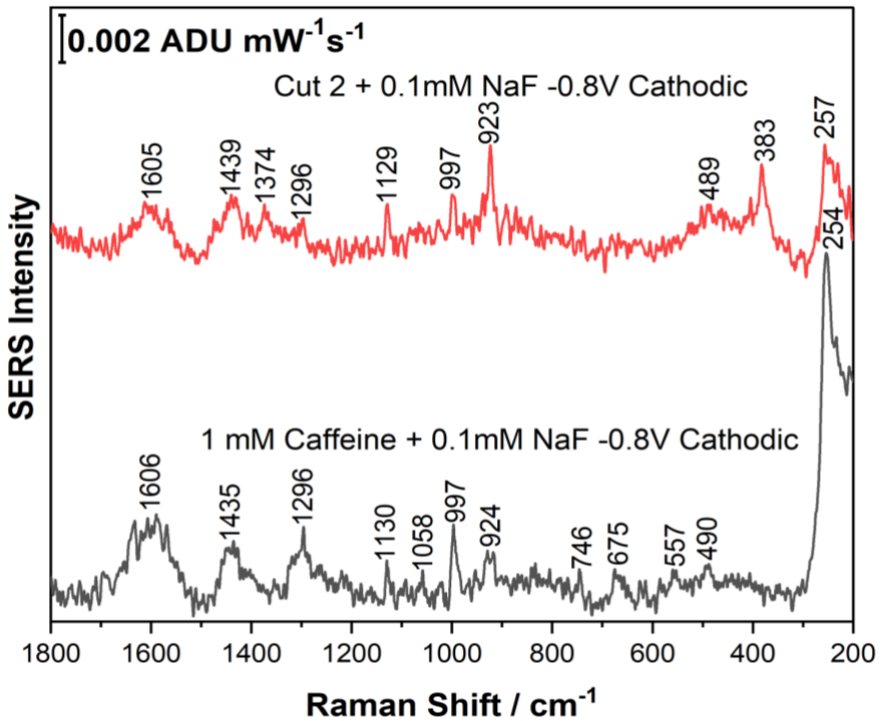

Figure 5.17: Comparison of EC-SERS spectra of 1mM caffeine standard and cut 2 at 0.5 V during the cathodic progression using an excitation wavelength of 780 nm with a laser power of 80 mW and acquisition time of 30 seconds.

The last cut that was analysed using EC-SERS was cut 4 as shown in Figure 5.18 and a table of peak assignments for this cut can be found in Table 5.8. There are several peaks present in cut 4 that are present in the other cuts such as ~ 612 cm^{-1} and ~1000 cm^{-1}, meaning that the compounds found in each of the three cuts may be similar to one another and may have similar functional groups. Similarly to cut 1, it would be useful to obtain catechin standards and have the results compared to the cuts to see of these catechins are present in this green tea.

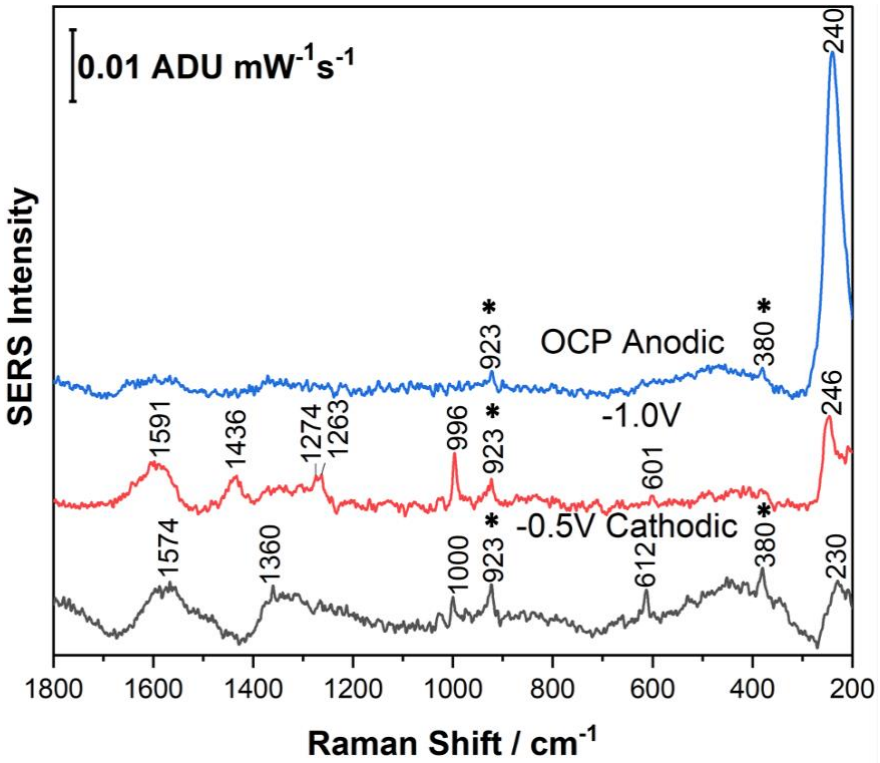

Figure 5.18: EC-SERS analysis of 1 mL of cut 4 mixed with 1 mL of 0.1 M NaF electrolyte (Cathodic, 0.1 V stepwise progression from 0 V to -1.0 V and Anodic, 0.1 V step-wise progression from 0 V to -1.0 V. Asterisks indicate peaks due to second-dimension mobile phase.) An excitation wavelength of 780 nm with a laser power of 80 mW and acquisition time of 30 seconds was used.

Table 5.8: SERS Peak Assignment of Cut 4. (δ = bending mode and υ = stretching mode)

Wavenumber (cm^{-1})	Peak assignment[134]
601 & 612	υ(CC) alicyclic, aliphatic chain vibrations
996 & 1000	υ(CC) aromatic ring chain vibrations
1263 & 1274	υ(CC) alicyclic, aliphatic chain vibrations
1360	δ(CH3)
1436	δ(CH2) & δ(CH3) asymmetric
1574 & 1591	υ(C=C) & υ(CC) aromatic ring chain vibrations

5.1.2.6 Mass Spectrometry

5.1.2.6.1 2D-LC fractions of Green Tea

Mass spectrometry was performed on cuts 1, 2 and 4 to help figure out what could be in these cuts through the use of a mass spectrometry database (NIST). MS was also performed on the second-dimension mobile phase which can be found in the appendix as Figure 9.2; this was collected as a reference. Figure 5.19 shows the mass spectrum of cut 2 with the peaks found in the second-dimension mobile phase spectrum previously subtracted to only show the peaks that were only found in cut 2. Figure 5.19, which compares the MS signal for cut 2 with a caffeine standard, indicates that cut 2 does indeed contain caffeine. The mass spectra for cuts one and four can be found in the appendix with Figure 9.3 and 9.4. It was challenging to determine what was in cuts one and four with the database comparison because the results provided from the database did not make sense (for example, suggesting narcotics present in the green tea). In addition, the comparison with the database was not as strong for these two cuts as it was for cut 2. The NIST database only contains (+)-catechin and (-)-epicatechin that are found in green tea and not others

such as (-)-epigallocatechin or (-)-epicatechin-3-gallate which can limit the identification of the compounds found in the cuts. Additionally, figuring out what could be in the cuts with MS can be challenging because the compounds within the cut might not have a high enough concentration or may contain more than one compound. Alternatively, the MS parameters chosen for this analysis might not have been the best and may have to be optimized in future studies.

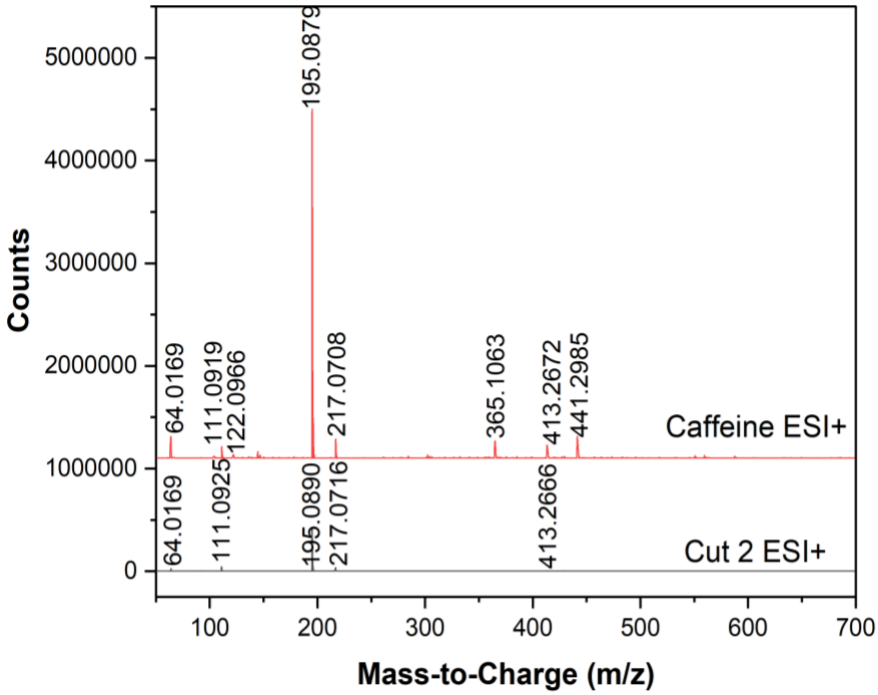

Figure 5.19: Comparison of ESI-Q-TOF MS/MS spectra of cut 2 and caffeine in positive mode.

5.1.2.7 Conclusion for Green Tea

Green tea was used for 2D-LC and EC-SERS method development for eventual DOM studies. Various parameters such as flow rate and mobile phase composition were optimized to achieve a good separation of green tea in the first- and second-dimensions. Subsequently, to successfully perform EC-SERS on green tea, it had to be mixed with the sodium fluoride electrolyte because drop coating of the green tea onto the electrode resulted in diffusion of the components into the electrolyte, and therefore, loss of signal. Therefore, the cuts taken from the 2D-LC were also combined with the electrolyte in order to do EC-SERS successfully. In conclusion, green tea was

used to showcase the offline combination of 2D-LC-EC-SERS, where caffeine was successfully identified in the green tea. ESI-MS was helpful in validating that caffeine was indeed in cut 2. At this point in the thesis work, 2D-LC-EC-SERS was explored to characterize dissolved organic matter (DOM) extracted from the Sackville River.

5.2 Dissolved Organic Matter Without Acidification before SPE

5.2.1 Solid Phase Extraction

For sample collection, the Sackville Trail site was chosen as indicated by the red circle in Figure 5.20. This site was chosen because there is a bridge present, and sampling from the bridge would avoid any disturbance of the river bottom sediment. The conditions during the time of sampling are presented in Table 5.9. It was important to collect the sample on a day without a precipitation event so as to avoid contamination of the river water from the runoff of precipitation. Five liters of water were collected from the Sackville Trail site and the DOM was concentrated using solid phase extraction. Five liters of water was filtered with combusted 0.7 μm filters and then the filtrate went through the SPE cartridge. The DOM was extracted from the SPE cartridge with twenty milliliters of methanol at a flow rate of one to two mL/minute. The DOM extract was a clear yellow solution as shown in Figure 5.21.

Table 5.9: Conditions of Sackville River Water Sampling.

Date	**January 5th, 2022**
Time	8:30 am
Coordinates	44.75, -63.66
Weather	Overcast
Air Temperature	0 °C
Relative Humidity	68%

Figure 5.20: Map of the Sackville River with the Sackville trail sampling site circled in red.

Figure 5.21: Image of DOM extract from SPE cartridge.

5.2.2 UV-Vis Spectroscopy

UV-Vis absorbance spectroscopy is an important technique used for DOM analysis.[32] Therefore, UV-Vis analysis was completed with the DOM extract obtained from the Sackville River water as shown in Figure 5.22. There are various absorption ratios used in DOM studies to explore the sources and the composition of chromophoric DOM (CDOM). Absorption ratios are defined as the ratios of the absorption coefficients at two different wavelengths. The absorbance ratio $\frac{A_{250}}{A_{365}}$ ($\frac{E2}{E3}$), is used to characterize the molecular size of CDOM found within the DOM sample.[29] $\frac{E2}{E3}$ is an inverse proxy for DOM molecular weight and as DOM molecular weight increases, $\frac{E2}{E3}$ tends to decrease.[136] Alternatively, $\frac{A_{254}}{A_{436}}$ is used to determine the sources and aromaticity such as an estimate of the relative composition of autochthonous versus terrestrial DOM.[29] Another absorption ratio, $\frac{A_{340}}{A_{254}}$ ($\frac{E3}{E4}$) is used to predict the dissolved organic carbon (DOC) concentration. The values for these ratios of the DOM sample extracted from the Sackville River are found in Table 5.10. The values were found to be in agreement with the ranges found in the literature.[29] A low $\frac{A_{250}}{A_{365}}$ ratio indicates less labile DOM present in the sample.[137] DOM being considered as labile means that the DOM is readily available for organisms to use.[138] A high $\frac{A_{254}}{A_{436}}$ reflects that the DOM found in the Sackville River is produced from autochthonous sources.[139] The value for $\frac{A_{340}}{A_{254}}$ was 0.31, indicating that the concentration of DOC in the water sample is moderate.

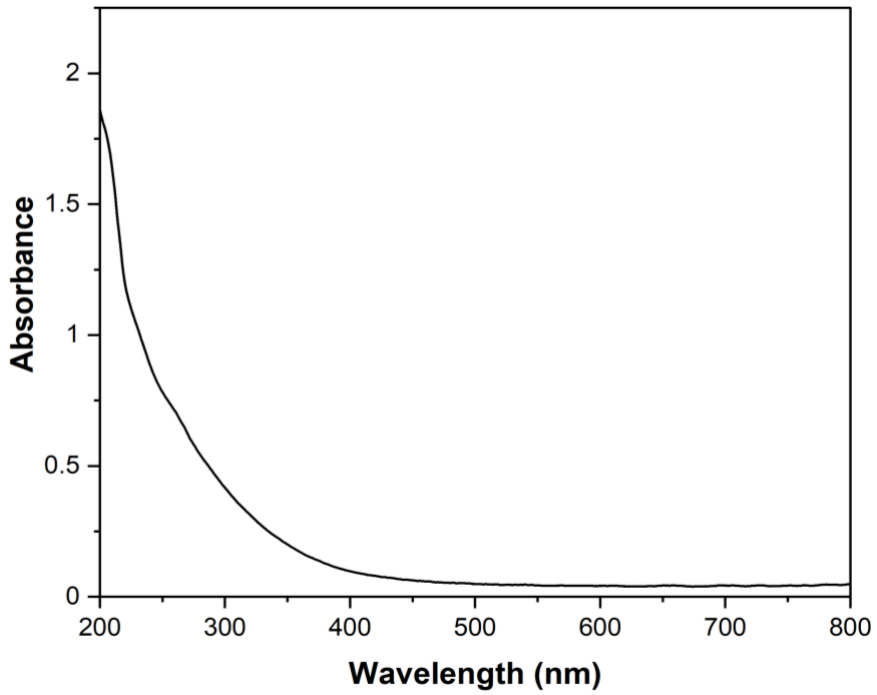

Figure 5.22: UV-Vis absorbance spectrum of DOM extract of from the Sackville Trail.

Table 5.10: Calculated Absorbance Ratios of Sackville River DOM.

Type	Absorbance ratio	Value	Literature Value[29]
$\frac{E2}{E3}$	$\frac{A_{250}}{A_{365}}$	4.93	4.16-5.72
$\frac{E2}{E4}$	$\frac{A_{254}}{A_{436}}$	10.73	4.37-11.34
$\frac{E3}{E4}$	$\frac{A_{340}}{A_{254}}$	0.31	0.20-0.38

5.2.3 2D-LC

5.2.3.1 First-Dimension Separation of DOM

The DOM extracted from the five liters of river water using solid phase extraction was used for 2D-LC analysis. The method established for green tea separation in the first-dimension as listed in Table 4.4 was first used for the separation of the DOM extract. Consistent with the green tea studies, an injection volume of five microliters was used. Figure 5.23 shows the first-dimension chromatogram. A large broad peak is present at 4 minutes and remains until the run-time is finished

at 15 minutes, therefore this method does not provide a sufficient separation for this DOM extract. This broad feature is commonly observed when performing chromatography on DOM samples and represents many unresolved peaks that co-elute in the middle region of the chromatogram of the applied methanol gradient, suggesting the analyte has intermediate polarity.[8,24,26] There are some unretained peaks eluting at the beginning of the chromatograms indicating the presence of a fraction of highly polar organic material.

Band broadening occurs when the rate of mass-transfer processes is slow between the mobile and stationary phases while a solute migrates through the column. Ways to fix band broadening are to (i) change the mobile and/or stationary phase and (ii) adjust the gradient as well as to (iii) adjust the mobile phase flow rate. Another feature to note in Figure 5.23 is that the run-time is possibly not long enough to finish the separation as there is a peak that is eluting before the run-time is finished. Therefore, several parameters were explored in an effort to try and improve the separation of DOM in the first-dimension.

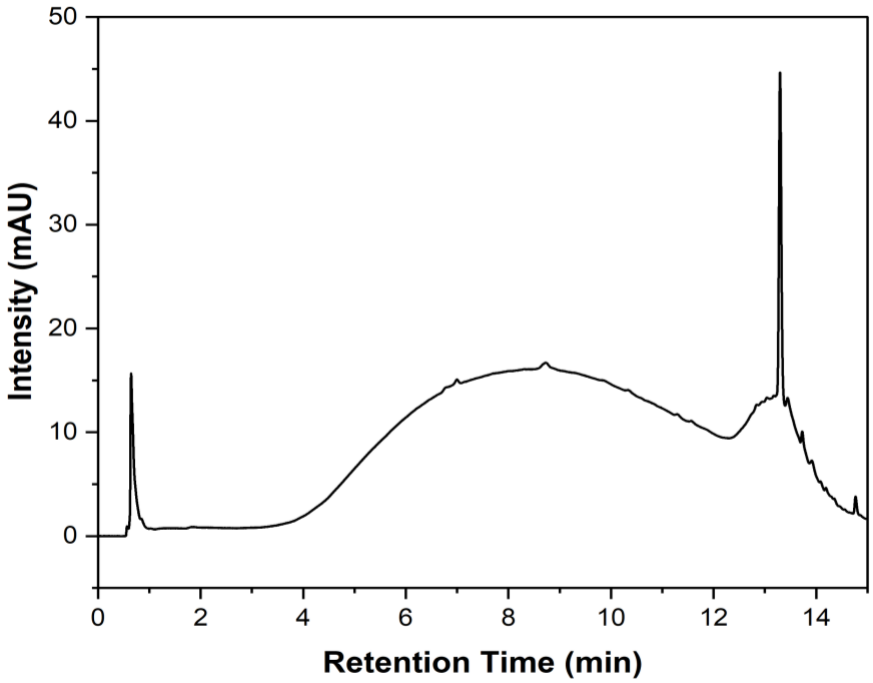

Figure 5.23: [1]D chromatogram of DOM extract at 254 nm. Milli-Q water and methanol used for the mobile phase. Injection volume was 5 μL.

5.2.3.1.1 Mobile Phase

Acetonitrile was used in place of methanol for the organic portion of the mobile phase and the run-time was increased to 32 minutes with the following gradient (Table 5.11).

Table 5.11: Gradient Parameters in the First-Dimension Separation of DOM.

Minute	Composition of Acetonitrile
0 min	5%
30 min	95%
32 min	95%

Acetonitrile was chosen because it is very commonly used as part of the mobile phase, especially in DOM chromatography research.[8,140,141] Methanol was used to extract the DOM from the SPE sorbent. Hence, using methanol as part of the mobile phase may not be the best choice for the organic component of the mobile phase. Figure 5.24 shows the chromatogram when acetonitrile was used as the organic portion of the mobile phase. When using acetonitrile, the width of the large peak was reduced but once again most of the detectable DOM components eluted as an unresolved hump earlier in the run-time. Additionally, there is again a large unretained peak eluting at the beginning of the chromatogram. One way to help resolve the coelution issue is to try and adjust the mobile phase gradient and/or composition.

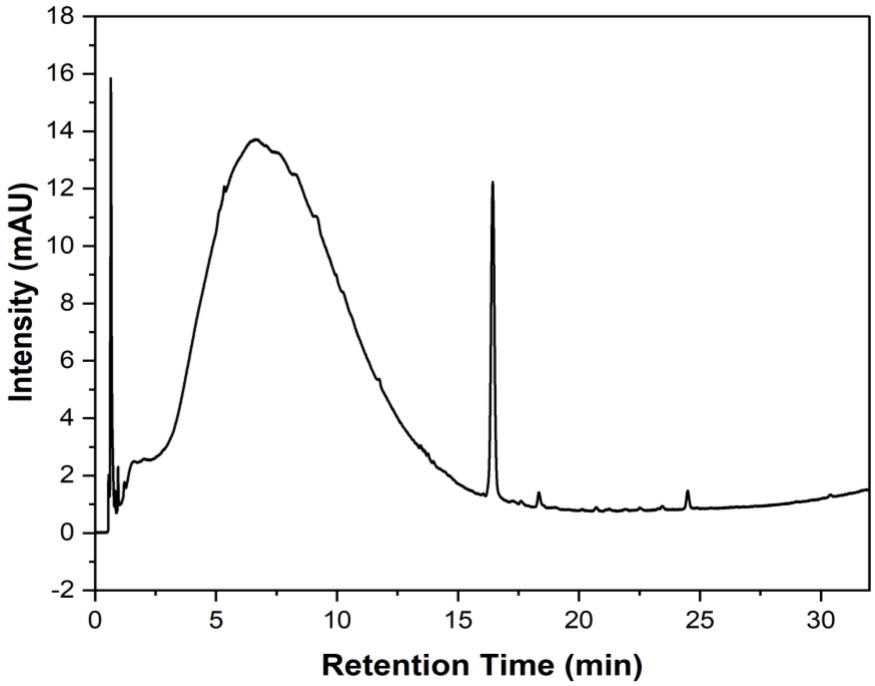

Figure 5.24: [1]D chromatogram of DOM extract at 254 nm. Milli-Q water and acetonitrile used for the mobile phase. Injection volume was 5 μL.

5.2.3.1.2 Mobile Phase Gradient and Composition Adjustment

Because compounds within the hump elute when there is a high organic content in the mobile phase, the gradient was changed to reflect this as shown in Table 5.12. While this change may help with the separation, all the compounds eluted out as one peak within the first two minutes of the run-time, which in turn, increased the intensity of the peaks (as shown in Figure 5.25). The run-time was reduced to 17 minutes as well because a longer run-time was no longer needed.

Table 5.12: Gradient Parameters in the First-Dimension Separation of DOM.

Minute	Composition of Acetonitrile
0 min	70%
15 min	95%
17 min	95%

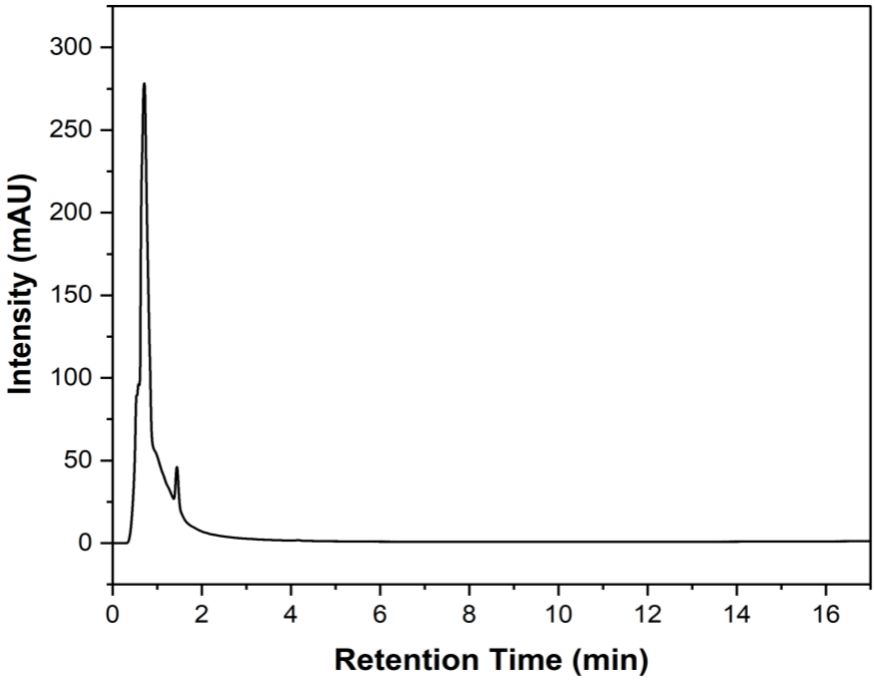

Figure 5.25: [1]D chromatogram of DOM extract at 254 nm. Milli-Q water and acetonitrile used for the mobile phase. Injection volume was 5 μL.

Subsequently, the organic phase was adjusted between 5% and 70% at 0 minute, therefore 20% acetonitrile was used. Hence, a new gradient was established that is listed in Table 5.13.

Table 5.13: Gradient Parameters in the First-Dimension Separation of DOM.

Minute	Composition of Acetonitrile
0 min	20%
15 min	95%
17 min	95%

Figure 5.26 is the chromatogram for the separation of compounds within the DOM extract with the following gradient changes of the mobile phase. The hump is no longer present and has severely flattened out, meaning that the compounds are not eluting all at once but rather over a longer time. The second peak that eluted has significant tailing as well which leads into coelution

with the flattened hump. Therefore, this change of gradient does not provide suitable results and needs to be further optimized.

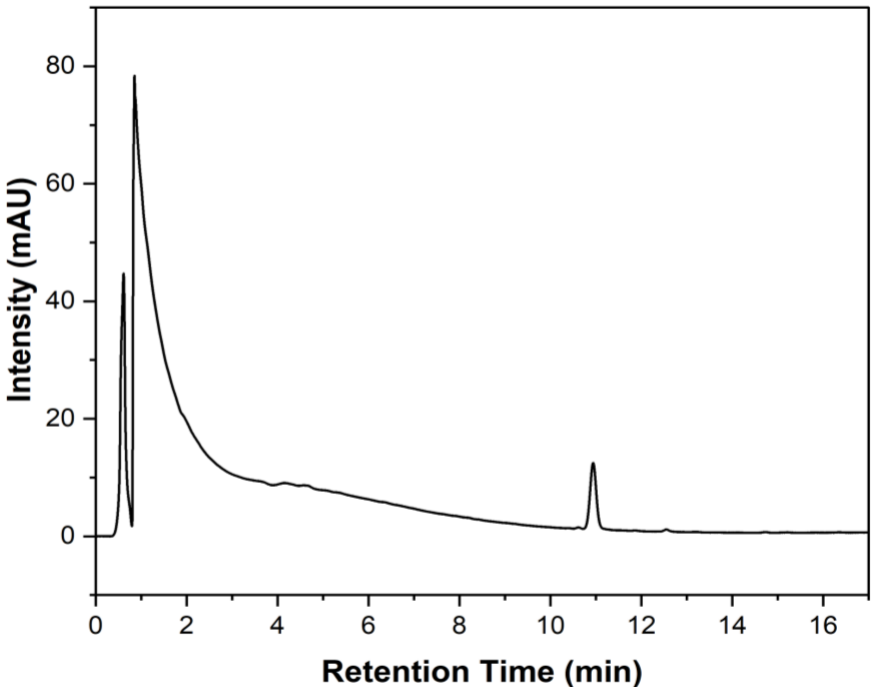

Figure 5.26: [1]D chromatogram of DOM extract at 254 nm. Milli-Q water and acetonitrile used for the mobile phase. Injection volume was 5 μL.

Acids are very often used in chromatographic mobile phases as they help with the resolution of the separation, providing sharper, more well resolved peaks. Acids deliver better peak shape because adding acidity to the mobile phase will help the silanol groups within the stationary phase be slightly suppressed of ionization. Formic acid is heavily used as a mobile phase additive for many chromatographic methods and therefore, formic acid was added to both the aqueous and organic portion of the mobile phase for this research. It can be observed in Figure 5.27 that when formic acid was added it did indeed sharpen the peaks. The hump that was not previously viewed in the last chromatogram is now present. Additionally, the two peaks in the beginning of the run are noticeably sharper with the second peak experiencing less tailing. Consequently, it was confirmed that adding an acid such as formic acid does improve peak shape and it was kept in the mobile phase for further separations in the first-dimension.

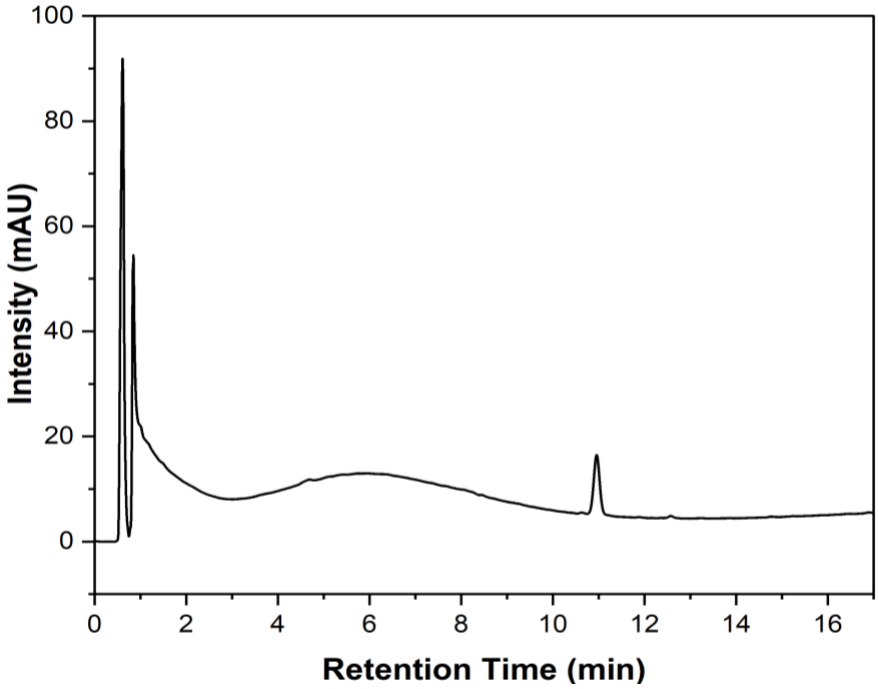

Figure 5.27: [1]D chromatogram of DOM extract at 254 nm. Milli-Q water + 0.1% formic acid and acetonitrile + 0.1% formic acid used for the mobile phase.

The gradient was changed once more to try and increase the intensity of the hump and possibly get a better separation in the first-dimension before trying the second-dimension for further separation. It is important to have a high intensity for the peaks of interest in the first-dimension because the concentration of these peaks will be severely diluted in the second-dimension, which would lead to harder detection and identification of the separated compounds. The new gradient parameters are in Table 5.14.

Table 5.14: Gradient Parameters in the First-Dimension Separation of DOM.

Minute	Composition of Acetonitrile
0 min	20%
1 min	50%
4 min	70%
15 min	95%

These parameters were chosen because it was thought that increasing the organic phase earlier in the run-time would help with the separation of the hump and its intensity. The changes in gradient did lead to increasing the intensity of peaks but did not help improve the separation of the hump as shown in Figure 5.28. However, the hump is not as broad as was observed previously. At this point in the thesis research, method optimization for the DOM first-dimension separation, while not perfect, was deemed good enough for second-dimension exploration.

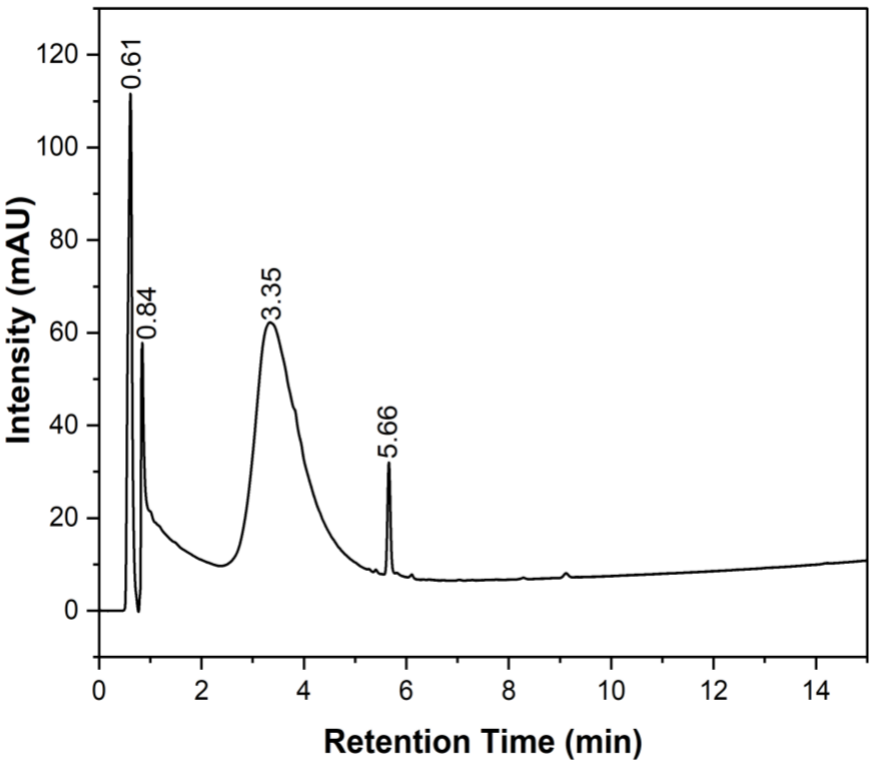

Figure 5.28: [1]D chromatogram of DOM extract at 254 nm. Milli-Q water + 0.1% formic acid and acetonitrile + 0.1% formic acid used for the mobile phase. Injection volume was 5 μL.

5.2.3.2 Second-Dimension Separation of DOM

Even though the intensities of the peaks in the first-dimension are not high, the second-dimension was attempted regardless. The first three peaks (0.61 min, 0.84 min and 6.36 min) were chosen because they had higher intensities compared to the fourth peak which only had an intensity of 30 mAU and would not be worth trying to further separate in the second-dimension. Figure 5.29 highlights which peaks were chosen in the first-dimension chromatogram to be analysed in the second-dimension. The second-dimension parameters used for this separation are the same that was used for green tea in the second-dimension as well and can be found in Table 4.5. The second-dimension chromatograms in Figure 5.29 emphasize how low the intensities are (below 4 mAU), therefore, the concentration of the separated compounds is very low, leading to challenging detection of these compounds. However, there is a separation occurring for each of the cuts in Figure 5.29 because there are many peaks found in the cuts chromatograms. Therefore, Figure

5.29 demonstrates how 2D-LC is useful for further separation of these DOM components. For further work and optimization, it is imperative that the concentration of DOM be increased. This could include, for example, putting larger volumes of water through the SPE cartridge as well as using less methanol for extraction. In addition, acidification of the water prior to running it through the SPE may be helpful.

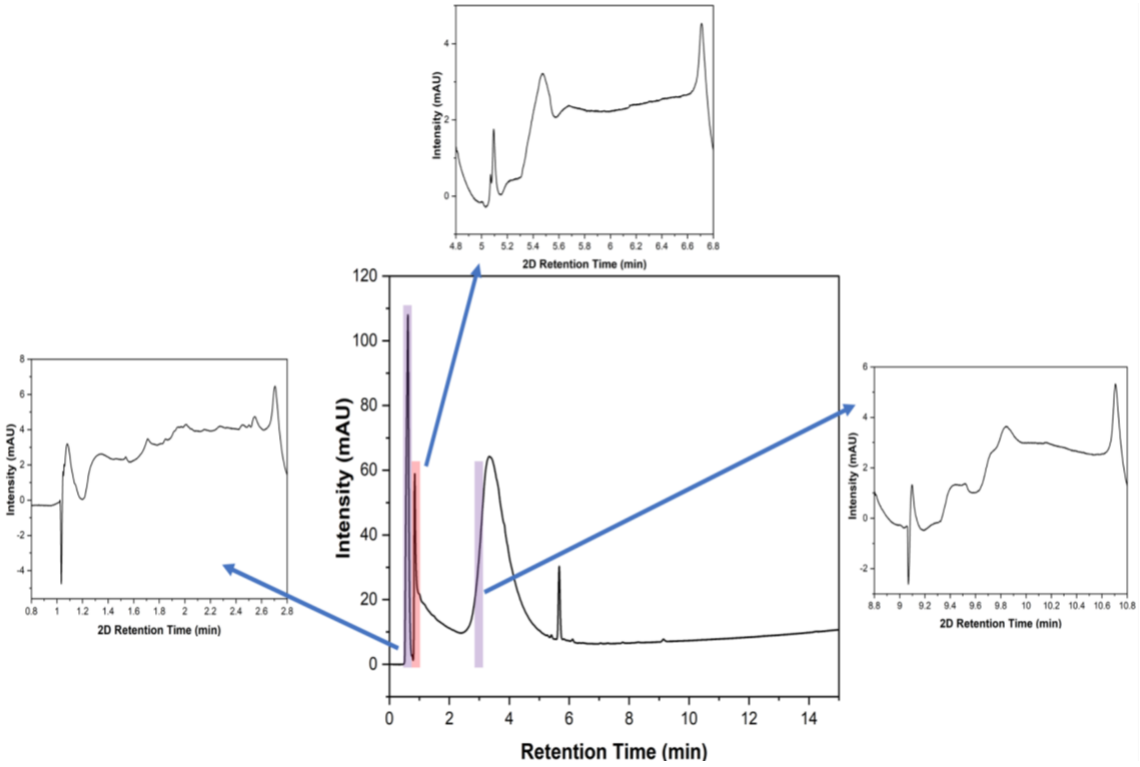

Figure 5.29: Chromatogram of DOM extract in the first-dimension (centre) and chromatograms in the second-dimension of cuts highlighted from the first-dimension at 254 nm. 1:9 acetonitrile/Milli-Q water (v/v) with 5 mM ammonium acetate buffer and 9.5:0.5 acetonitrile/Milli-Q water (v/v) with 5 mM ammonium acetate buffer used for the second-dimension mobile phase.

Once the final first-dimension LC method was developed, it was important to run a control study of the blank containing only methanol that was run through a SPE cartridge after being conditioned. Figure 5.30 is the chromatogram of the three runs of the blank with the retention times of the peak stated above. The intensities of the peaks are small, all below 20 mAU which is good because when the DOM sample was analysed, the peaks of interest had an intensity of above 20

mAU. However, an interesting observation is that there really should not be this many peaks found in the chromatogram for the blank, suggesting that there could be potential blank contamination into the solvent.

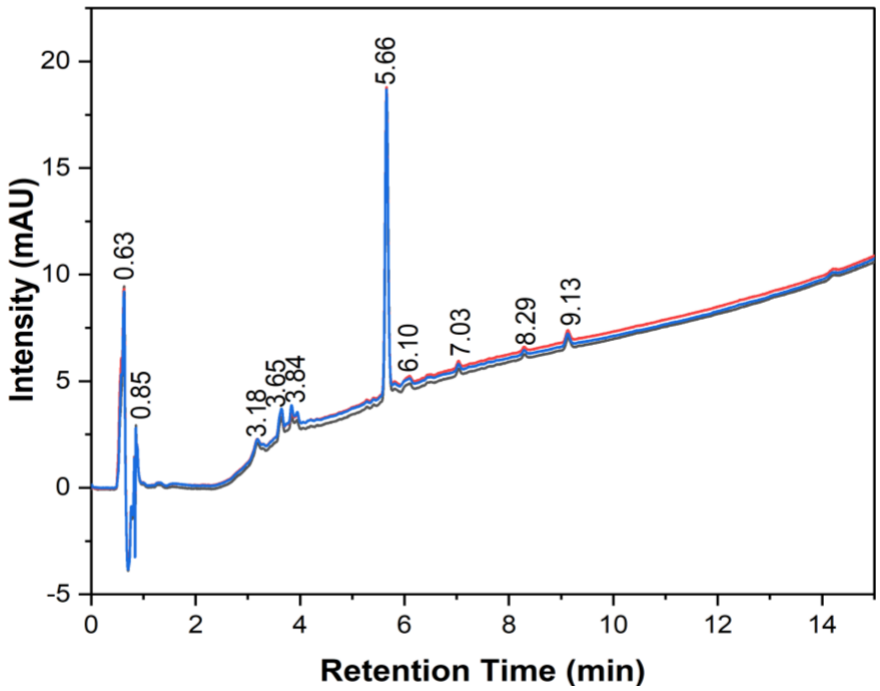

Figure 5.30: [1]D chromatogram of three trials of SPE control at 254 nm. Milli-Q water + 0.1% formic acid and acetonitrile + 0.1% formic acid used for the mobile phase.

Figure 5.31 is a comparison of chromatograms of the SPE control and DOM extract. Unfortunately, there are many peaks present in both chromatograms, suggesting that many of the peaks separated in the DOM extract are not of importance since they are also found in the control study. The only peak that is of interest is the large, broad unresolved peak centered at 3.30 minutes. In addition, the intensity of this peak is very low, implying that there is not a large concentration of compound(s) eluted in this peak. However, it was found that it is important to acidify the water before SPE, which helps the compounds in the water to bind to the sorbent before extraction. For example, Dittmar *et al.* acidified their DOM water samples to pH 2 to 2.6 with 6 N HCl prior to SPE.[19] Acidification has been shown to increase retention of natural organic matter, especially phenolic and carboxylic components, onto hydrophobic resins, thus increasing subsequent extract

recoveries.[142] However, acidification of water had not been attempted thus far in this thesis work, meaning that there could have been loss of sample and breakthrough could have occurred.

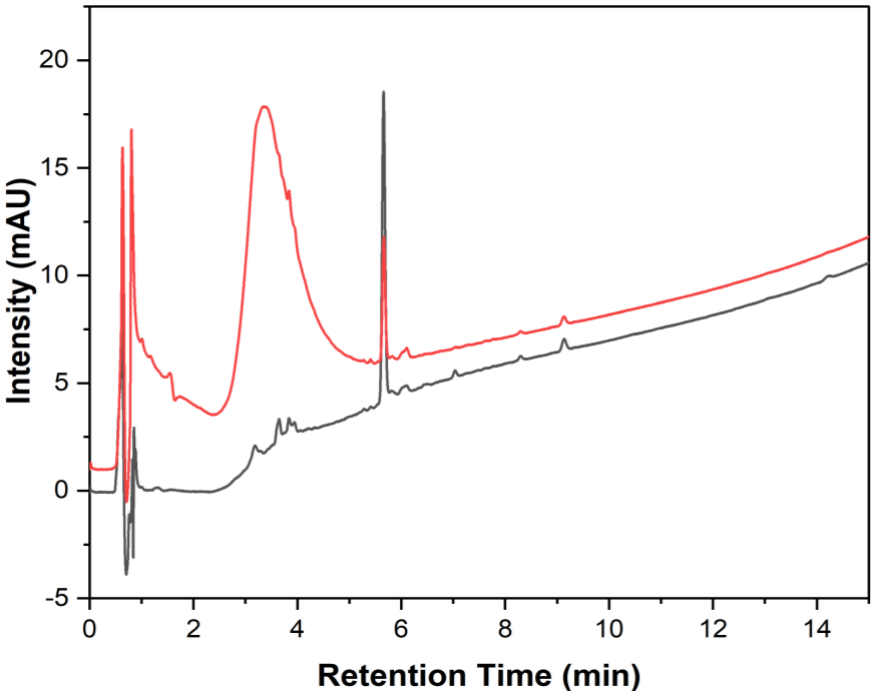

Figure 5.31: Comparison of ^{1}D chromatogram of SPE control (black) and DOM extract (red) at 254 nm. Milli-Q water + 0.1% formic acid and acetonitrile + 0.1% formic acid used for the mobile phase.

5.2.4 EC-SERS

Since the intensities of the peaks in the second-dimension were low, EC-SERS could not be performed on those cuts and was only completed on the DOM extract recovered from the SPE. The same method was done as with the green tea cuts; one milliliter of DOM extract with one milliliter of 0.1 M NaF electrolyte were combined, and EC-SERS measurements were run in this solution. Figure 5.32 provides the EC-SERS spectra for this analysis. Figures 5.33 and 5.34 are the EC-SERS analysis of the SPE control of methanol and the comparison of -0.5V of the DOM extract and the SPE control. It can be observed from the comparison in Figure 5.34 that there are many peaks found in both the SPE control and the DOM extract cathodic spectra, confirming that the compounds in the DOM extract are not present in high enough concentration to be readily

detected. However, the anodic progression of the DOM extract is quite different than the anodic progression of the SPE control. The two main peaks found in the anodic progression (at around 1020 cm^{-1} and 1429 cm^{-1}) of the control study are from the normal Raman of methanol, but for the DOM extract there is more than those two peaks present in the anodic progression, indicating there is another compound being detected besides just the methanol in Figure 5.32. An interesting peak found in both the control study and the DOM extract is the peak at 529 cm^{-1} which contributes to either a disulfide bond or a Si-O-Si bond. The sorbent is composed of a styrene-divinylbenzene polymer modified with a proprietary nonpolar surface. It is possible that the sulfur or silicon might be from the nonpolar surface of the SPE sorbent and somehow was bled out of the cartridge along with the DOM extract during solid phase extraction. This may suggest that further pre-conditioning of the SPE cartridge prior to extraction may be beneficial for 2D-LC studies of DOM.

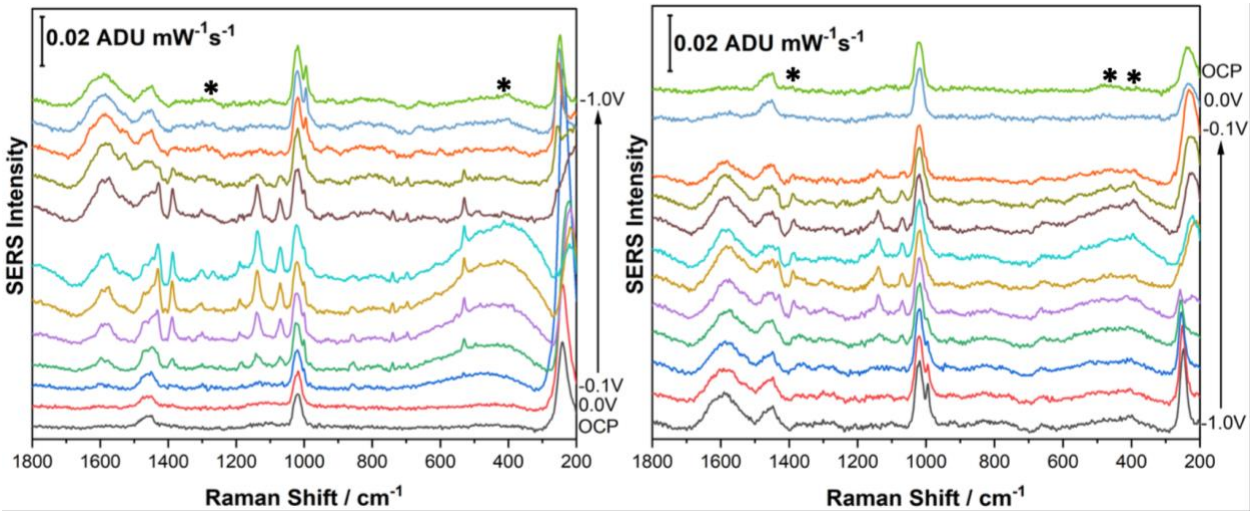

Figure 5.32: EC-SERS analysis of 1 mL of DOM extract mixed with 1 mL of 0.1 M NaF electrolyte (Cathodic, 0.1 V stepwise progression from 0 V to -1.0 V and Anodic, 0.1 V step-wise progression from 0 V to -1.0 V) using an excitation wavelength of 780 nm with a laser power of 80 mW and acquisition time of 30 seconds. Asterisks indicate peaks due to possible DOM compounds.)

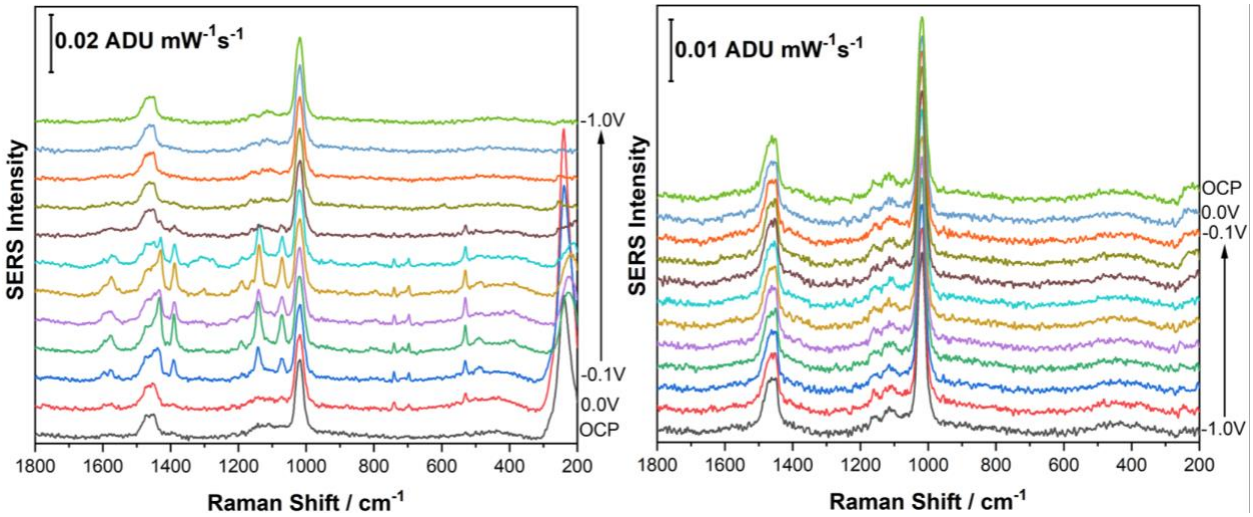

Figure 5.33: EC-SERS analysis of 1 mL of SPE control mixed with 1 mL of 0.1 M NaF electrolyte (Cathodic, 0.1 V stepwise progression from 0 V to -1.0 V and Anodic, 0.1 V step-wise progression from 0 V to -1.0 V) using an excitation wavelength of 780 nm with a laser power of 80 mW and acquisition time of 30 seconds.

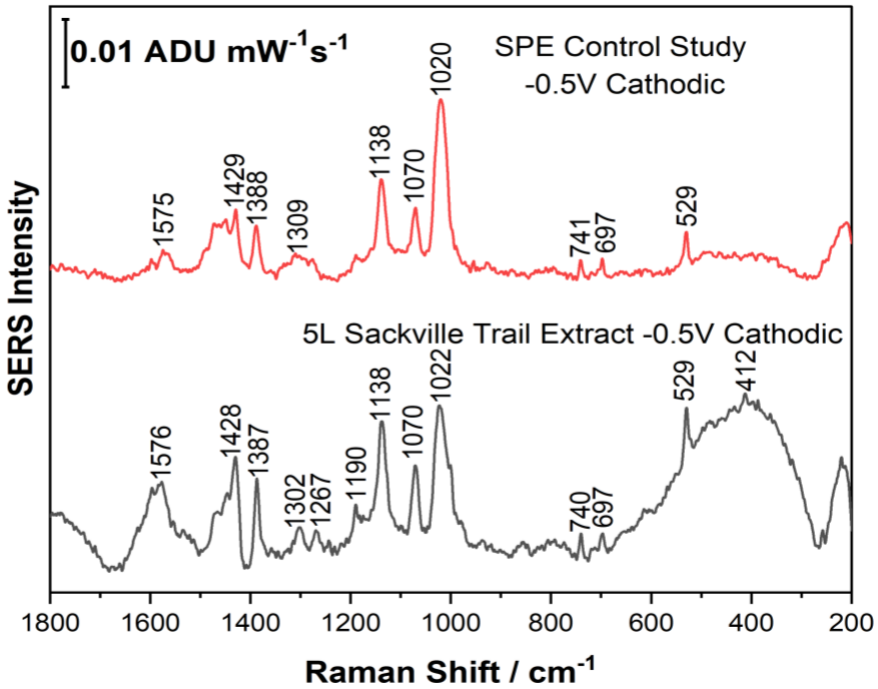

Figure 5.34: Comparison of EC-SERS spectra of DOM extract and SPE control at -0.5 V during the cathodic progression using an excitation wavelength of 780 nm with a laser power of 80 mW and acquisition time of 30 seconds.

5.2.5 Infrared (IR) Spectroscopy

IR spectroscopy was performed on the SPE sorbent to try and figure out what was in the sorbent besides the styrene-divinylbenzene. Figure 5.35 is the IR spectrum and Table 5.15 lists the peak assignment of the SPE sorbent. Most of the peaks are contributed from the polymer and so did not provide any additional information.

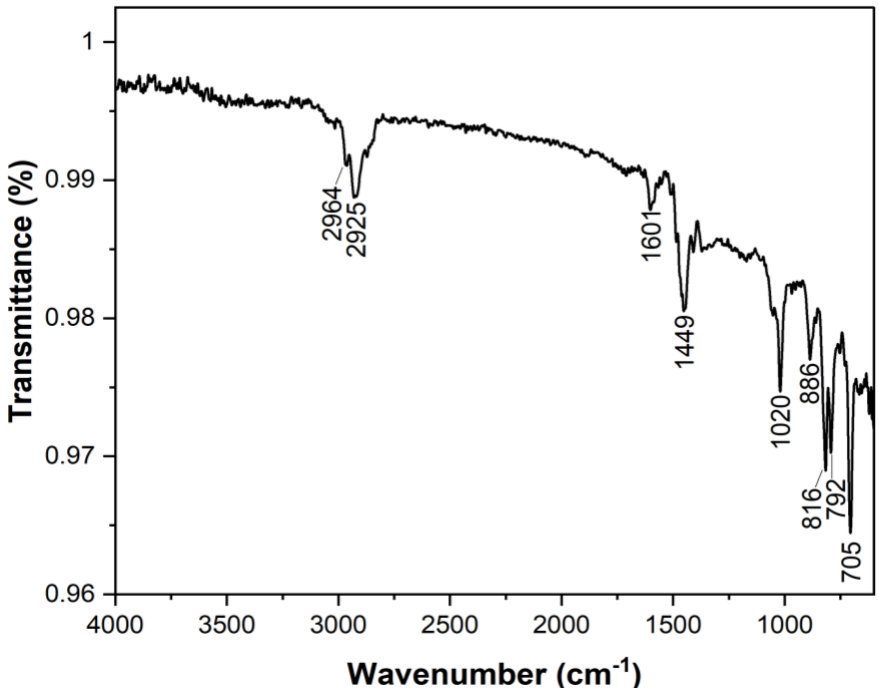

Figure 5.35: ATR-FTIR of unused SPE sorbent on a ZnSe crystal for 60 scans.

Table 5.15: IR Peak Assignment of SPE sorbent.

Wavenumber (cm^{-1})	Peak Assignment
2964 & 2925	C-H stretching (alkane)
1601	C=C aromatic
1449	CH_2 bending
1020	C-O stretching
886 & 816	C=C bending (alkene)
792 & 705	C=C bending (alkene, benzene)

5.2.6 Energy-dispersive X-ray (EDX) Spectroscopy

Figures 5.36 and 5.37 are EDX spectra of the SPE used to do the DOM extraction from the Sackville River water and a SPE that had not been used. It was expected to find sulfur or silicon since it is known to be part of the SPE sorbents.[143,144] However, as shown in the following figures silicon or sulfur were not detected in the EDX spectra, but unexpectedly bromine (17%) was detected. Based on a literature review, bromine is not known to be used in SPE sorbents. Although, this agrees with the EC-SERS spectra of the SPE control because the peak at 697 cm^{-1} may correspond to υ(C-Br). The detected carbon and oxygen in the EDX spectra is attributed to the styrene-divinylbenzene polymer. Chlorine was detected in the EDX analysis, but the amount of chlorine is below one percent.

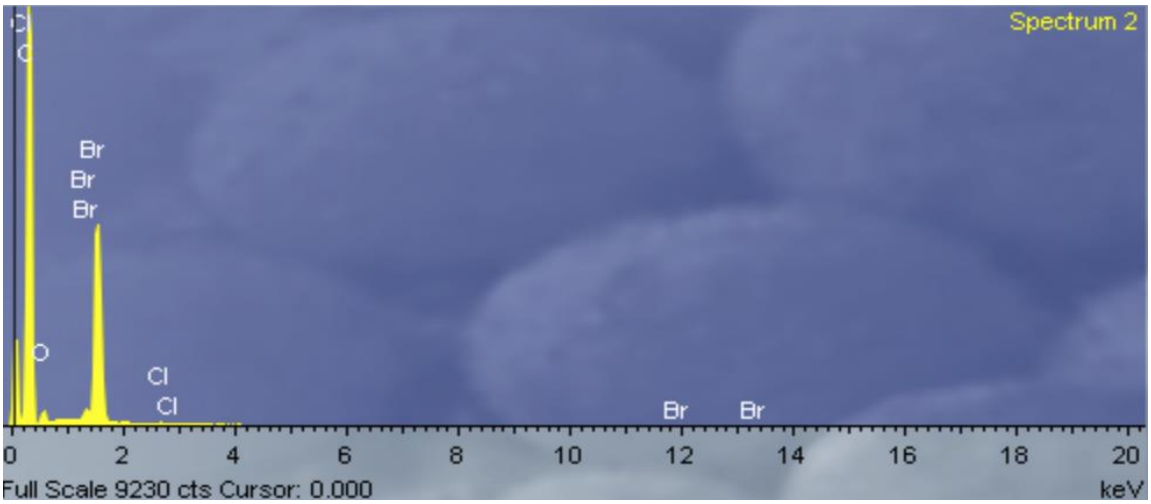

Figure 5.36: EDX analysis on a used SPE sorbent.

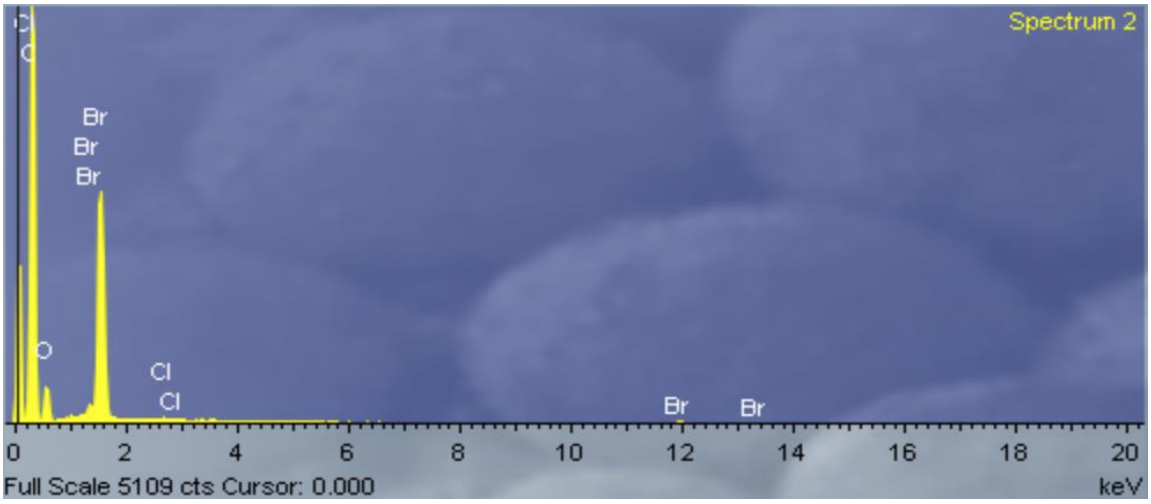

Figure 5.37: EDX analysis on an unused SPE sorbent.

Figure 5.38 is the EDX spectrum of the DOM extract to observe if the extract contained any bromine which would mean that there is some breakthrough occurring from the SPE cartridge. It can be observed that bromine is present but below one percent possibly indicating that any breakthrough occurring from the SPE cartridge is very minute. The silicon present in the EDX spectrum is not from the DOM extract but from the silicon wafer that the DOM extract was put onto. The other interesting element present in Figure 5.38 is calcium which could come from the siltation that occurs in the Sackville River.

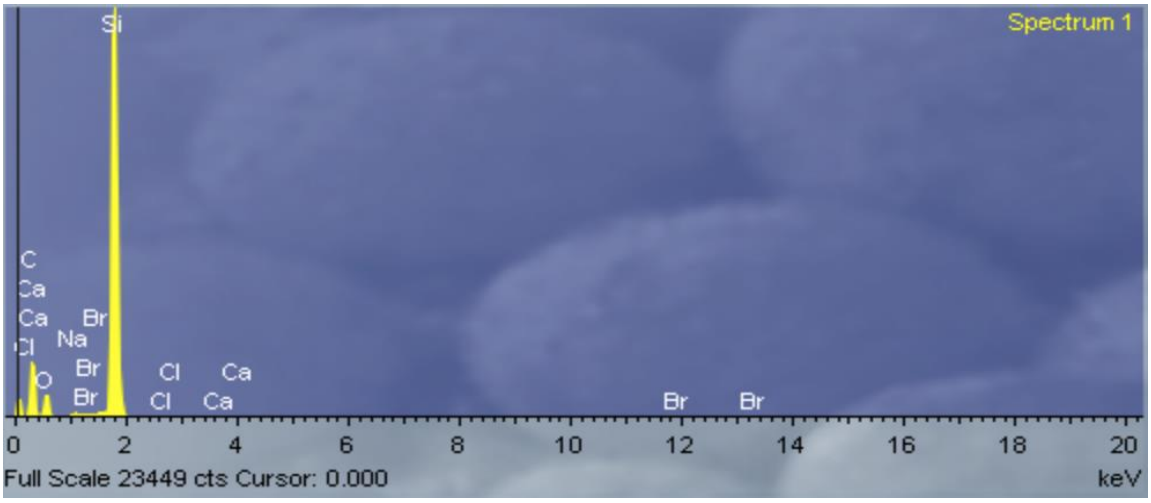

Figure 5.38: EDX analysis on DOM extract.

5.2.6.1 Conclusion for DOM Extract without Acidification before SPE

Five liters of water was collected from the Sackville River and SPE was performed on the filtrate after filtering with 0.7 μm combusted filter paper. The DOM extract from the SPE sorbent was a light clear yellow solution. When 2D-LC was performed on the DOM extract in the first-dimension, the intensities of the peaks found in the chromatogram were very low (~100 mAU or below). Since the intensities of the peaks are low in the first-dimension, the intensities were extremely low (below 6 mAU) in the second-dimension and therefore EC-SERS could not be performed on fractions of theses peaks obtained from the 2D-LC. When a control study was analyzed in the first-dimension of the 2D-LC, many of the peaks matched with the peaks in the chromatogram in the DOM extract. The only peak of interest was the large wide peak in the DOM extract chromatogram since it was not present in the SPE control chromatogram. The mobile phase and gradient in the first-dimension were optimized to try and resolve this large peak.

EC-SERS was performed on the DOM extract and the SPE control, and many of the same peaks were found in both EC-SERS spectra. The sorbent is likely bleeding through the cartridge and being detected through EC-SERS and actually no compounds from the DOM extract are being detected. It is important to note that no acidification of the water filtrate was done before doing SPE. Not doing acidification of the water filtrate before SPE could have played a role as to why there was not a large concentration of DOM compounds in the extract because acidifying the water would help with the compound in the filtrate bind to the sorbent before being extracted with methanol. As a result, acidification of the water sample prior to SPE was attempted next.

5.3 DOM Extract with Acidification before SPE

5.3.1 Solid Phase Extraction

Once again, the Sackville Trail site was used to collect five liters of water as indicated by the red circle in Figure 5.20, and Table 5.16 lists the conditions and information when sampling. The water was filtered with combusted 0.7 μm filters and then acidified to pH 2 with 2 M HCl. Subsequently the filtered and acidified water went through a SPE cartridge. The DOM was extracted from the SPE cartridge with twenty milliliters of methanol at a flow rate of one to two mL/minute. The DOM extract this time was a clear dark orange brown solution as shown in Figure 5.39. This DOM extract is much darker in colour than the original DOM extract (refer to Figure 5.21) meaning that there is likely a higher concentration of DOM compounds found in the extract due to having the water acidified before solid phase extraction.

Table 5.16: Conditions of Sackville River Water Sampling.

Date	March 3rd, 2022
Time	8:30 am
Coordinates	44.75, -63.66
Weather	Overcast with flurries
Air Temperature	-4.4°C
Relative Humidity	85%

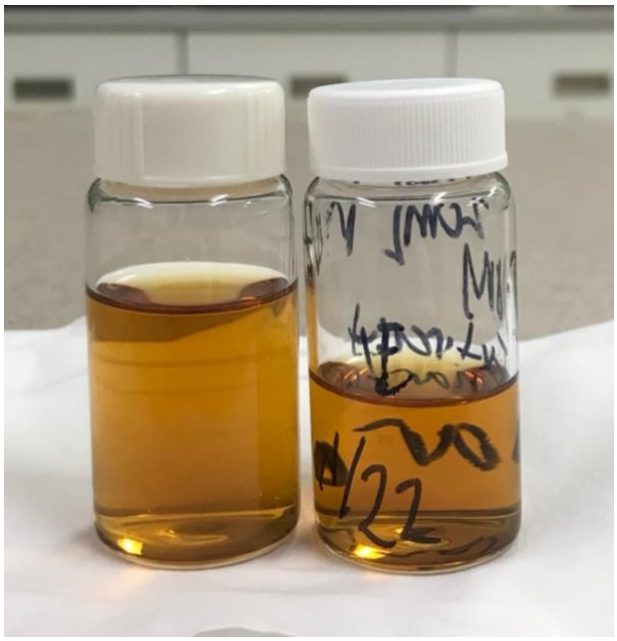

Figure 5.39: Image of DOM extract from SPE cartridge of acidified Sackville River water.

5.3.2 UV-Vis

Figure 5.40 shows the absorbance spectra of the Sackville River water before filtering and SPE and the DOM extract obtained after filtering, acidifying and SPE was completed on the water samples. After performing SPE, the slope in the UV-Vis is steeper indicating a greater decrease in absorption of the compounds within the sample with increasing wavelength. The same absorption values were calculated and can be found in Table 5.17. The values for $\frac{A_{250}}{A_{365}}$ and $\frac{A_{254}}{A_{436}}$ are higher than they were with the first DOM extract implying that the acidification helps with concentrating the DOM in the water sample. The value for $\frac{A_{254}}{A_{436}}$ is higher than the range found in the literature indicating the DOM found in the Sackville River is produced from autochthonous sources. The value for $\frac{A_{254}}{A_{436}}$ agrees with the range found in the literature, however the value for this DOM extract is slightly lower than the one obtained previously, which is interesting because it would have been assumed that it would be higher since the DOM concentration probably increased with the acidification step included before extraction.

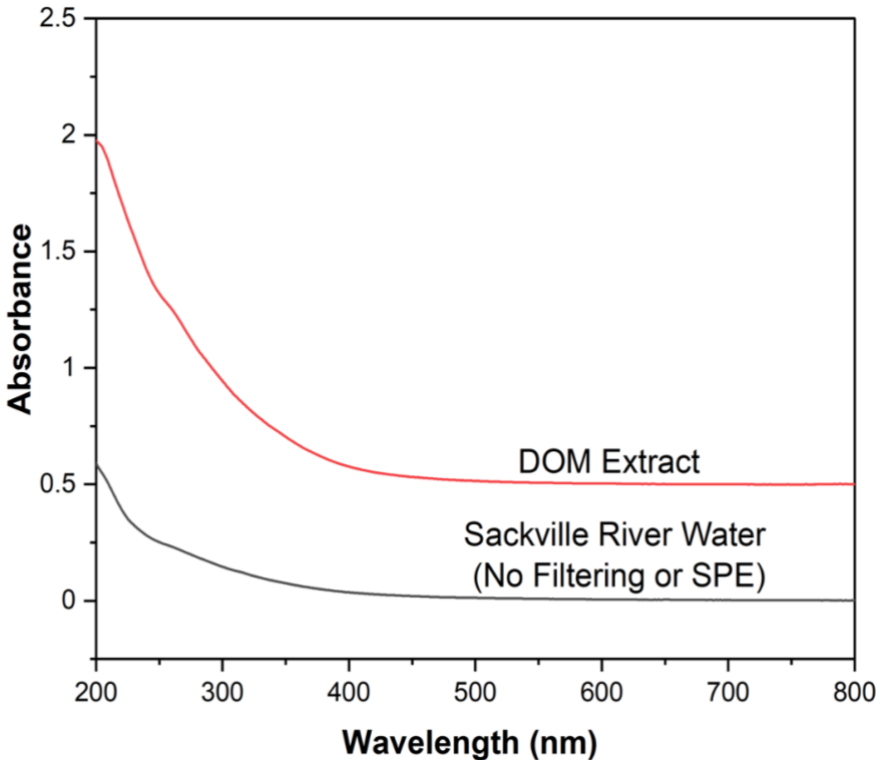

Figure 5.40: UV-Vis absorbance spectrum of DOM extract obtained from the acidified Sackville River water.

Table 5.17: Calculated Absorbance Ratios of Acidified Sackville River DOM.

Type	Absorbance ratio	Value	Literature Value[29]
$\frac{E2}{E3}$	$\frac{A_{250}}{A_{365}}$	5.34	4.16-5.72
$\frac{E2}{E4}$	$\frac{A_{254}}{A_{436}}$	19.92	4.37-11.34
$\frac{E3}{E4}$	$\frac{A_{340}}{A_{254}}$	0.29	0.20-0.38

5.3.3 2D-LC

5.3.3.1 First-Dimension Separation of DOM

The DOM extracted from the five liters of filtered and acidified river water using solid phase extraction was used for 2D-LC analysis. The method established in the first-dimension for the previous DOM extract as listed in Table 4.6 was first used for the separation of this new DOM extract. Consistent with previous 2D-LC studies, an injection volume of five microliters was used.

Figure 5.41 shows the first-dimension chromatogram. The chromatogram contains three peaks, the peaks at 0.61 and 0.64 minutes are the highly polar compound(s) in the DOM extract whereas the peak at 3.28 minutes contains the compound(s) that are less polar. The intensities of these peaks are significantly greater than observed previously in Figure 5.28, which were below ~120 mAU. Due to the high intensity in the first-dimension, these peaks were further separated in the second-dimension.

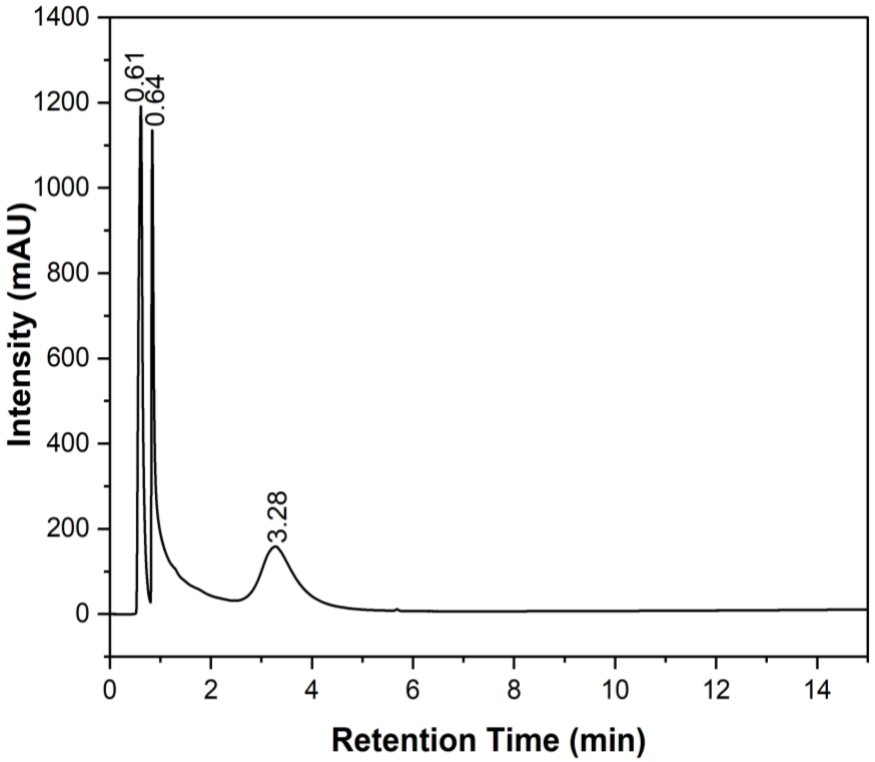

Figure 5.41: [1]D chromatogram of DOM extract with acidification at 254 nm. Milli-Q water + 0.1% formic acid and acetonitrile + 0.1% formic acid used for the mobile phase. Injection volume was 5 μL.

5.3.3.2 Second-Dimension Separation of DOM

The second-dimension parameters used for this separation were the same that were used for green tea and the previous DOM extract in the second-dimension, these parameters can be found in Table 4.7. Figure 5.42 highlights the cuts that were chosen in the first-dimension to be further separated in the second-dimension. All of the peaks in the first-dimension were originally chosen

to be further separated in the second-dimension, however after the ^{2}D analysis of the peaks was done, only the first two peaks could be analyzed and not the third peak at 3.28 minutes possibly because the absorbance threshold might not have been chosen. The second-dimension separation emphasizes that in both cuts 1 and 2 there is a further separation of compounds that were originally co-eluting in the first-dimension, therefore demonstrating the effectiveness of 2D-LC for analyzing DOM. However, it can be observed in the second-dimension chromatogram that the ^{2}D run-time is not long enough for the separation of cuts 1 and 2 since the peaks at 2.76 and 6.72 minutes are not within their ^{2}D run-time. Therefore, the run-time needs to be increased in order for the separation to occur within the ^{2}D run-time.

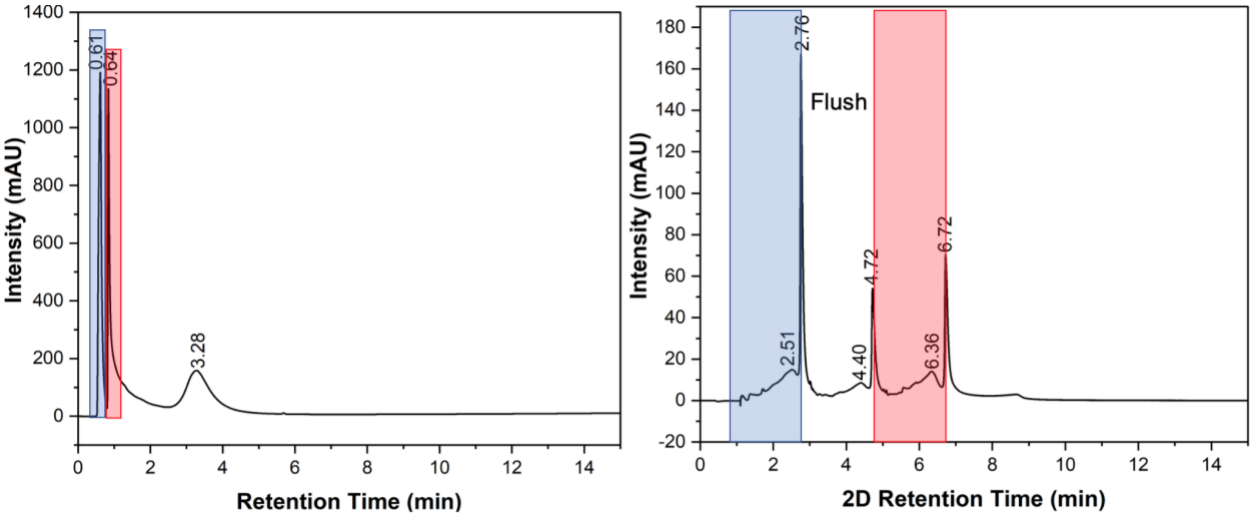

Figure 5.42: Chromatogram of DOM extract in the first-dimension (left) and in the second-dimension (right) of cuts highlighted from the first-dimension at 254 nm (cut 1 is in blue and cut 2 is in red). 1:9 acetonitrile/Milli-Q water (v/v) with 5 mM ammonium acetate buffer and 9.5:0.5 acetonitrile/Milli-Q water (v/v) with 5 mM ammonium acetate buffer used for the second-dimension mobile phase.

5.3.3.2.1 Second-Dimension Run-time

The run-time was changed from 2.0 minutes to 2.5 minutes. Figure 5.43 validates that changing the run-time to 2.5 minutes helped with containing most of the peaks further separated in the second-dimension within the ^{2}D run-time of that cut. However, there are still peaks present in the flush part of the chromatogram. The flush occurs between cuts to ensure the column is

sufficiently cleaned before proceeding to the next cut and to re-equilibrate the gradient mixer to allow the mobile phase to reach the initial composition used in the gradient. Therefore, the peaks found in the flush are from cut 1 that again are not eluting within the ^{2}D run-time of 2.5 minutes. There is also a peak present at 9.67 minutes that is probably from cut 2 but eluting beyond the ^{2}D run-time of 2.5 minutes. Additionally, the peaks further separated in the second-dimension such as peaks 2.47 and 2.76 minutes in cut 1, and 7.34 and 7.73 minutes in cut 2 are not fully resolved. Therefore, the gradient was changed in order to help resolve this issue.

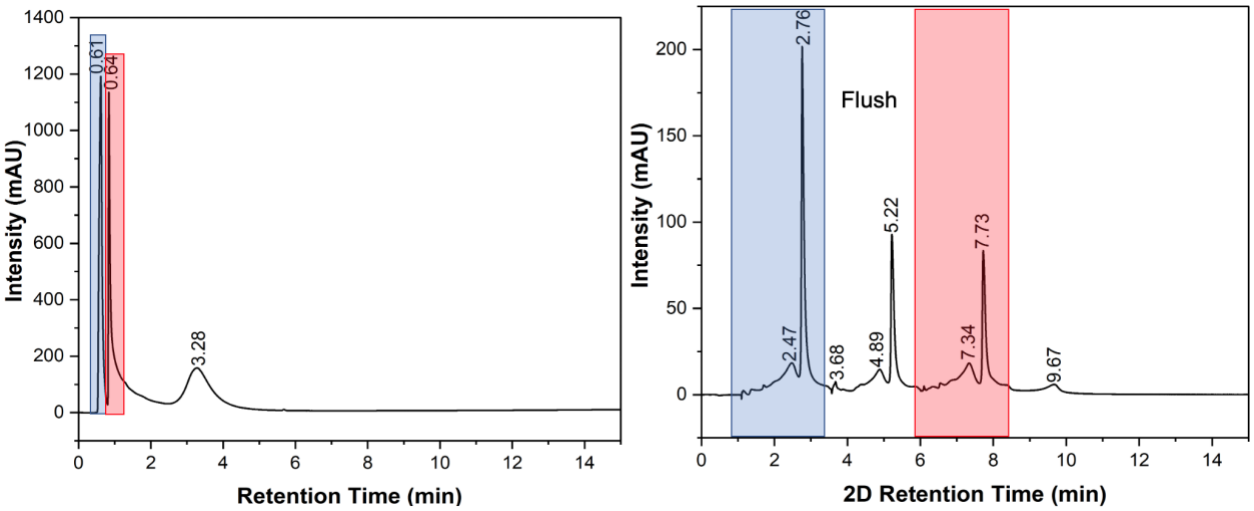

Figure 5.43: Chromatogram of DOM extract in the first-dimension (left) and in the second-dimension (right) of cuts highlighted from the first-dimension at 254 nm (cut 1 is in blue and cut 2 is in red). 1:9 acetonitrile/Milli-Q water (v/v) with 5 mM ammonium acetate buffer and 9.5:0.5 acetonitrile/Milli-Q water (v/v) with 5 mM ammonium acetate buffer used for the second-dimension mobile phase.

5.3.3.2.2 Second-Dimension Mobile Phase Gradient

The gradient was changed to have a higher amount of 5 mM ammonium acetate in 9.5:0.5 acetonitrile/Milli-Q water (v/v) (Solvent B) sooner in the ^{2}D run-time as indicated in Table 5.18. The main change was that at 0.5 minutes the composition of mobile phase was at 90% of solvent B. Figure 5.44 includes the second-dimension chromatogram reflecting the change of mobile phase gradient. It was observed that the peaks at 2.47 and 2.76 minutes in cut 1, and 7.34 and 7.73

minutes in cut 2 are more resolved. However, again the flush contains peaks that are from cut 1 as was observed previously but at this point in the thesis research, method optimization for the DOM second-dimension separation, while not complete, was deemed sufficient for second-dimension fraction collection for EC-SERS analysis.

Table 5.18: Gradient Parameters in the First-Dimension Separation of DOM.

Minute	Composition of Acetonitrile
0 min	10%
0.50 min	90%
1.40 min	90%
1.50 min	90%
1.60 min	10%
2.00 min	10%
2.50 min	10%

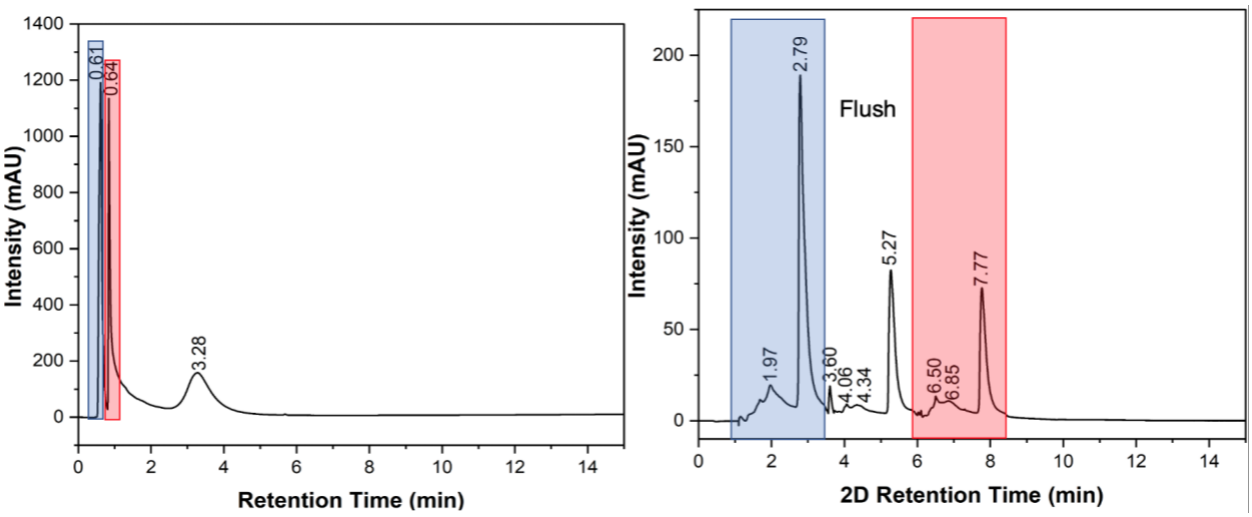

Figure 5.44: Chromatogram of DOM extract in the first-dimension (left) and in the second-dimension (right) of cuts highlighted from the first-dimension at 254 nm (cut 1 is in blue and cut 2 is in red). 1:9 acetonitrile/Milli-Q water (v/v) with 5 mM ammonium acetate buffer and 9.5:0.5 acetonitrile/Milli-Q water (v/v) with 5 mM ammonium acetate buffer used for the second-dimension mobile phase.

5.3.4 EC-SERS of DOM Extract

The same method was done as with the green tea cuts and the previous DOM extract; one milliliter of DOM extract with one milliliter of 0.1 M NaF electrolyte were combined in the electrochemical cell, and EC-SERS measurements were run in this solution. Figure 5.46 provides the EC-SERS spectra of the analysis of the new DOM extract. The only peaks present at 1020 and 1429 cm^{-1} are because of the methanol used to extract the DOM from the SPE cartridge. Unfortunately, no compounds in the DOM extract were detected through EC-SERS. It is believed that because the DOM extract is very coloured, the solution is absorbing most of the light from the laser instead of scattering the light; therefore, no SERS signal can be obtained. However, when compared to the previous EC-SERS analysis of the DOM extract and SPE control study (refer to Figure 5.33 and 5.34), none of other peaks are present in Figure 5.45. This is likely because the concentration of the new DOM extract is much higher than the previous extract, and so the small amounts of material bleeding off the PPL cartridge are less of an issue. Since the combination of

one milliliter of DOM extract and one milliliter of 0.1 M NaF electrolyte did not provide sufficient results, other methods were explored for EC-SERS analysis.

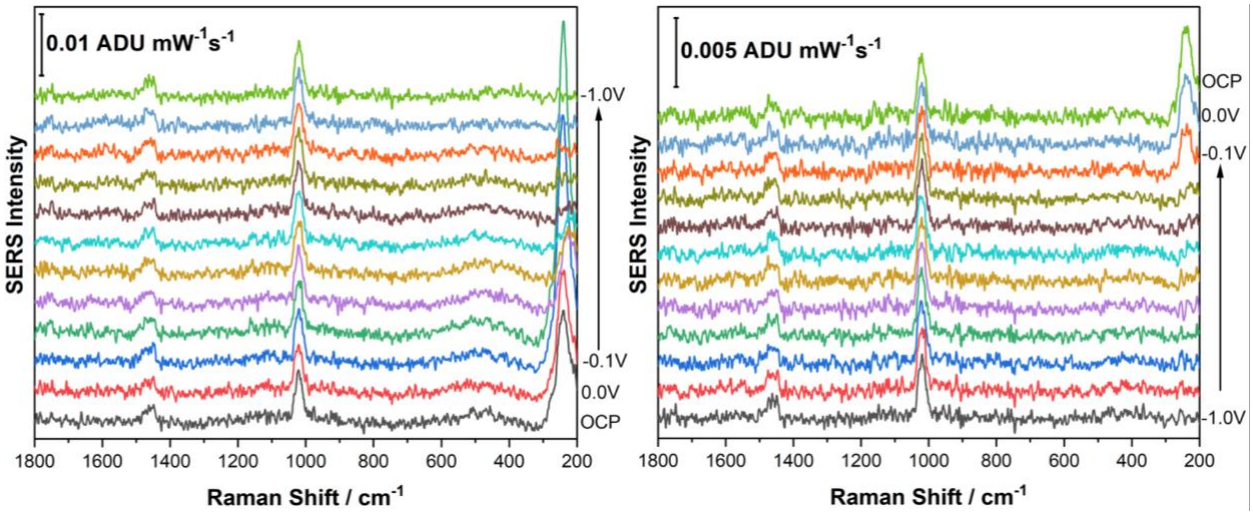

Figure 5.45: EC-SERS analysis of 1 mL of DOM extract with acidification prior to SPE mixed with 1 mL of 0.1 M NaF electrolyte (Cathodic, 0.1 V stepwise progression from 0 V to -1.0 V and Anodic, 0.1 V step-wise progression from 0 V to -1.0 V) using an excitation wavelength of 780 nm with a laser power of 80 mW and acquisition time of 30 seconds.

5.3.4.1 Collecting 2 Fractions of Cut 1 of DOM Extract

After performing a 2D-LC separation of the new DOM extract, cut 1 (refer to Figure 5.44) was chosen to collect as a fraction from the second-dimension for EC-SERS analysis because it had the highest intensity in the second-dimension. For the EC-SERS analysis of the cuts, one milliliter of the cut and then one milliliter of 0.1 M NaF supporting electrolyte would be added to the electrochemical cell. As a result, in order to collect the required volume of the fraction, two runs were completed, and the fractions were combined for EC-SERS analysis. Figure 5.46 shows the EC-SERS analysis of cut 1 of the DOM extract. Similar to the fractions from the 2D-LC of the green tea, there appears to be acetonitrile from the mobile phase present with peaks at 380-382 cm^{-1} and 923-924 cm^{-1}, and 1373-1374 cm^{-1} (as indicated with asterisks in Figure 5.46). However, there are other peaks present that are not from acetonitrile in the mobile phase. These peaks are very low in signal but were determined to be above the signal limit of detection (intensity is greater

than $3\sigma_b$). Figure 9.5 (located in the appendix) is a comparison of various cathodic and anodic spectra of the cut and the ^{2}D mobile phase at -1.0V which may help observing the peaks attributed from the compounds found in the cut. Detection of a compound in a cut from the 2D-LC through EC-SERS is an exciting result because this is the first time where 2D-LC-EC-SERS has been successfully demonstrated. Table 5.19 provides the SERS peak assignment for cut 1. From the peak assignment it appears that the cut contains compound(s) which may feature aromatic rings, alkenes, and alkanes as well possibly some sulfur compounds.

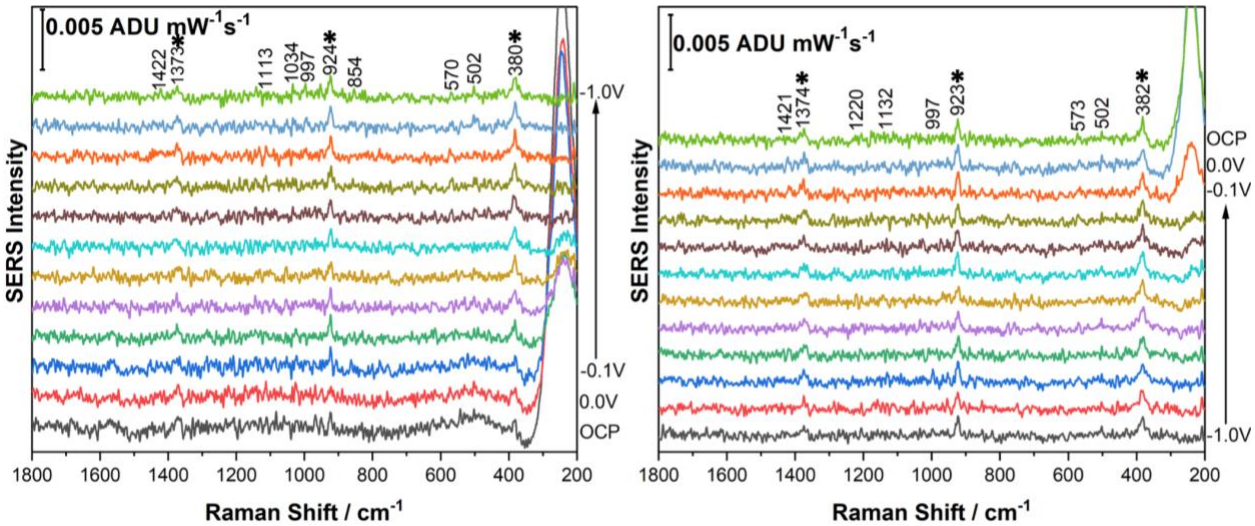

Figure 5.46: EC-SERS analysis of 1 mL of cut 1 of the DOM extract with acidification prior to SPE mixed with 1 mL of 0.1 M NaF electrolyte (Cathodic, 0.1 V stepwise progression from 0 V to -1.0 V and Anodic, 0.1 V step-wise progression from 0 V to -1.0 V. Asterisks indicate peaks due to second-dimension mobile phase.) An excitation wavelength of 780 nm with a laser power of 80 mW and acquisition time of 30 seconds was used.

Table 5.19: SERS Peak Assignment of Cut 1 of DOM Extract. (δ = bending mode and υ = stretching mode)

Wavenumber (cm^{-1})	Peak assignment[134]
501 & 573	υ(S-S)
997	υ(CC) aromatic ring chain vibrations
1034	υ(CC) alicyclic, aliphatic chain vibrations
1113 & 1132	υ(C-O-C) asymmetrical
1422	δ(CH2) & δ(CH3) asymmetrical

5.3.5 Increasing DOM Extract Concentration

To help with the EC-SERS analysis of the fractions collected from the second-dimension, the volume of methanol was decreased to help increase the DOM concentration and consequently would increase the intensities of peaks in both the first- and second-dimensions. Roughly 10 mL of DOM extract was decreased to 1 mL by evaporating the methanol with argon gas to obtain the concentrated DOM extract. Figure 5.47 is the first- and second-dimension chromatograms of the concentrated DOM extract. The intensities in both dimensions are increased significantly meaning that when it comes time to collect fractions from the second-dimension to preform EC-SERS, possibly only one or two collections of fractions would need to be collected in order to obtain a sufficient SERS signal of the compound(s) found in the fraction(s).

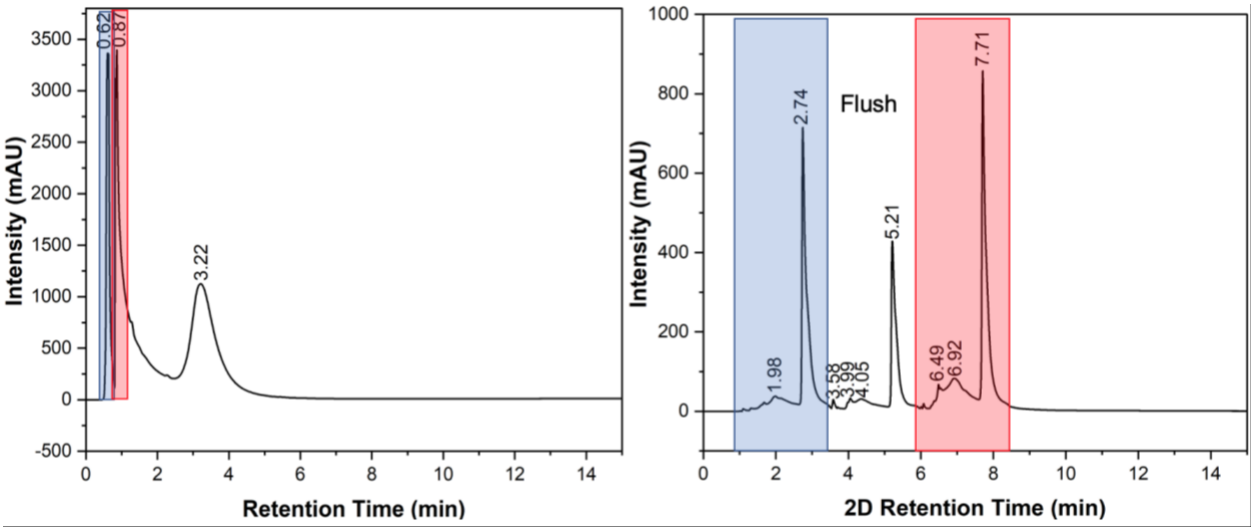

Figure 5.47: Chromatogram of concentrated DOM extract in the first-dimension (left) and in the second-dimension (right) of cuts highlighted from the first-dimension at 254 nm (cut 1 is in blue and cut 2 is in red). 1:9 acetonitrile/Milli-Q water (v/v) with 5 mM ammonium acetate buffer and 9.5:0.5 acetonitrile/Milli-Q water (v/v) with 5 mM ammonium acetate buffer used for the second-dimension mobile phase.

After performing a 2D-LC separation of the concentrated DOM extract, cut 1 (refer to Figure 5.47) was collected as a fraction from the second-dimension five times for EC-SERS analysis. Cut 1 was chosen to keep the EC-SERS analysis of the fraction consistent such that a comparison to the results shown in Figure 5.46 could be made. Cut 1 was collected five times in order to obtain one milliliter of the fraction and then one milliliter of 0.1 M NaF supporting electrolyte was also added to the electrochemical cell. Figure 5.48 shows the EC-SERS analysis of cut 1 of the concentrated DOM extract. Again, there appears to be acetonitrile from the mobile phase present with peaks at 382 cm^{-1}, 923 cm^{-1}, and 1374 (as indicated with asterisks in Figure 5.48). However, there are other peaks present that are not due to the acetonitrile present in the mobile phase. The peaks presents are higher in intensity than in Figure 5.46 and were determined to be above the signal limit of detection (intensity is greater than $3\sigma_b$). When comparing Figures 5.46 and 5.48, there are peaks present in both spectra such as at 997, 1034, 1132, 1422 cm^{-1} in Figure 5.46, and at 996, 1027, 1139 and 1433 cm^{-1} in Figure 5.48. Figure 5.49 shows the anodic EC-SERS spectra

within the region of 996 and 1374 cm^{-1} to better display the peaks within this region and it can be observed there is an additional peak present at 969 cm^{-1}. Furthermore, applying a voltage does help with detecting the compound(s) found in this cut and subsequently enhances its SERS intensity as shown as well in Figure 5.50. In the OCP cathodic spectrum there is no detection of compounds other than acetonitrile found in the mobile phase, but as voltage is introduced other peaks become present especially in the anodic progression of the EC-SERS analysis such as at -0.4V. Table 5.20 provides the SERS peak assignment for cut 1 of the concentrated DOM extract. From the peak assignment it appears that the cut contains compound(s) which may contain functional groups, such as aromatic rings, alkenes, and alkanes.

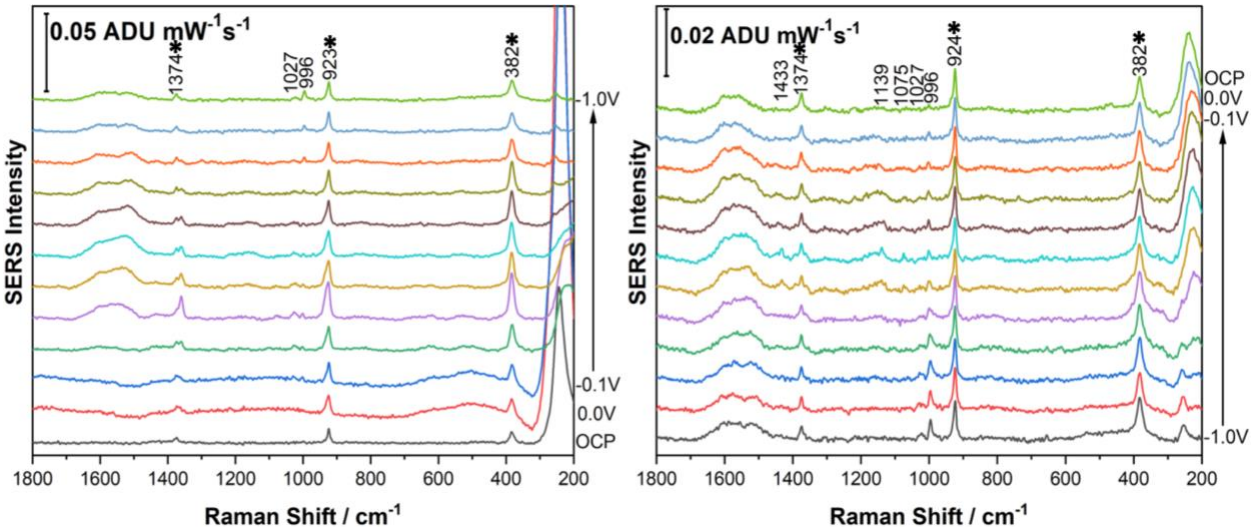

Figure 5.48*:* EC-SERS analysis of 1 mL of cut 1 of the concentrated DOM extract with acidification prior to SPE mixed with 1 mL of 0.1 M NaF electrolyte (Cathodic, 0.1 V stepwise progression from 0 V to -1.0 V and Anodic, 0.1 V step-wise progression from 0 V to -1.0 V. Asterisks indicate peaks due to second-dimension mobile phase.) An excitation wavelength of 780 nm with a laser power of 80 mW and acquisition time of 30 seconds was used.

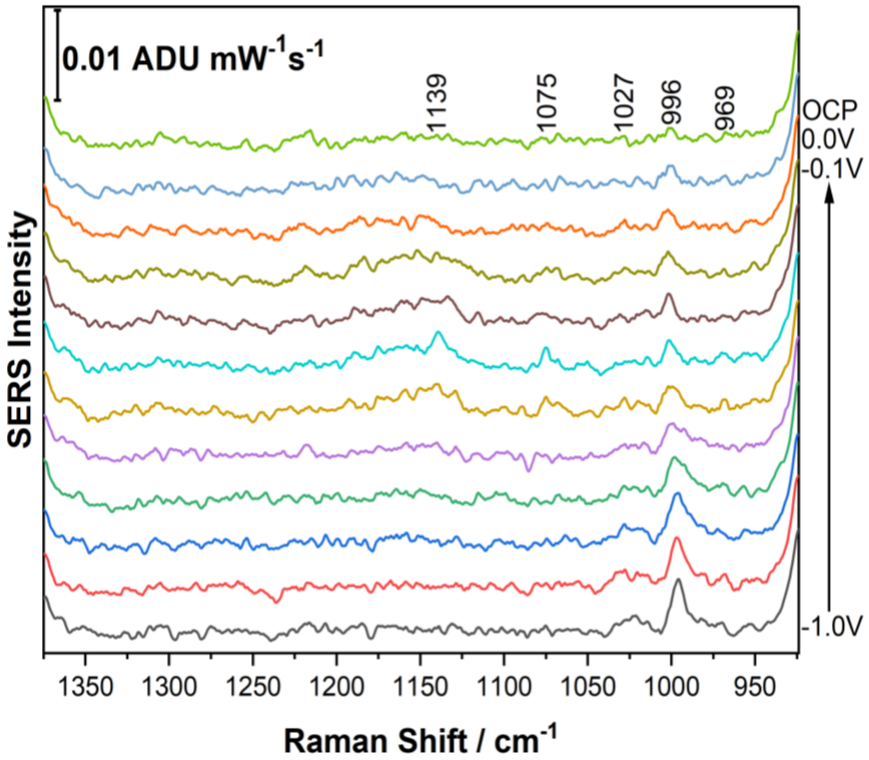

Figure 5.49*:* Anodic EC-SERS spectra between 1375-924 cm^{-1} of 1 mL of cut 1 of the concentrated DOM extract with acidification prior to SPE mixed with 1 mL of 0.1 M NaF electrolyte (0.1 V step-wise progression from 0 V to -1.0 V. Asterisks indicate peaks due to second-dimension mobile phase). An excitation wavelength of 780 nm with a laser power of 80 mW and acquisition time of 30 seconds was used.

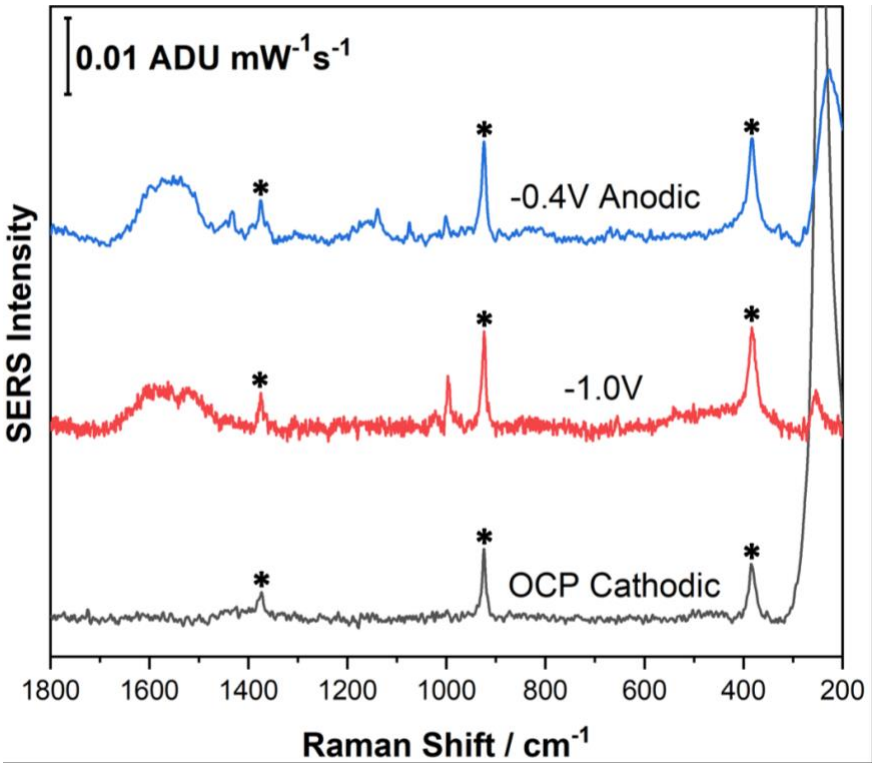

Figure 5.50: EC-SERS spectra of 1 mL of cut 1 of the concentrated DOM extract with acidification prior to SPE mixed with 1 mL of 0.1 M NaF at OCP cathodic, -1.0 V and -0.4 V anodic using an excitation wavelength of 780 nm with a laser power of 80 mW and acquisition time of 30 seconds. (Asterisks indicate peaks due to second-dimension mobile phase).

Table 5.20: SERS Peak Assignment of Cut 1 of Concentrated DOM Extract. (δ = bending mode and υ = stretching mode)

Wavenumber (cm^{-1})	**Peak assignment[134]**
969	υ(C-O-C) vibrations
996	υ(CC) aromatic ring chain vibrations
1027 & 1075	υ(CC) alicyclic, aliphatic chain vibrations
1139	υ(C-O-C) asymmetric
1433	δ(CH_2) & δ(CH_3) asymmetric

5.3.5.1 Conclusion for DOM Extract with Acidification before SPE

Another five liters of water was collected from the Sackville River. The water was filtered with 0.7 μm combusted filter paper and the filtrate was acidified with 2 M HCl before SPE was performed. The DOM extract from the SPE sorbent was a clear dark orange brown solution. When 2D-LC was performed on the new DOM extract in the first-dimension, the intensities of the peaks found in the chromatogram were much higher than observed before with the previous DOM extract. Since the intensities of the peaks are high in the second-dimension as well, the second-dimension could be optimized to achieve a sufficient ^{2}D separation by changing the ^{2}D run-time and mobile phase gradient.

EC-SERS could be performed on the one fraction obtained from the 2D-LC because of the high intensities of the peaks in the second-dimension. It was found that there were peaks present in the EC-SERS analysis of the fraction that were not attributed from the second-dimension mobile phase but from the separated compound(s) found in the fraction, albeit at a very low SERS intensity. EC-SERS was performed on the DOM extract and there was no detection besides the methanol in the solution. It is believed that since the DOM extract is very coloured, the solution is absorbing most of the light from the laser instead of scattering the light; therefore, no SERS signal can be obtained. The methanol was then evaporated from the DOM extract to increase the concentration of DOM and then 2D-LC was performed on the solution. This increased the intensities of the peaks significantly in both the chromatographic analysis of the DOM extract and EC-SERS analysis of cut 1 fraction. There are peaks present in the EC-SERS spectra that are not attributed from the acetonitrile found in the second-dimension mobile phase, but actually from the compound(s) present in the fraction of cut 1. As a result, acidification of the water sample prior to SPE improved extraction of the DOM from the water sample considerably.

Chapter 6: Conclusion

DOM and green tea are very complex samples that require enhanced separation and subsequent sensitive detection to obtain comprehensive results. 2D-LC is gaining notoriety as an enhanced separation technique, providing results that a conventional HPLC instrument may not be able to provide. EC-SERS combines SERS and electrochemistry, where analytes adhere onto the metallic nanostructured surface of a working electrode wherein electrolyte is present and voltage is applied. The SERS signal can be enhanced significantly due to the applied voltage. Therefore, combining 2D-LC and EC-SERS can be very advantageous for analyzing complex samples such as DOM and green tea by obtaining both an enhanced separation and detection of the various components within these samples. This thesis research demonstrated the potential of this hyphenated technique (2D-LC-EC-SERS) for the first time to analyze green tea which was used a model of DOM for chromatographic and spectroscopic method development.

One of the first important steps was to develop a 2D-LC method for separating green tea in the first and second-dimensions. Reverse phase chromatography was used in both dimensions; the first-dimension contains an alkyl chain whereas the second-dimension has an additional amide connection. In the first-dimension, gradient elution using water and methanol as the mobile phase was used. The separation of green tea was completed in fifteen minutes with some of the peaks not being fully resolved, making 2D-LC particularly useful since a second-dimension can help resolving these peaks. For the second-dimension, a 1:9 acetonitrile/water (% v/v) and 9.5:0.5 acetonitrile/water (% v/v) with 5 mM ammonium acetate buffer was used. This mobile phase was able to provide a satisfactory separation in the second-dimension and therefore was used in all second-dimension chromatographic separations of green tea. Additionally, the flow rate was

reduced from 1 mL/min to 0.5 mL/min in order to allow the compounds in green tea to interact with the stationary phase longer, leading to a better separation.

The next step of this thesis work was to synthesize and characterize nanoparticles appropriate for this work. Silver nanoparticles produced from a Lee-Meisel method were chosen since they are easy to synthesize and provide near-monodispersed nanoparticles with diameters of ~30 nm. UV-Vis and SEM characterization were completed on the silver nanoparticles. Another aspect that was crucial to observe was whether the second-dimension mobile phase would interfere with the detection of the compounds found in the 2D-LC fractions. Fractions from the 2D-LC are mostly composed of second-dimension mobile phase and the compounds found in the analyte are severely diluted. EC-SERS was completed on both 1:9 acetonitrile/water (v/v) and 9.5:0.5 acetonitrile/water (v/v) with 5 mM ammonium acetate buffer, and there was minimal signal detected, fortunately.

The concentration of the sample is significantly reduced due to diffusion when using 2D-LC since the sample is experiencing two separation steps. This is a very common problem when performing 2D-LC, therefore using an ultrasensitive detection modality such as EC-SERS would be ideal for further investigation and identification of the compound(s) found in the fraction. Several methods were explored to try to obtain a SERS signal of the compounds within the 2D-LC fractions, and the optimal method was to collect the fraction and complete the EC-SERS measurements in the fraction directly, with added electrolyte. This procedure led to superior results for cuts 1, 2 and 4. Cut 2 contains caffeine which was determined through using a caffeine standard. ESI-Q-TOF MS/MS was used for further examination of the cuts, and it was confirmed that caffeine was in cut 2 but did not provide ideal results for cuts 1 and 4.

Finally, 2D-LC and EC-SERS methods for green tea were established and therefore the thesis research moved on to investigate the DOM sample from the Sackville River. The DOM sample extracted from the sorbent with methanol was yellow in colour and clear. It should be mentioned that no acidification step of the water was done before SPE. UV-Vis was performed on the DOM sample and absorption ratios comprised of absorption intensities at different wavelengths were calculated. The values agreed with the ranges found in the literature. 2D-LC was then performed on the DOM sample using the same method developed for green tea. The results in the first-dimension were unsatisfactory because there was a large hump present which eluted in the middle of the separation. Many parameters of the method had to be optimized such as mobile phase and gradient to try resolve the large hump, however further work needs to be done. Another problem experienced in the first-dimension was that the intensity was very low i.e., typically below 100 mAU. Therefore, when certain peaks in the first-dimension were further separated in the second-dimension was ~4 mAU. Since the intensity was very low, fractions were not collected from the 2D-LC for EC-SERS analysis. It became apparent that acidification of the water sample prior to the SPE step was likely needed.

Subsequently, another five liters water was collected from the Sackville River to do the acidification step prior to SPE. 2D-LC was performed on the DOM extract in both the first- and second-dimension and it was observed that the intensity was significantly higher than the original DOM extract, by about 1-2 orders magnitude. The first-dimension method developed with the original DOM extract was used for the new extract and the second-dimension was optimized by changing the mobile phase gradient and ^{2}D run-time. In the second-dimension separation, there was a further separation that occurred for cut 1 and 2. When EC-SERS was performed on cut 1 of the DOM extract obtained from the 2D-LC there were compound(s) besides the second-dimension

mobile phase being detected. This result indicates that 2D-LC-EC-SERS was successfully demonstrated, but more optimization work is needed.

In conclusion, it was observed that green tea and DOM are very different matrices and require different methodologies in order to be successfully separated using 2D-LC and detected through EC-SERS. In fact, green tea may not be the best model of DOM for method development, and further work is needed in this area. Offline 2D-LC-EC-SERS was successful in separating the various compounds in green tea and identifying caffeine which was validated using ESI-Q-TOF MS/MS. Solid phase extraction was performed on the Sackville River water and subsequently 2D-LC and EC-SERS were conducted on the sample. 2D-LC-EC-SERS was successfully performed on the acidified DOM sample obtained from the Sackville River, paving the way for future exploration of this hyphenated analytical technique.

Chapter 7: Future Work

This thesis research was focused on combining two analytical techniques, multidimensional chromatography and electrochemical surface-enhanced Raman spectroscopy, for the first time. The samples of interest in this work included green tea, which is fairly well studied, and dissolved organic matter, which remains understudied. Clearly, this thesis research opens up many new avenues of scientific exploration. One important issue to address in the future would be the relatively poor separation in the first-dimension separation of DOM. While this is a known challenge, it makes the second-dimension separation more challenging. In the future, different stationary phases, such as HILIC columns, should be investigated. In addition, different mobile phases with and without a buffer present should be explored for the separation of green tea and DOM in the second-dimension. Additionally, it would be interesting to collect DOM fractions from the second dimension and to then send these back through the 2D-LC to observe if there is a further separation.

For the EC-SERS component of this project, it would be very beneficial to develop an electrochemical cell small enough to hold one fraction collection of a cut from the 2D-LC. More than one collection of fractions is very time consuming and therefore a smaller cell would save a great deal of time. It would also be beneficial to create better SERS databases to help identify the various compounds detected with EC-SERS.

MS should be used on the cut of the DOM extract from the 2D-LC as well as other cuts to help with identification of the compounds found in the DOM extract. Obtaining different catechin standards could help in identifying the compounds found in the cuts of green tea through 2D-LC, EC-SERS and MS. Lastly, another aspect to look more into is to observe the difference and similarities of water collected from other sites along the Sackville River during different seasons

as well. Employing comprehensive 2D-LC for the analysis of DOM may be useful for the comparison of DOM for various sites and time points.

Chapter 8: References

(1) Stoll, D. R.; Carr, P. W. Two-Dimensional Liquid Chromatography: A State of the Art Tutorial. *Anal. Chem.* **2017**, *89* (1), 519–531.

(2) O. Jones. *Two-Dimensional Liquid Chromatography: Principles and Practical Applications.*; Springer: Singapore, 2020.

(3) Carr, P. W.; Stoll, D. R. *Agilent Technologies Inc, Germany* **2015**, 182.

(4) Lin, V. S. *Environ. Sci.: Processes Impacts* **2015**, *17* (12), 2002–2005.

(5) Zark, M.; Dittmar, T. *Nat. Commun.* **2018**, *9* (1), 3178.

(6) Xu, H.; Guo, L. *Water Res.* **2018**, *135*, 187–194.

(7) Duarte, R. M. B. O.; Barros, A. C.; Duarte, A. C. *J. Chromatogr. A* **2012**, *1249*, 138–146.

(8) Sandron, S.; Rojas, A.; Wilson, R.; Davies, N. W.; Haddad, P. R.; Shellie, R. A.; Nesterenko, P. N.; Kelleher, B. P.; Paull, B. *Environ. Sci.: Processes Impacts* **2015**, *17* (9), 1531–1567.

(9) Wang, X.; Huang, J.; Fan, W.; Lu, H. *Anal. Methods* **2015**, *7* (2), 787–792.

(10) Chan, E. W.; Soh, E. Y.; Tie, P. P.; Law, Y. P. *Pharmacogn. Res.* **2011**, *3* (4), 266.

(11) Que, W.; Wang, B.; Li, F.; Chen, X.; Jin, H.; Jin, Z. *Chem. Geol.* **2020**, *540*, 119565.

(12) Gaffney, J. S.; Marley, N. A.; Clark, S. B. In *Humic/Fulvic Acids and Organic Colloidal Materials in the Environment*; American Chemical Society: Washington, DC, 1996.

(13) What are humic substances? https://humic-substances.org/what-are-humic-substances-2/ (accessed 2021 -05 -29).

(14) Velintine, V. A.; Wee, B. S.; Droepenu, E. K.; Chin, S. F.; Kok, K. Y. *Biointerface Res. Appl. Chem.* **2020**, *11* (4), 11256–11271.

(15) Ogawa, H.; Tanoue, E. *J. Oceanogr.* **2003**, *59* (2), 129–147.

(16) Lønborg, C.; Carreira, C.; Jickells, T.; Álvarez-Salgado, X. A. *Front. Mar. Sci.* **2020**, *7*, 466.

(17) Arrieta, J. M.; Mayol, E.; Hansman, R. L.; Herndl, G. J.; Dittmar, T.; Duarte, C. M. *Science* **2015**, *348* (6232), 331–333.

(18) Minor, E. C.; Swenson, M. M.; Mattson, B. M.; Oyler, A. R. *Environ. Sci.: Processes Impacts* **2014**, *16* (9), 2064–2079.

(19) Dittmar, T.; Koch, B.; Hertkorn, N.; Kattner, G. *Limnol. Oceanogr.: Methods* **2008**, *6* (6), 230–235.

(20) Li, Y.; Harir, M.; Uhl, J.; Kanawati, B.; Lucio, M.; Smirnov, K. S.; Koch, B. P.; Schmitt-Kopplin, P.; Hertkorn, N. *Water Res.* **2017**, *116*, 316–323.

(21) Li, Y.; Harir, M.; Lucio, M.; Kanawati, B.; Smirnov, K.; Flerus, R.; Koch, B. P.; Schmitt-Kopplin, P.; Hertkorn, N. *Anal. Chem.* **2016**, *88* (13), 6680–6688.

(22) Bodhipaksha, L. C.; Sharpless, C. M.; Chin, Y.-P.; Sander, M.; Langston, W. K.; MacKay, A. A. *Environ. Sci. Technol.* **2015**, *49* (6), 3453–3463.

(23) Jordan, T. B.; Nichols, D. S.; Kerr, N. I. *Anal. Bioanal. Chem.* **2009**, *394* (8), 2257–2266.

(24) Mills, G. L.; Quinn, J. G. *Mar. Chem.* **1981**, *10* (2), 93–102.

(25) Koch, B. P.; Ludwichowski, K.-U.; Kattner, G.; Dittmar, T.; Witt, M. *Mar. Chem.* **2008**, *111* (3), 233–241.

(26) Dittmar, T.; Whitehead, K.; Minor, E. C.; Koch, B. P. *Mar. Chem.* **2007**, *107* (3), 378–387.

(27) D'Andrilli, J.; Dittmar, T.; Koch, B. P.; Purcell, J. M.; Marshall, A. G.; Cooper, W. T. *Rapid Commun. Mass. Spectrom.* **2010**, *24* (5), 643–650.

(28) Murphy, K. R.; Stedmon, C. A.; Waite, T. D.; Ruiz, G. M. *Mar. Chem.* **2008**, *108* (1–2), 40–58.

(29) Li, P.; Hur, J. *Crit. Rev. Environ.* **2017**, *47* (3), 131–154.

(30) Weishaar, J. L.; Aiken, G. R.; Bergamaschi, B. A.; Fram, M. S.; Fujii, R.; Mopper, K. *Environ. Sci. Technol.* **2003**, *37* (20), 4702–4708.

(31) Helms, J. R.; Stubbins, A.; Ritchie, J. D.; Minor, E. C.; Kieber, D. J.; Mopper, K. *Limnol. Oceanogr.* **2008**, *53* (3), 955–969.

(32) Reader, H. E.; Stedmon, C. A.; Nielsen, N. J.; Kritzberg, E. S. *Front. Mar. Sci.* **2015**, *2*, 88.

(33) Hansen, A. M.; Kraus, T. E.; Pellerin, B. A.; Fleck, J. A.; Downing, B. D.; Bergamaschi, B. A. *Limnol. Oceanogr.* **2016**, *61* (3), 1015–1032.

(34) Fleischmann, M.; Hendra, P. J.; McQuillan, A. J. *Chem. Phys. Lett.* **1974**, *26* (2), 163–166.

(35) Jeanmaire, D. L.; Duyne, R. P. V. *J. Electroanal. Chem.* **1977**, *84* (1), 1–20.

(36) Willets, K. A.; Duyne, R. P. V. *Annu. Rev. Phys. Chem.* **2007**, *58*, 267–297.

(37) Cañamares, M. V.; Reagan, D. A.; Lombardi, J. R.; Leona, M. *J. Raman Spectrosc.* **2014**, *45* (11–12), 1147–1152.

(38) Haynes, C. L.; McFarland, A. D.; Duyne, R. P. V. *Anal. Chem.* **2005**, *77*, 338A-345A.

(39) Heaps, D. A.; Griffiths, P. R. *Appl. Spectro.* **2005**, *59* (11), 1305–1309.

(40) Robinson, A. M.; Harroun, S. G.; Bergman, J.; Brosseau, C. L. Portable Electrochemical Surface-Enhanced Raman Spectroscopy System for Routine Spectroelectrochemical Analysis. *Anal. Chem.* **2012**, *84* (3), 1760–1764.

(41) Zhu, Q.; Cao, Y.; Cao, Y.; Chai, Y.; Lu, F. *Anal. Bioanal. Chem.* **2014**, *406* (7), 1877–1884.

(42) Huang, R.; Han, S.; Li, X. (Sheryl). *Anal. Bioanal. Chem.* **2013**, *405* (21), 6815–6822.

(43) Carron, K. T.; Kennedy, B. J. *Anal. Chem.* **1995**, *67* (18), 3353–3356.

(44) Cowcher, D. P.; Jarvis, R.; Goodacre, R. *Anal. Chem*. **2014**, *86* (19), 9977–9984.

(45) Riordan, C. M.; Jacobs, K. T.; Negri, P.; Schultz, Z. D. *Faraday Discuss.* **2016**, *187*, 473–484.

(46) Nguyen, A. H.; Deutsch, J. M.; Xiao, L.; Schultz, Z. D. *Anal. Chem.* **2018**, *90* (18), 11062–11069.

(47) Trachta, G.; Schwarze, B.; Sägmüller, B.; Brehm, G.; Schneider, S. *J. Mol. Struct.* **2004**, *693* (1–3), 175–185.

(48) Natural http://sackvillerivers.ns.ca/sackville-river-watershed/history/natural/ (accessed 2021 -01 -20).

(49) Sackville River Watershed http://sackvillerivers.ns.ca/sackville-river-watershed/ (accessed 2021 -01 -20).

(50) Bell, N. G.; Smith, A. J.; Zhu, Y.; Beishuizen, W. H.; Chen, K.; Forster, D.; Ji, Y.; Knox, E. A. *Sci. Rep.* **2020**, *10* (1), 1–13.

(51) Cotrufo, M. F.; Wallenstein, M. D.; Boot, C. M.; Denef, K.; Paul, E. *Glob. Change Biol.* **2013**, *19* (4), 988–995.

(52) Pietta, P. G.; Simonetti, P.; Gardana, C.; Brusamolino, A.; Morazzoni, P.; Bombardelli, E. *BioFactors* **1998**, *8* (1, 2), 111–118.

(53) Chacko, S. M.; Thambi, P. T.; Kuttan, R.; Nishigaki, I. *Chin. Med.* **2010**, *5* (1), 1–9.

(54) Reich, E.; Schibli, A.; Widmer, V.; Jorns, R.; Wolfram, E.; DeBatt, A. *J. Liq. Chromatogr. Relat. Technol.* **2006**, *29* (14), 2141–2151.

(55) Jiang, H.; Engelhardt, U. H.; Thräne, C.; Maiwald, B.; Stark, J. *Food Chem.* **2015**, *183*, 30–35.

(56) Zhou, B.; Wang, Z.; Yin, P.; Ma, B.; Ma, C.; Xu, C.; Wang, J.; Wang, Z.; Yin, D.; Xia, T. *Food Chem.* **2022**, *368*, 130855.

(57) Fernandez, P. L.; Martin, M. J.; Gonzalez, A. G.; Pablos, F. *Analyst* **2000**, *125* (3), 421–425.

(58) Wangkarn, S.; Grudpan, K.; Khanongnuch, C.; Pattananandecha, T.; Apichai, S.; Saenjum, C. *Molecules* **2021**, *26* (19), 6052.

(59) Kalili, K. M.; Villiers, A. de. *J. Sep. Sci.* **2010**, *33* (6-7), 853–863.

(60) Theppakorn, T.; Wongsakul, S. *NUJST* **2013**, *20* (2), 1–11.

(61) Scoparo, C. T.; Souza, L. M. de; Dartora, N.; Sassaki, G. L.; Gorin, P. A.; Iacomini, M. *J. Chromatogr. A* **2012**, *1222*, 29–37.

(62) Krieger, S. *LC GC N. Am.* **2015**, *33* (12), 67.

(63) Lin, X.; Sun, D.-W. *Trends Food Sci. Technol.* **2020**, *104*, 163–176.

(64) Jeong, J.-H.; Jang, H.-J.; Kim, Y. *Korean Chem. Soc.* **2019**, *63* (2), 78–84.

(65) Buyukgoz, G. G.; Soforoglu, M.; Basaran Akgul, N.; Boyaci, I. H. *J. Food Sci. Technol.* **2016**, *53* (3), 1709–1716.

(66) Zeiri, L. *J. Raman Spectrosc.* **2007**, *38* (7), 950–955.

(67) Zareef, M.; Hassan, M. M.; Arslan, M.; Ahmad, W.; Ali, S.; Ouyang, Q.; Li, H.; Wu, X.; Chen, Q. *Microchem. J.* **2020**, *159*, 105431.

(68) V.R. Meyer. *Practical High-Performance Liquid Chromatography*, 4th ed.; John Wiley & Sons, Inc: Hoboken, New Jersey, 2004.

(69) D. A. Skoog; D. M. West; F. J. Holler. *Fundamentals of Analytical Chemistry*, 8th ed.; Brook/Cole: Belmont, CA, 2004.

(70) A. Manz; P. S. Dittrich; N. Pamme; D. Iossifidis. *Bioanalytical Chemistry*; Imperial College Press: 2nd, 2015.

(71) Morris Goodwin. The Theory of HPLC Band Broadening, 2017.

(72) Stoll, D. R.; Carr, P. W. *Anal. Chem.* **2017**, *89* (1), 519–531.

(73) D.R. Stoll. *Handbook of Advanced Chromatography/Mass Spectrometry Techniques*; Academic Press and AOCS Press: London, 2017.

(74) Pirok, B. W. J.; Stoll, D. R.; Schoenmakers, P. J. *Anal. Chem.* **2019**, *91* (1), 240–263.

(75) Brandão, P. F.; Duarte, A. C.; Duarte, R. M. *TrAC-Trend. Anal. Chem.* **2019**, *116*, 186–197.

(76) Li, D.; Schmitz, O. J. *Anal. Bioanal. Chem.* **2013**, *405* (20), 6511–6517.

(77) Movasaghi, Z.; Rehman, S.; Rehman, I. U. *Appl. Spectrosc. Rev.* **2007**, *42* (5), 493–541.

(78) Browne, W. R.; McGarvey, J. J. *Coordin. Chem. Rev.* **2007**, *251* (3–4), 454–473.

(79) M. J. Pelletier. *Analytical Applications of Raman Spectroscopy*; Blackwell Science Ltd.,: Michigan, USA, 1999.

(80) Kudelski, A. *Talanta* **2008**, *76* (1), 1–8.

(81) J. R. Ferraro; K. Nakamoto. *Introductory Raman Spectroscopy*; Academic Press Limited, Inc.: San Diego, USA, 1994.

(82) D.C. Harris; M. D. Bertolucci. *Symmetry and Spectroscopy: An Introduction to Vibrational and Electronic Spectroscopy*; Dove Publication: New York, 1989.

(83) Turrell, G.; Corset, J. *Raman Microscopy: Developments and Applications*; Academic Press, 1996.

(84) M. C. Ocampo. Construction, Optimization and Testing a Coherent Anti-Stokes Raman Scattering Microscope, Ohio State University, Ohio, 2011.

(85) Kazuo Nakamoto. *Infrared and Raman Spectra of Inorganic and Coordinations Compounds. Part A: Theory and Applications in Inorganic Chemistry*, 5th edition.; John Wiley & Sons: New York, NY, 1997.

(86) Doering, W. E.; Piotti, M. E.; Natan, M. J.; Freeman, R. G. *Adv. Mater.* **2007**, *19* (20), 3100–3108.

(87) Lyandres, O.; Shah, N. C.; Yonzon, C. R.; Walsh, J. T.; Glucksberg, M. R.; Duyne, R. P. V. *Anal. Chem.* **2005**, *77* (19), 6134–6139.

(88) Sharma, B.; Frontiera, R. R.; Henry, A.-I.; Ringe, E.; Duyne, R. P. V. *Mater. Today* **2012**, *15* (1–2), 16–25.

(89) Das, G.; Patra, N.; Gopalakrishnan, A.; Zaccaria, R. P.; Toma, A.; Thorat, S.; Fabrizio, E. D.; Diaspro, A.; Salerno, M. *Analyst* **2012**, *137* (8), 1785–1792.

(90) Albrecht, M. G.; Creighton, J. A. *J. Am. Chem. Soc.* **1977**, *99* (15), 5215–5217.

(91) Bantz, K. C.; Meyer, A. F.; Wittenberg, N. J.; Im, H.; Kurtuluş, Ö.; Lee, S. H.; Lindquist, N. C.; Oh, S.-H.; Haynes, C. L. *Phys. Chem. Chem. Phys.* **2011**, *13* (24), 11551–11567.

(92) Stiles, P. L.; Dieringer, J. A.; Shah, N. C.; Duyne, R. P. V. *Annu. Rev. Anal. Chem.* **2008**, *1*, 601–626.

(93) Kho, K. W.; Fu, C. Y.; Dinish, U. S.; Olivo, M. *J. Biophotonics* **2011**, *4* (10), 667–684.

(94) Porter, M. D.; Lipert, R. J.; Siperko, L. M.; Wang, G.; Narayanan, R. *Chem. Soc. Rev.* **2008**, *37* (5), 1001–1011.

(95) Rycenga, M.; Cobley, C. M.; Zeng, J.; Li, W.; Moran, C. H.; Zhang, Q.; Qin, D.; Xia, Y. *Chem. Rev.* **2011**, *111* (6), 3669–3712.

(96) Moskovits, M. *J. Raman Spectrosc.* **2005**, *36* (6-7), 485–496.

(97) Wei, A. *In Nanoparticles: Building Blocks for Nanotechnology*; Kluwer Academic/ Plenum Publishers: New York, 2011.

(98) Moskovits, M. *J. Chem. Phys.* **1982**, *77* (9), 4408–4416.

(99) Ru, E. C. L.; Meyer, S. A.; Artur, C.; Etchegoin, P. G.; Grand, J.; Lang, P.; Maurel, F. *Chem. Commun.* **2011**, *47* (13), 3903–3905.

(100) A. Eftekhari. *In Nanostructured Materials in Electrochemistry*; Wiley-VCH: Weinheim, Germany, 2008.

(101) Zhang, J. Z. *Optical Properties and Spectroscopy of Nanomaterials.*; World Scientific Publishing Co. Pte. Ltd: Singapore, 2009.

(102) Y. Wang; E. Wang. *Nanoparticle SERS Substrates*; Wiley-VCH: Weinheim, Germany, 2011.

(103) Horikoshi, S.; Serpone, N. Introduction to Nanoparticles. In *Microwaves in Nanoparticle Synthesis*; John Wiley & Sons, Ltd; pp 1–24.

(104) Lee, P. C.; Meisel, D. *J. Phys. Chem.* **1982**, *86* (17), 3391–3395.

(105) Aroca, R. *Surface-Enhanced Vibrational Spectroscopy*; John Wiley & Sons: Chichester, England, 2006.

(106) Zhao, L.; Blackburn, J.; Brosseau, C. L. Quantitative Detection of Uric Acid by Electrochemical-Surface Enhanced Raman Spectroscopy Using a Multilayered Au/Ag Substrate. *Anal. Chem.* **2015**, *87* (1), 441–447.

(107) G.T. Barnes; I.R. Gentle. *Interfacial Science: An Introduction*; Oxford Univeristy Press, 2005.

(108) Farling, C. G.; Stackaruk, M. C.; Pye, C. C.; Brosseau, C. L. *Phys. Chem. Chem. Phys.* **2021**, *23* (36), 20065–20072.

(109) Radziuk, D.; Moehwald, H. *Phys. Chem. Chem. Phys.* **2015**, *17* (33), 21072–21093.

(110) Nie, S.; Emory, S. R. *Science* **1997**, *275* (5303), 1102–1106.

(111) J. Wang. *Analytical Electrochemistry*, 2nd ed.; Wiley-VCH: New York, USA, 2000.

(112) Bard, A.; Faulkner, L. R. *Electrochemical Methods: Fundamentals and Applications*, 2nd ed.; John Wiley & Sons, Inc: New York, USA, 2001.

(113) Derek, P. *First Course in Electrode Processes*, 2nd ed.; Royal Society of Chemistry, 2009.

(114) Wang, H.; Pilon, L. *Electrochim. Acta.* **2012**, *64*, 130–139.

(115) Shaw, D. J. *Introduction to Colloid and Surface Chemistry*; Reed Educational and Professional Publishing Ltd., 1992.

(116) Zoski, C.G. *Handbook of Electrochemistry*, 1st ed.; Elsevier: Amsterdam, Netherlands, 2007.

(117) Ren, B; Cui, Y; Wu, D.Y; Tian, Z. Q. *Electrochemical SERS and Its Application in Analytical, Biophysical and Life Science*; Wiley-VCH: Weinheim, Germany, 2011.

(118) Lynk, T. P.; Sit, C. S.; Brosseau, C. L. Electrochemical Surface-Enhanced Raman Spectroscopy as a Platform for Bacterial Detection and Identification. *Anal. Chem.* **2018**, *90* (21), 12639–12646.

(119) Goodall, B. L.; Robinson, A. M.; Brosseau, C. L. *Phys. Chem. Chem. Phys.* **2013**, *15* (5), 1382–1388.

(120) Abdelsalam, M. E.; Bartlett, P. N.; Baumberg, J. J.; Cintra, S.; Kelf, T. A.; Russell, A. E. *Electrochem. Commun.* **2005**, *7* (7), 740–744.

(121) Eisnor, M.; McLeod, K.; Bindesri, S.; Svoboda, S.; Wustholz, K.; Brosseau, C. L. Electrochemical Surface-Enhanced Raman Spectroscopy (EC-SERS): A Tool for the Identification of Polyphenolic Components in Natural Lake Pigments. *Phys. Chem. Chem. Phys.* **2021**.

(122) Karaballi, R. A.; Nel, A.; Krishnan, S.; Blackburn, J.; Brosseau, C. L. *Phys. Chem. Chem. Phys.* **2015**, *17* (33), 21356–21363.

(123) Greene, B. H. C.; Alhatab, D. S.; Pye, C. C.; Brosseau, C. L. Electrochemical-Surface Enhanced Raman Spectroscopic (EC-SERS) Study of 6-Thiouric Acid: A Metabolite of the Chemotherapy Drug Azathioprine. *J. Phys. Chem. C* **2017**, *121* (14), 8084–8090.

(124) Wain, A. J.; O'Connell, M. A. *Adv. Phys.: X* **2017**, *2* (1), 188–209.

(125) Liu, W. H.; Yuan, R. H.; Teng, Y. J.; Ma, C.-A. *Acta. Physico-Chim. Sin.* **2013**, *29* (12), 2599–2607.

(126) Reipa, V.; Gaigalas, A.; Abramowitz, S. *J. Electroanal. Chem.* **1993**, *348* (1–2), 413–428.

(127) Dendisová, M.; Němečková, Z.; Člupek, M.; Prokopec, V. *Appl. Surf. Sci.* **2019**, *470*, 716–723.

(128) Cook, S.; Peacock, M.; Evans, C. D.; Page, S. E.; Whelan, M.; Gauci, V.; Khoon, K. L. *Mires Peat* **2016**, *18* (25), 1–8.

(129) Boyes, B.; Dong, M. *LC GC N. Am.* **2018**, *36* (10), 752–768.

(130) M. M. Eisnor. Investigation of a Yellow Lake Pigment Using 2D-LC and EC-SERS, Saint Mary's Univeristy, 2020.

(131) Clyde, C.; Blake, S.; Obrien, S.; Igwilo, I.; Lurie, I. S. *Anal. Methods* **2015**, *7* (23), 9763–9772.

(132) Tuschel, D. *Spectroscopy* **2014**, *29*, 14–23.

(133) Neelakantan, P. Raman Spectrum of Acetonitrile. *Proc. Indian Acad. Sci.* **1964**, *60*, 422–424.

(134) Yvon, H. J. Raman spectroscopy for analysis and monitoring https://static.horiba.com/fileadmin/Horiba/Technology/Measurement_Techniques/Molecular_Spectroscopy/Raman_Spectroscopy/Raman_Academy/Raman_Tutorial/Raman_bands.pdf.

(135) Kang, J.; Gu, H.; Zhong, L.; Hu, Y.; Liu, F. *Spectrochim. Acta A Mol. Biomol. Spectrosc.* **2011**, *78* (2), 757–762.

(136) McCabe, A. J.; Arnold, W. A. *Limnol. Oceanogr.* **2018**, *63* (5), 1992–2014.

(137) Wang, Z.; Roulet, N. *Plant Soil* **2017**, *417* (1), 197–216.

(138) Wright, A. L.; Reddy, K.R. Dissolved organic matter in wetlands https://edis.ifas.ufl.edu/ss507 (accessed 2020 -11 -12).

(139) Cascone, C.; Murphy, K. R.; Markensten, H.; Kern, J. S.; Schleich, C.; Keucken, A.; Köhler, S. J. *Environ. Sci.: Water Res. Technol.* **2022**, *8*, 836–848.
(140) He, X.-S.; Xi, B.-D.; Li, W.-T.; Gao, R.-T.; Zhang, H.; Tan, W.-B.; Huang, C.-H. *J. Chromatogr. A* **2015**, *1420*, 83–91.

(141) Li, W.-T.; Xu, Z.-X.; Li, A.-M.; Wu, W.; Zhou, Q.; Wang, J.-N. *Water Res.* **2013**, *47* (3), 1246–1256.

(142) Swenson, M. M.; Oyler, A. R.; Minor, E. C. *Limnol. Oceanogr.: Methods* **2014**, *12* (10), 713–728.

(143) Walker, V.; Mills, G. A. *Ann. Clin. Biochem.* **2002**, *39* (5), 464–477.

(144) Malik, M. A. *Ind. Eng. Chem. Res.* **2009**, *48* (15), 6961–6965.

Appendix

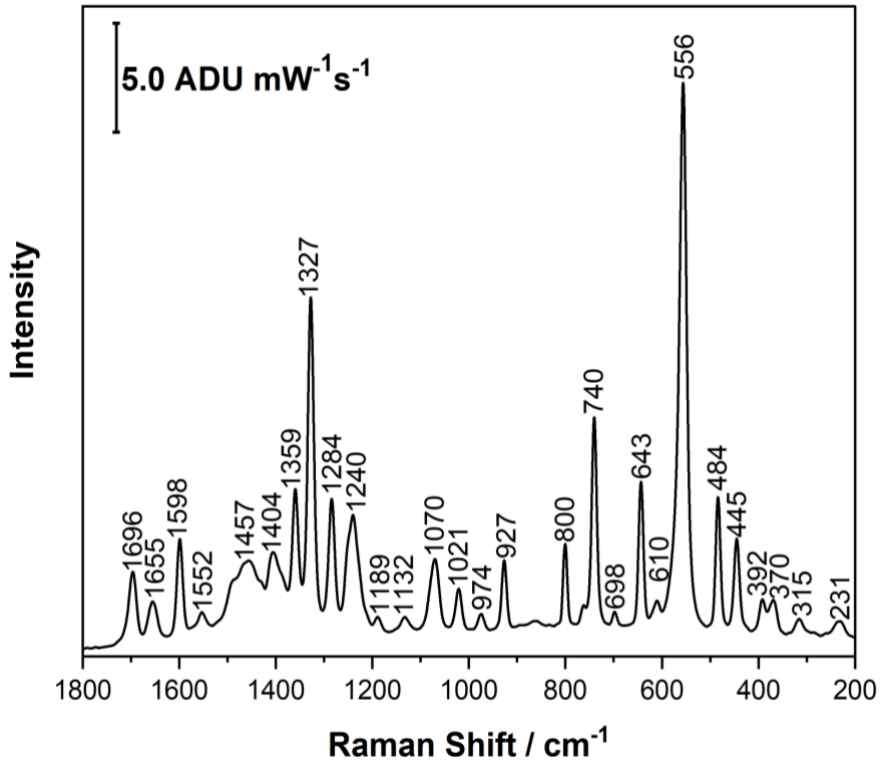

Figure 9.1: Raman spectrum of caffeine powder for 30 seconds at a high laser power at 780 nm excitation.

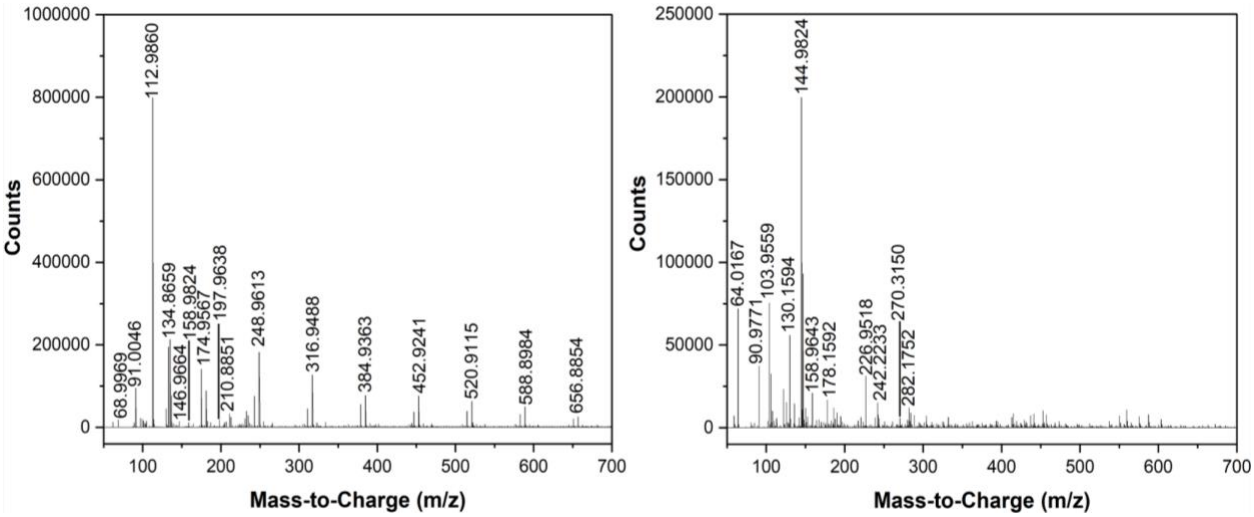

Figure 9.2: ESI-Q-TOF MS/MS spectra of ^{2}D mobile phase. Negative mode (left) and positive mode (right).

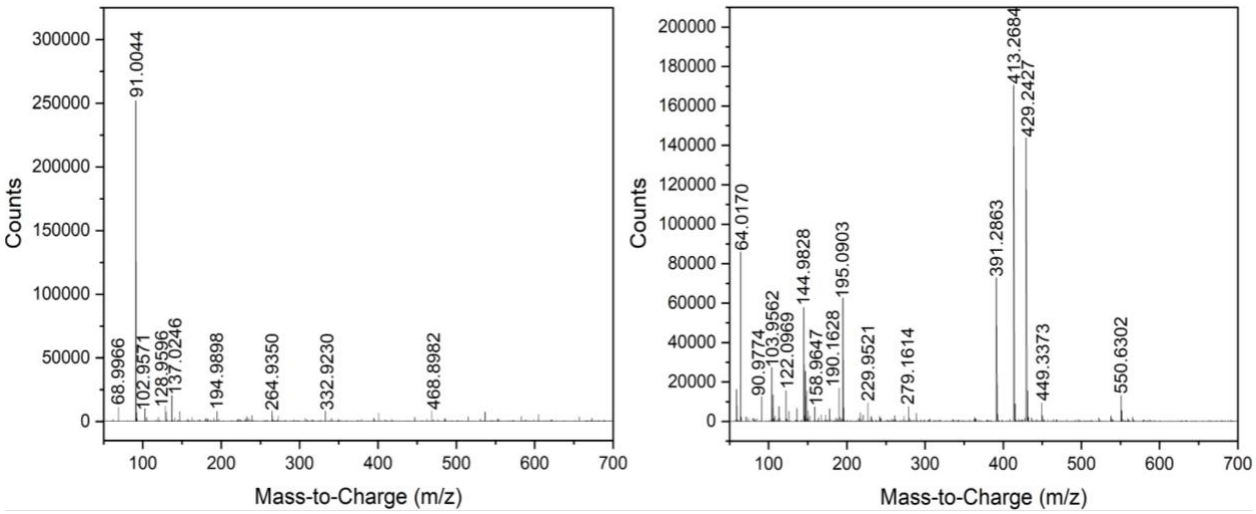

Figure 9.3: ESI-Q-TOF MS/MS spectra of cut 1. Negative mode (left) and positive mode (right).

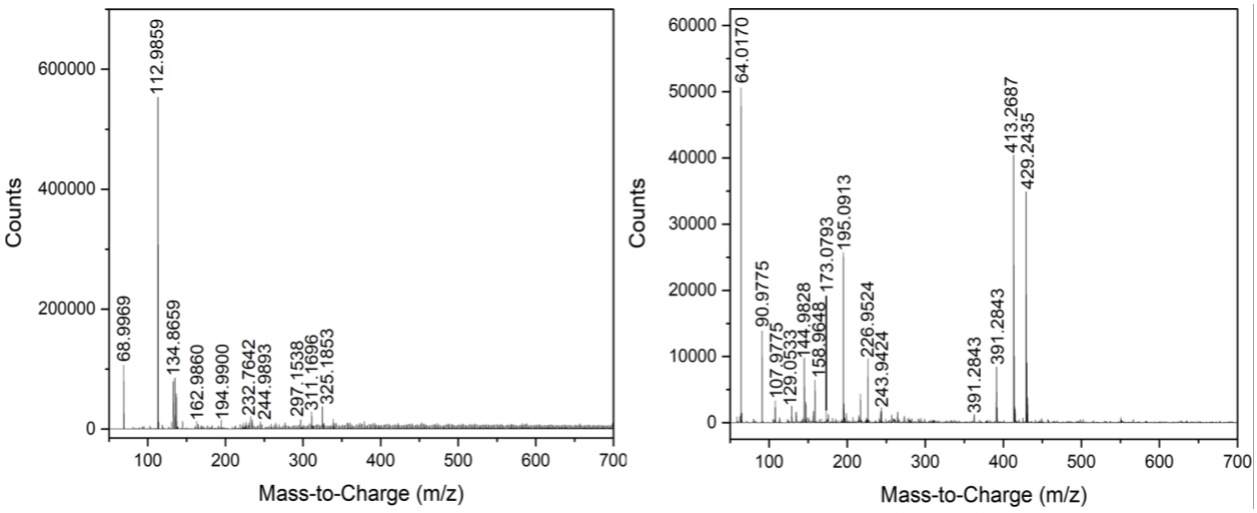

Figure 9.4: ESI-Q-TOF MS/MS spectra of cut 4. Negative mode (left) and positive mode (right).

Table 9.1: SERS Peak Assignment of DOM Extract. (δ = bending mode and υ = stretching mode)

Wavenumber (cm^{-1})	**Peak assignment**
412	δ(CC) aliphatic chains
529	υ(C-Br)
697	υ(C-Br)
740	υ(CC) alicyclic, aliphatic chain vibrations
1022	δ(CH_2, CH_3) asymmetric
1070	υ(C-O-C) asymmetric
1138	υ(C-O-C)
1190	υ(CC) aromatic ring chain vibrations
1267	υ(CC) alicyclic, aliphatic chains vibrations
1302	υ(CC) alicyclic, aliphatic chains vibrations
1387	δ(CH_3)
1428	δ(CH_2, CH_3) asymmetric
1576	υ(CC) aromatic ring chain vibrations, υ(C=C)

Table 9.2: SERS Peak Assignment of SPE Control Study. (δ = bending mode and υ = stretching mode)

Wavenumber (cm^{-1})	Peak assignment
529	υ(C-Br)
697	υ(C-Br)
741	υ(CC) alicyclic, aliphatic chain vibrations
1020	δ(CH_2, CH_3) asymmetric
1070	υ(C-O-C) asymmetric
1138	υ(C-O-C)
1190	υ(CC) aromatic ring chain vibrations
1309	υ(CC) alicyclic, aliphatic chains vibrations
1388	δ(CH_3)
1429	δ(CH_2, CH_3) asymmetric
1575	υ(CC) aromatic ring chain vibrations, υ(C=C)

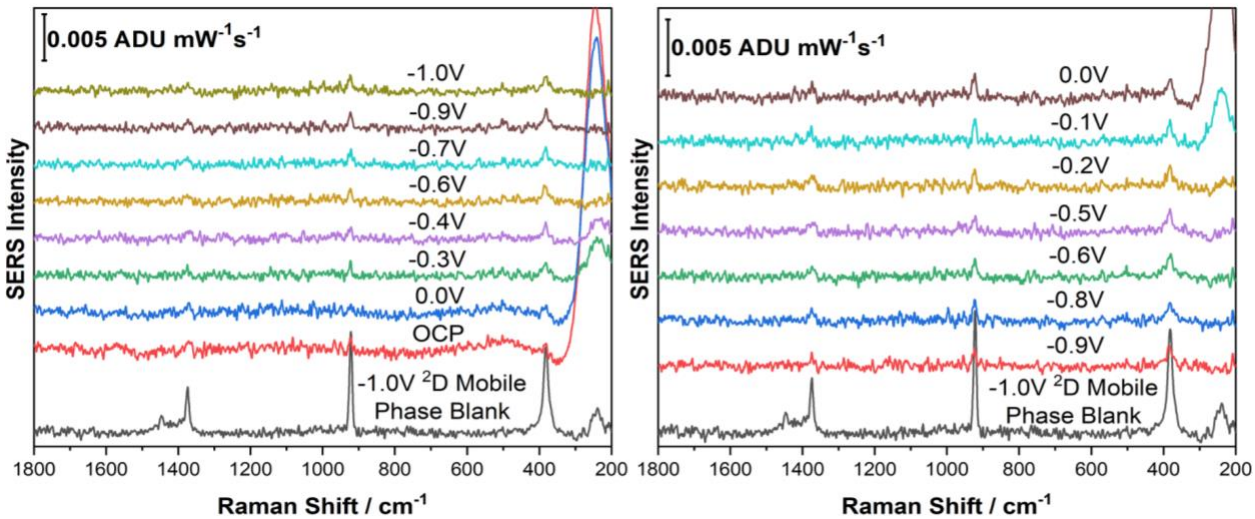

Figure 9.5: Comparison of EC-SERS spectra of cut 1 of DOM extract with second-dimension mobile phase.